

ISSN 1307-3729

REHVA  
**3E**

Federation of  
European Heating,  
Ventilation and  
Air Conditioning  
Associations

# The REHVA European HVAC Journal

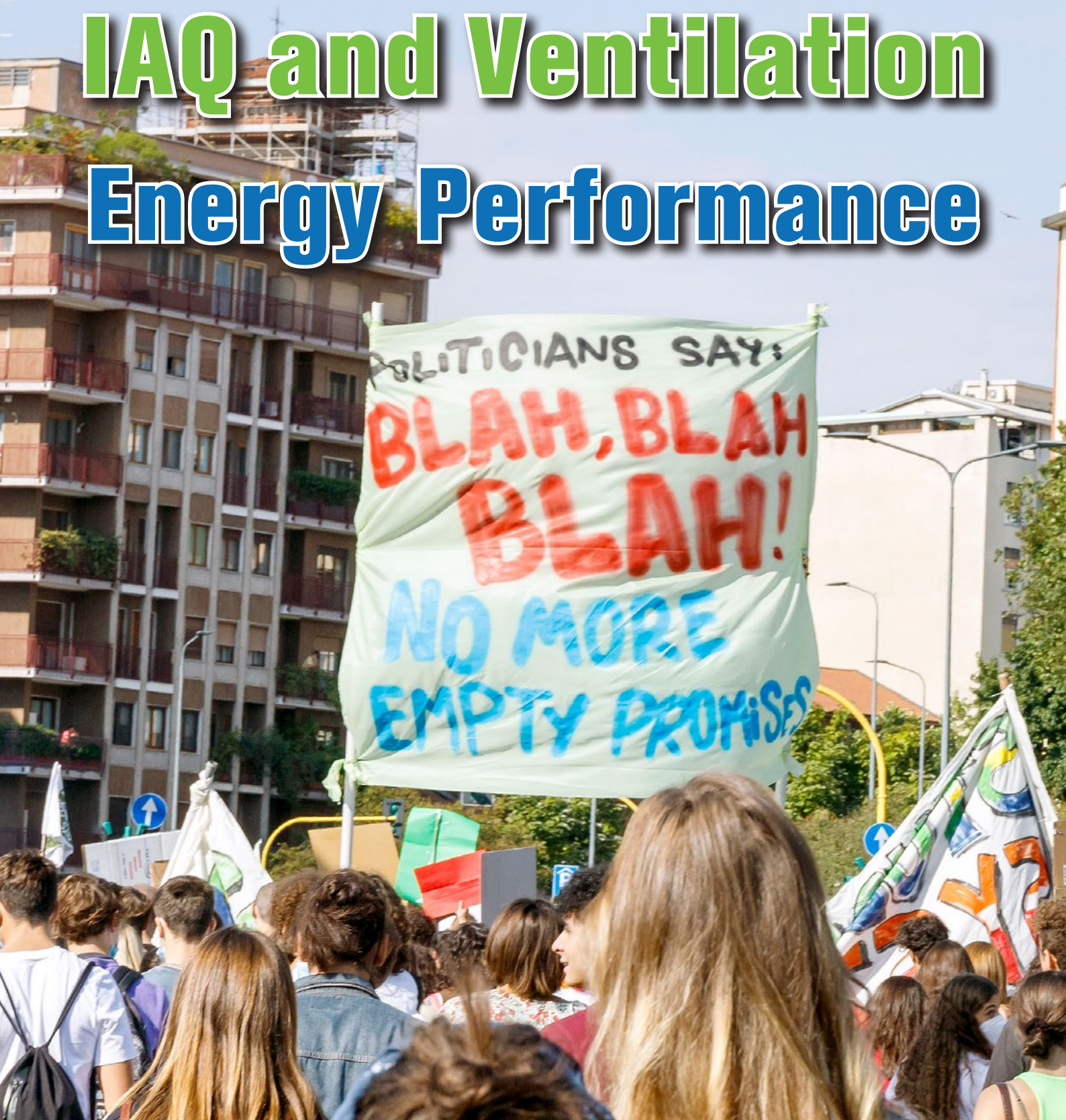
Volume: 60

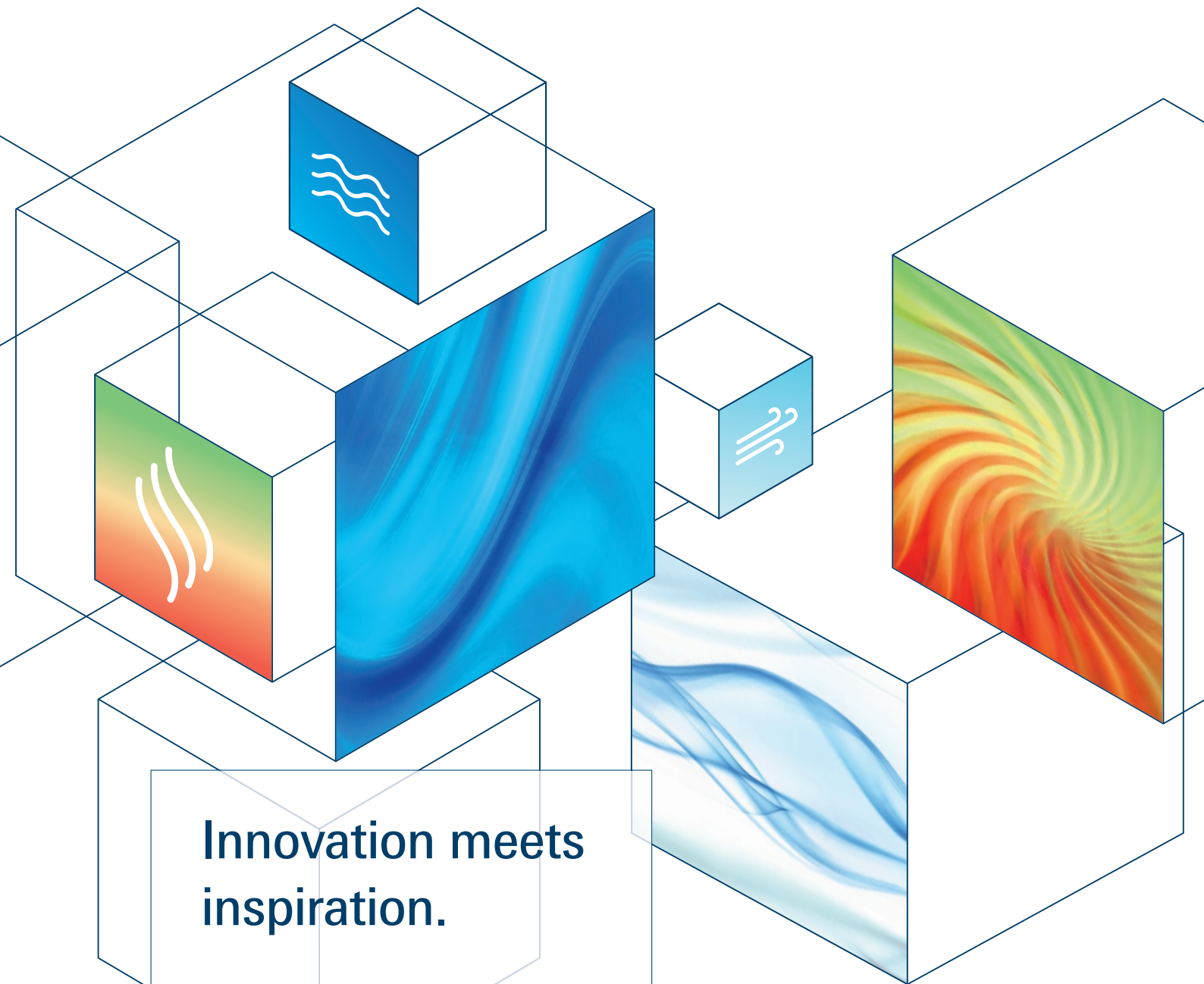
Issue: 1

February 2023

[www.rehva.eu](http://www.rehva.eu)

## IAQ and Ventilation Energy Performance

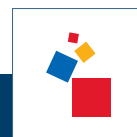




# Innovation meets inspiration.

Discover trailblazing innovations, fresh ideas and intelligent solutions for a **sustainable** future.

World's leading trade fair for  
HVAC + Water



# ISH

13.–17. 3. 2023  
Frankfurt am Main

## Editor-in-Chief:

Jaap Hogeling  
jh@rehva.eu

## Editorial Assistant:

Marie Joannes  
mj@rehva.eu

## General Executive:

Ismail Ceyhan, Turkey

## REHVA BOARD

### President:

Cătălin Lungu

### Vice Presidents:

Lada Hensen Centnerová

Livio Mazzarella

Pedro Vicente-Quiles

Johann Zirngibl

Ivo Martinac

Kemal Gani Bayraktar

## EDITORIAL BOARD

Murat Cakan, Turkey

Guangyu Cao, Norway

Tiberiu Catalina, Romania

Francesca R. d'Ambrosio, Italy

Ioan Silviu Dobosi, Romania

Lada Hensen, The Netherlands

Karel Kabele, Czech Republic

Risto Kosonen, Finland

Jarek Kurnitski, Estonia

Livio Mazzarella, Italy

Dejan Mumovic, United Kingdom

Ilinca Nastase, Romania

Natasa Nord, Norway

Dusan Petras, Slovakia

Olli Seppänen, Finland

Branislav Todorovic, Serbia

Peter Wouters, Belgium

## CREATIVE DESIGN AND LAYOUT

Jarkko Narvanne, jarkko.narvanne@gmail.com

## ADVERTISEMENTS

Nicoll Marucciová, nm@rehva.eu

## SUBSCRIPTIONS AND

## CHANGES OF ADDRESSES

### REHVA OFFICE:

Washington Street 40

1050 Brussels, Belgium

Tel: +32-2-5141171

info@rehva.eu, www.rehva.eu

## PUBLISHER

TEKNİK SEKTÖR YAYINCILIĞI A.Ş.

Fikirtepe Mah., Rüzgar Sk. No: 44C

A3 Blok, Kat:11 D:124 Kadıköy/Istanbul, Turkey

REHVA Journal is distributed in over 50 countries through the Member Associations and other institutions. The views expressed in the Journal are not necessarily those of REHVA or its members. REHVA will not be under any liability whatsoever in respect of contributed articles.

Cover photo: Kom Pornnarong / shutterstock.com

## Contents

Download the articles from [www.rehva.eu](http://www.rehva.eu) -> REHVA Journal

## EDITORIAL

- 4 2023 the Year of Fundamental Paradigm Swifts? – The signs cannot be ignored**  
Jaap Hogeling

## ARTICLES

- 5 Effects of Feed-In Power Limitations of Photovoltaic Systems**  
Matthias Krammer & Florian Wenig
- 10 Operational building energy performance**  
Ondřej Horák & Karel Kabele
- 15 Identification of Performance Gaps of Heat Pump Systems in Real Operation with Model-Based Data Analysis**  
Sebastian Dragosits & Roman Stelzer
- 20 Farm Constructions in Relation to the Quality of the Environment**  
Jana Lendelová, Ingrid Karandušovská, Miroslav Žitňák & Milada Balková
- 25 Indoor Climate After Energy Renovation of Family house**  
Anna Predajnianska, Eva Švarcová & Dušan Petráš
- 31 SMART Solutions for Energy Saving and Better Indoor Environment**  
Jiří Hirš & Ali Badai
- 35 Laboratory for testing of heating/cooling radiant systems**  
Martin Šimko, Dušan Petráš & Daniel Szabó
- 40 Comparison of Daylighting in Different Climatic Conditions**  
Iveta Skotnicová, Vojtěch Kolarčík & Ondřej Fadrný
- 45 Study of the Pressure Resistance of Odour Traps**  
Martin Sokol & Jana Peráčková

- 50 Mycoerosol in historic places – calculated ill health potential**  
Elena Piecková, Renáta Lehotská & Soňa Wimmerová
- 54 Estimation of Cross-Ventilation Through Roof Windows in Attics**  
Valérie Leprince, Nolwenn Hurel & Christoffer Plesner
- 60 Energy Savings with Aeroseal Ductwork Sealing in Europe**  
Nolwenn Hurel, Valérie Leprince & Simon Tölke
- 65 Integration of Domestic Ventilation Systems with Vertical Axis Wind Turbine Ventilation Technology**  
Jirayut Sitthipuk
- 69 Statistical analysis of the French building airtightness database**  
Bassam Moujalled, Adeline Mélois, Valérie Leprince & Gaëlle Guyot

## REHVA WORLD

- 75 REHVA is happy to welcome a new supporter: Saint-Gobain!**

## IAQ CORNER

- 77 The Seven Essentials of Healthy Indoor Air**

## EVENTS & FAIRS

- 78 Exhibitions, Conferences and Seminars in 2023**
- 79 ISH 2023 interim result: growing anticipation**
- 81 SuDBE International Conference 2023**
- 81 EFS 2023**

## Advertisers

- ✓ ISH ..... 2 ✓ REHVA SUPPORTERS..... 83
- ✓ BELIMO..... 76 ✓ REHVA GUIDEBOOKS..... 84
- ✓ REHVA MEMBERS ..... 82

## Next issue of REHVA Journal

Instructions for authors are available at [www.rehva.eu](http://www.rehva.eu) (> Publications & Resources > Journal Information). Send the manuscripts of articles for the journal to Jaap Hogeling [jh@rehva.eu](mailto:jh@rehva.eu).

# *2023 the Year of Fundamental Paradigm Swifts?*

## *– The signs cannot be ignored*

---

The war in Ukraine causes immense suffering to the Ukrainian people which is not to compare with the discomfort in Europe due to the gas dependency on Russia.

**T**he RepowerEU plan, the EU Green Deal, Renovation Wave, Fit for 55 by 2030 and the ongoing revision of the EPBD are the policy actions that will have a great impact on the HVAC&R industry in 2023. The European Commission advises to change from gas-fired boilers to electric Heat Pump systems to reduce the European gas consumption. This should be done anyway as the phasing out of fossil fuel use in buildings, is clearly mentioned in the draft EPBD. Using gas-fired boilers to heat our buildings should be phased out to be able to decarbonise our building stock by 2050. The war situation and the last IPCC report on climate change indicating that it will be almost impossible to stay below our 1.5–2.0 degree threshold, made it just more urgent.

When discussing with your customers energy saving measures, phasing out fossil fuels and investing in sustainable energy systems the cost effectiveness of our proposals is always on the table. Supporting financial incentives available at national level may support your proposals, convincing arguments that it is our obligation to save the world for the future generations should help. And in the case that you are able to produce an acceptable offer we encounter shortage of professional capacity and delayed delivery schedules of products.

And not to forget in this first post-epidemic year we still have to improve our ventilation systems and solutions as the health authorities warn us that a new epidemic is possible and we should use our time to

make our buildings more epidemic resilient. We have to advice residents who are working more from home compared to the pre-covid years given the fact that this will not change in the future. Homes are often not designed for using spaces as office, ventilation, thermal comfort acoustics and lighting are not always meeting the standards. This may affect health and productivity. When upgrading homes to make them more energy efficient and sustainable, this situation has to be taken in account.

To summarise: the keywords for 2023 are improving the energy performance of our buildings, decarbonisation, health and ventilation. I expect that as in this RJ issue, these themes will be prominent in 2023, sometimes addressing details but also global holistic approaches. I thank the contributing authors who will address these issues during 2023.■



**JAAP HOGELING**  
Editor-in-Chief  
REHVA Journal

# Effects of Feed-In Power Limitations of Photovoltaic Systems



**MATTHIAS KRAMMER**

Center for Building Technology  
Forschung Burgenland, Pinkafeld, Austria  
[matthias.krammer@forschung-burgenland.at](mailto:matthias.krammer@forschung-burgenland.at)



**FLORIAN WENIG**

Center for Building Technology  
University of Applied Sciences Burgenland,  
Pinkafeld, Austria

Limiting the feed-in power of residential photovoltaic systems is an important tool for electric grid operators to maintain a reliable energy supply. PV curtailment is effectively loss of green energy, therefore, this article aims to raise awareness that the PV potential lost through curtailment is far less than it is widely believed.

**Keywords:** photovoltaic; curtailment; feed-in limitation; inverter oversizing; grid management

The basic principle of a power system is that the produced electric power must be equal to the current consumption. Due to the falling costs in production, the solar photovoltaic (PV) capacity is projected to more than double by 2030 and overtake coal in the mid-2030s to become the second-largest installed global capacity [1]. The growing number of photovoltaic systems, however, which are mainly connected to low-voltage electric grids, lead to new challenges for grid operators in terms of maintaining a safe and reliable grid operation. On days with high solar radiation grid operators are faced with periods of overproduction of electricity and the high simultaneity of solar energy generation, especially in poorly developed grids, can lead to overloading of the grid. An alternative to cost-intensive grid reinforcement is the so-called feed-in management of photovoltaic systems. The simplest form is to limit or curtail the AC feed-in power of the generator to a constant value below the rated DC power of the photovoltaic array. PV curtailment can be done at two points in the grid - directly at the inverter or at the feed-in point. Curtailment at the inverter can occur by oversizing the inverter. Oversizing of inverters describes the situation when a PV array is assembled with a higher capacity than the rated size of the inverter. This is quite possible, as PV systems often produce less than their rated power. In times of optimal performance, the inverter limits the AC output by controlling the voltage and current. This means that the PV power is curtailed by the inverter

[2]. Curtailment of PV power at the feed-in point may be necessary to match supply and demand within the grid. One of the key issues is to maintain sufficient flexibility and balancing capability within the grid to balance demand and supply with controllable energy generators [3]. A prescribed feed-in curtailment may hinder reaching the full potential of the maximum available renewable energy generation at a specific location, because PV arrays may tend to be designed smaller to avoid running into the curtailment. Hence, this article discusses the effects on the annual electricity yield of a small-scale residential photovoltaic system under multiple curtailment scenarios. The effects of self-consumption and/or an optional battery storage are not taken into account. These assumptions ensure that only the PV electricity generated is taken into account in the evaluation and that the results are independent of individual boundary conditions. As a result, the outcome of this report has a higher informative value and applies both to a curtailment by the inverter and to a feed-in limitation by the local grid operator.

## Methodology

In order to investigate the effects of feed-in power limitations on the annual yield, an Example Plant was defined. The representative plant has a rated power of 10 kilowatt-peak (kWp) and is composed of twenty “FuturaSun FU 500 SILK Premium”-modules and a “Fronius Symo 10.0-3-M”-inverter and was situated in

five European capitals. In order to obtain representative results, the locations for the calculations have been chosen in such a way that they are evenly distributed over the longitudes of Europe. Not only was the location of the Example Plant varied, but also the orientation and inclination. The fictitious PV system was aligned in six different orientations and for each of these orientations, the modules were set up with an inclination of 30°, 60°, and 90°. Since the orientation does not matter for an inclination of 0°, this setup was simulated only once for each site. The selected locations and some additional information are listed in **Table 1 a)**, **b)** and **c)**, from the northernmost location to the southernmost. A list of the parameter variation performed at each simulation site is given in this table as well. For the elaboration of the results in this article, a total of 95 simulations were performed. All data featured in this paper was simulated with PV\*SOL premium 2022 [4]. The output of the simulations is the course of the grid feed-in in kWh over an entire year in a one-minute resolution. This value is used to calculate the electrical grid feed-in power of the PV system in kW. To keep the time required for the simulations low, they were carried out without curtailment. The PV curtailment was implemented in post-processing with MATLAB. The approach of introducing a feed-in limit in post-processing makes it possible to apply a power limitation to any value over the entire range of the rated power. Thus, a statement can be made not only about a certain curtailment value. For the purpose of this paper, the ratio of the maximum permitted feed-in power to the nominal power of the PV generator is referred to as the feed-in limit.

After curtailing the simulation data, the corresponding curtailed annual electrical yield can be calculated for each feed-in limit. The ratio between the yield under curtailment and the yield of a PV system without curtailment is referred to as yield-ratio in this paper and provides information on how a curtailed system performs compared to a system in unimpaired operation. This yield-ratio can take any value between 0 and 1 and the actual relative yield loss due to curtailment is defined as the difference between 1 and the yield-ratio.

Before the curtailment results are presented, the next section shows the different results from the parameter study. For the following illustrations, the values of the y-axis are in relation to the nominal power of the PV generator. **Figure 1** shows the summed monthly yield for a south-facing plant with a 30° inclination at all locations. It can be seen that the southernmost plant has the highest yield on average and the northernmost the lowest. **Figure 1** also shows for a representative week how the subsequent curtailment of the simulation results was carried out, using the example of a 25%, 50%, and 75% feed-in limit. A fictitious feed-in limit was applied over the entire simulation horizon, the values above this limit are considered as curtailment loss, and the values below the limit as curtailed PV power. Due to the higher global radiation and the higher proportion of direct radiation, it can be seen that the power limit is exceeded more often for the PV system in Rome than for the system in Oslo.

**Table 1 a).** List of Locations, used for the study.

Location; Latitude; Longitude; Database; Time Period; annual sum of global radiation (% diffuse)
Oslo; 59.95°; 10.72°; Meteonorm 7.2c3; 1991-2010; 900 kWh/m <sup>2</sup> (51.1%)
Berlin; 52.52°; 13.41°; DWD; 1995-2012; 1042 kWh/m <sup>2</sup> (52.1%)
Vienna; 48.23°; 16.50°; Meteonorm 6.1; 1991-2010; 1188 kWh/m <sup>2</sup> (47.5%)
Ljubljana; 46.07°; 14.52°; Meteonorm 8.1; 1996-2015; 1229 kWh/m <sup>2</sup> (47.9%)
Rome; 41.88°; 12.46°; UNI 10349; 1986-2005; 1611 kWh/m <sup>2</sup> (38.1%)

**Table 1 b).** List of Orientations (Azimuth) used for the study.

Orientation (Azimuth)
east/west(-)
east (90°)
south/east (135°)
south (180°)
south/west (225°)
west (270°)

**Table 1 c).** List of Inclinations used for the study.

Inclination
0°(south)
30°
60°
90°

## Results

The figures in this section show the most important findings from the calculations. To illustrate the results, the ratio of curtailed yield to maximum yield is plotted over the feed-in limit. In **Figure 2**, the AC power values after the inverter are plotted according to their frequency over the entire simulation year. The area under the curve thus represents the electrical yield in kWh. As can already be seen in **Figure 1**, a higher PV output is achieved in Rome and thus also a higher yield. The yield above the feed-in limit is considered a loss due to the curtailment. **Figure 2** also shows the difference between the individual sites with a southern orientation and 30° inclination. It can be seen that in the southern locations the curtailment in the lower area

has a greater effect on the yield losses. This is due to the fact that global irradiation is higher in these areas, resulting in more frequent and higher peaks in PV generation. Above a feed-in limit of 75%, no major differences can be observed between the individual locations.

Similar behavior can also be observed with a change in orientation and inclination, as shown in **Figure 3** - more direct irradiation of the modules by the sun leads to greater losses in yield due to the increased PV generation. A further comparison between the locations Oslo and Rome is carried out in **Figure 3**. “Rome - South - 30°” represents the PV system with the highest curtailment loss.

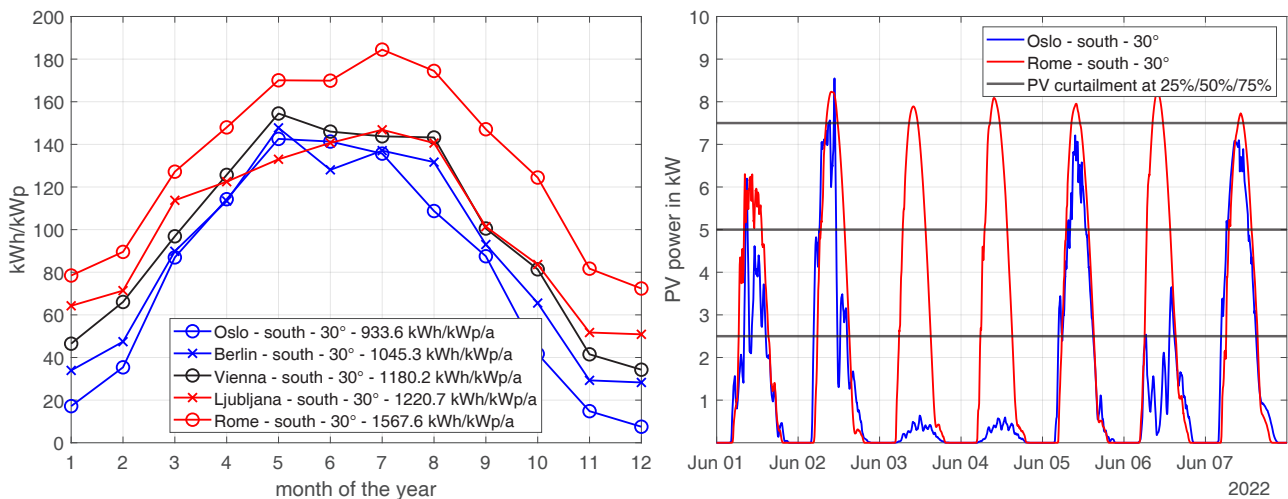


**Figure 1.** Comparing the monthly yield over all locations (left) and Example of curtailing the simulated PV power in MATLAB (right).

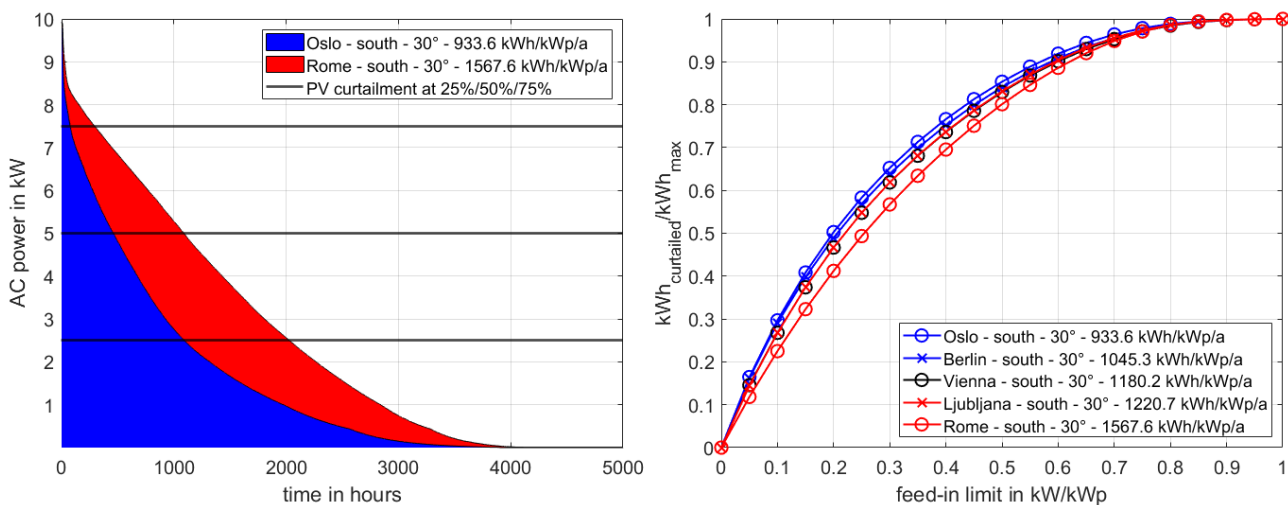


**Figure 2.** AC load distribution after inverter for Oslo and Rome (left) and Comparing the yield-ratio over all locations (right).

*Table 2. Yearly yield-loss at different levels of curtailment for the majority of the simulations.*

Yearly yield-loss at feed-in limit in %		30°			60°			90°		
		25%	50%	75%	25%	50%	75%	25%	50%	75%
Oslo	east/west	23.9	2.5	0.0	19.4	0.2	0.0	14.0	0.1	0.0
	east	34.8	9.2	0.8	37.3	13.0	1.7	33.3	10.2	0.8
	south/east	40.2	13.5	1.8	43.1	16.7	2.9	37.6	11.3	0.9
	south	41.7	14.7	2.1	44.6	17.3	2.9	38.0	10.7	0.9
	south/west	39.9	13.1	1.6	43.1	16.4	2.6	37.8	11.4	0.9
	west	33.7	8.5	0.6	36.2	12.0	1.3	32.4	9.4	0.5
Berlin	east/west	28.1	4.4	0.1	21.1	0.2	0.0	13.0	0.1	0.0
	east	37.0	11.6	1.1	36.9	13.4	1.8	30.6	9.3	0.5
	south/east	42.4	15.6	2.6	44.0	17.9	3.2	37.3	11.4	0.8
	south	43.1	15.9	2.8	44.1	17.1	2.8	35.5	9.7	0.9
	south/west	40.8	14.0	2.1	41.6	15.5	2.5	34.5	9.6	0.7
	west	34.7	9.6	0.8	34.3	11.3	1.2	28.4	8.0	0.4
Vienna	east/west	30.6	5.6	0.1	22.8	0.3	0.0	13.7	0.1	0.0
	east	39.4	12.6	1.3	38.7	14.1	1.8	31.9	9.7	0.6
	south/east	44.2	16.2	2.6	44.4	17.3	2.7	36.0	9.8	0.7
	south	45.2	17.0	2.9	45.1	17.0	2.6	34.9	8.9	0.9
	south/west	43.9	15.7	2.4	43.8	16.7	2.4	36.5	10.5	0.8
	west	38.4	11.4	1.0	37.9	12.7	1.4	31.1	8.5	0.4
Ljubljana	east/west	30.9	5.8	0.2	22.5	0.3	0.0	13.4	0.1	0.0
	east	39.0	12.0	1.2	38.5	13.5	1.7	31.7	9.4	0.6
	south/east	44.1	16.0	2.4	44.7	17.4	2.7	36.7	10.6	0.9
	south	45.2	16.9	2.7	45.4	17.2	2.9	35.7	10.1	1.1
	south/west	43.8	15.5	2.2	44.3	17.0	2.5	36.4	10.4	1.0
	west	38.1	11.1	0.9	37.4	12.3	1.2	30.6	8.2	0.4
Rome	east/west	37.2	8.2	0.2	26.0	0.3	0.0	14.4	0.1	0.0
	east	45.5	15.2	1.5	44.2	15.9	1.8	35.5	10.1	0.6
	south/east	50.1	19.3	2.7	49.5	19.4	2.6	39.4	10.4	0.8
	south	50.7	19.9	2.9	49.1	18.2	2.5	36.1	9.1	0.7
	south/west	49.4	18.6	2.5	48.6	18.2	2.1	38.0	9.2	0.6
	west	44.4	14.1	1.2	42.7	14.0	1.1	33.6	8.0	0.3

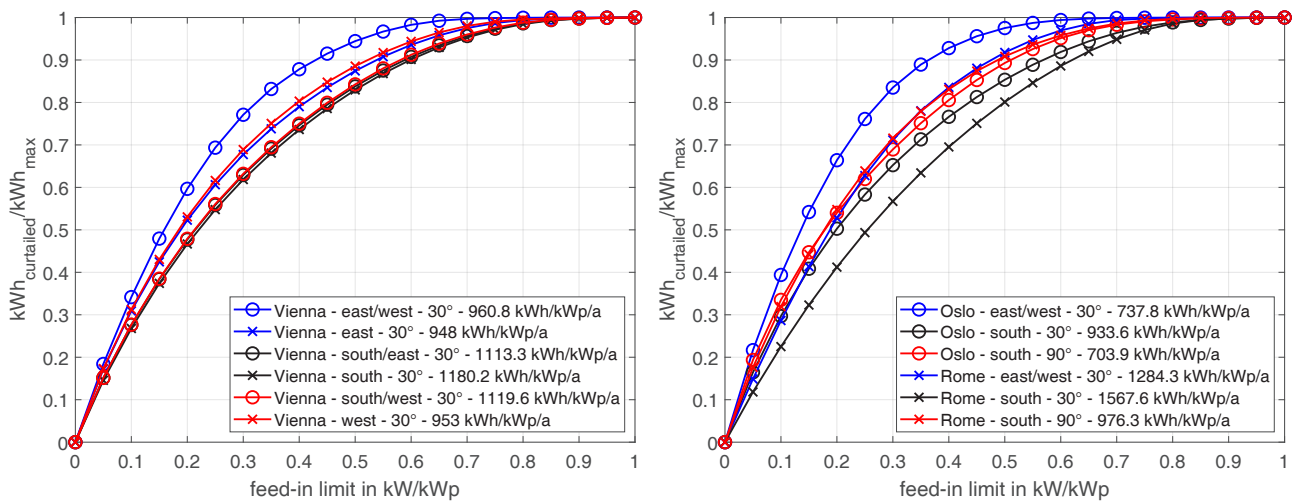


**Figure 3.** Comparing the yield-ratio for Vienna over all orientations (left) and Comparing the yield-ratio for the extreme scenarios Oslo and Rome (right).

## Conclusion

For the future maintenance of grid stability, curtailment of the PV power fed into the electricity grid is of great importance, as the discrepancy between supply and demand is minimized. It is also clear that through this measure, some of the green energy generated is lost. In general, it can be said that due to an optimal placement of the PV modules, power peaks occur more often and the curtailment intervenes more frequently. Due to these circumstances, the curtailment losses also increase. However, by evaluating the 95 simulation results, it can be stated that these losses are less than expected compared to the yield of a PV system with no curtailment. At a feed-in limit of 75% of the nominal power, a maximum loss of only 3.2% can be observed. When the relative losses of all simulations are averaged at this feed-in limit, the average loss is only 1.3%. At lower feed-in limits the

overall yield of the PV system decreases. However, a large portion of the yield is still available for use. If the feed-in power is reduced to 50%, there is a 19.9% loss of yield in the worst case. Taking all 95 simulation results into account, the average loss is 11.2% at this feed-in limit. In the worst case, the feed-in power must be reduced to 25% of the nominal power in order to record 50% of the yield as a loss. The resulting yield losses from the majority of the simulations are listed in **Table 2** for defined feed-in limits. One way to further reduce the losses caused by curtailment at the feed-in point is to integrate a battery storage system. On high-yield days, however, the battery storage is often fully charged at the time of maximum PV generation. This can be remedied by forecast-based battery charging. With this method, the charging of the battery storage is postponed to times with high PV power output [5]. ■

## References

- [1] International Energy Agency (IEA), 2018. World Energy Outlook 2018. International Energy Agency.
- [2] Neill, S., Stapleton, G., & Martell, C. (2017). Solar Farms: The Earthscan Expert Guide to Design and Construction of Utility-scale Photovoltaic Systems. Routledge.
- [3] Kato, T., Imanaka, M., Kurimoto, M., & Sugimoto, S. (2020). Impact of Power Output Curtailment Control of Photovoltaic Power Generation on Grid Frequency. IFAC-PapersOnLine, Vol. 53 Issue 2, 12157-12162.
- [4] Valentin Software GmbH: PV\*SOL premium 2022(R7), Stralauer Platz 34, 10243 Berlin, Germany.
- [5] Weniger, J., Bergner, J., Tjaden, T., & Quaschnig, V. (2016). Effekte der 50%-Einspeisebegrenzung des KfW-Förderprogramms für Photovoltaik-Speichersysteme. Hochschule für Technik und Wirtschaft Berlin (HTW Berlin), Berlin, Studie.

# Operational building energy performance



**ONDŘEJ HORÁK**

Czech Technical University in Prague  
Faculty of Civil Engineering  
Department of Indoor Environmental  
and Building Services Engineering  
[ondrej.horak.1@fsv.cvut.cz](mailto:ondrej.horak.1@fsv.cvut.cz)



**KAREL KABELE**

Czech Technical University in Prague  
Faculty of Civil Engineering  
Department of Indoor Environmental and  
Building Services Engineering  
[kabele@fsv.cvut.cz](mailto:kabele@fsv.cvut.cz)

Building Energy Performance is evaluated in form of a certificate before the construction. However, how can we ensure low energy consumption during building operation? The paper presents the user-friendly interface that provides information about all energy flows in assessed building.

**Keywords:** building energy performance, intelligent buildings, building systems data evaluation, low-energy buildings

Building energy performance in Czechia is evaluated on the basis of the Czech Decree on the Energy Performance of Buildings [1]. The main output is in the form of Energy Performance Certificate, which is calculated on monthly basis and even before the construction or refurbishment of the building starts.

Therefore, the paper deals with the topic of assessment of operational building energy performance. The structure of the assessment is based on above mentioned legislation with the aim of user-friendliness and clearness of the interface.

## TRIO Project, Energy Performance functionality

The paper presents the Energy Performance functionality, which is part of the “Smart House product management system extension” project, on which the Department of Indoor Environmental and Building Services Engineering of the Faculty of Civil Engineering of the CTU in Prague collaborates with Brand-tech company. The project is part of the “TRIO” Applied Research and Experimental Development Program announced by the Ministry of Industry and Trade of the Czechia. [2] The whole system consists of 11 functionalities which are focused on all building systems, energy sources, facility management etc. The project outputs are part of a functional sample called Modular House Monitoring System with Advanced Environmental and Energy Systems Assessment. [3]

The Energy Performance functionality has the aim of evaluating the energy flows in an assessed building during its operation. The main principle is the comparison between evaluated year of operation with so called reference year. The reference year may be based on Energy Performance Certificate, building simulation or one of the previous years of operation. The functionality structure corresponds with the Certificate (Evaluation of Total Energy Delivered and partial energies, Non-renewable primary energy, division to energy carriers). Beyond the scope of legislation, the evaluation of electricity consumption by appliances is also included.

## Evaluation procedure

The operational energy performance is evaluated according to the algorithm in **Figure 1**. First of all, an evaluation period of 1 year has to be selected (Step 1). Subsequently, in Step 2, the data from the building’s measurement system, which are relevant for the evaluation, are read and in Step 3, their summarization is carried out. Step 4 is used to evaluate the data of the reference year. Then the reference and evaluation data are compared and in Step 5, a percentage evaluation of the evaluated data is performed against the reference data in Step 6. Step 7 contains a menu for displaying details for shorter time periods and in Step 8 these are then displayed (in graphical and tabular form).

To make the outputs understandable, they are structured similarly to the building energy performance certificate. The interface consists of screens depicting

the energy flows in monthly time steps. Above them there are main screens that summarize the total energy delivered and non-renewable primary energy.

The main screen shows the main navigation of the functionality and a summary evaluation of the total energy delivered and partial energies: evaluated compared to the reference year, the percentual evaluation and triage by emoticon for clarity at a glance. By clicking on “Details” the monthly data are shown. It is also possible to select the evaluated and reference year on the main screen. By clicking on “Primary Energy” the screen of energy carries, electricity consumption by appliances and Primary energy from non-renewable sources is evaluated in the same principle.

### Case Study of a Family House

The functionality is tested on a low-energy family house located in town Rýmařov, Czechia. It is a one-story, low-energy wooden building with an unheated attic.

The main source of heat is a stove with a fireplace, where the piece wood is burnt. The fireplace is equipped with a heat exchanger to a hot water two-pipe heating system. The second source is an electric boiler.

Domestic hot water is prepared in an accumulation tank connected to the heating system. There is another circuit for DHW preparation connected with solar thermal collectors. The tank is also equipped by electric heat cartridge.

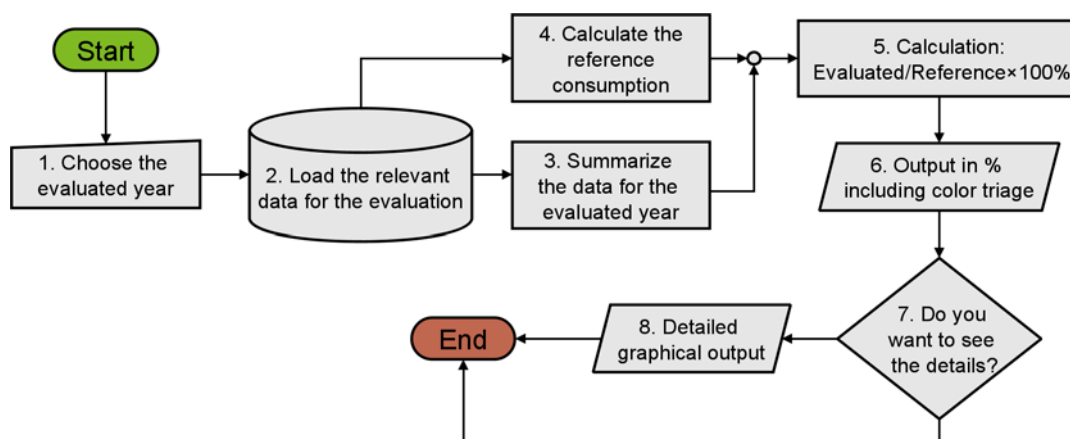


**Figure 1.** Scheme of algorithm which evaluates the operational energy performance.

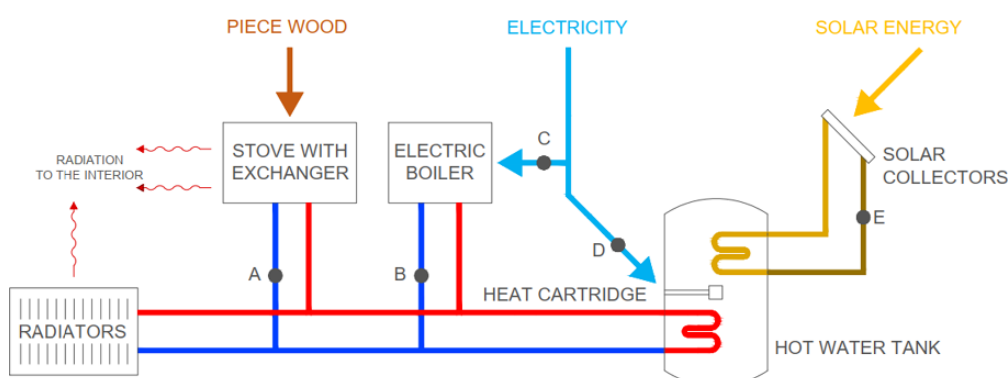


**Figure 2.** Family house in Rýmařov and its scheme of technical systems. [4,5]

The whole house is equipped by sensors which are measuring all the energy flows, indoor air quality and outside meteorological conditions. The data have been collecting starting January 2016 in 15-minute time step.

### Evaluation and outputs – Delivered energy

The figures below show the evaluations of total energy delivered and partial energies during the operation of the building. The dark-beige-coloured buttons are serving for navigation and clicking between screens. It is also possible to choose evaluated and reference year. In this case study, the authors evaluate the period from 1st July 2021 to 30rd June 2022. Year 2017 was chosen as a reference.

The principle of tabular evaluation is always to display the measured energy (left column with beige numbers), the reference value of supplied energy (middle column with grey numbers). The third column then indicates the percentage rating  $\text{Measured/Reference} \times 100\%$ .

This rating is accompanied by an emoticon to inform the user how the given energy flow is doing.

By clicking on “Details” the monthly graphic and tabular evaluation of delivered energy is shown. The percentual evaluation and emoticon triage have the same principle.

The main screen on **Figure 3** shows the annual results of comparison between measured and reference data. Between the reference and the evaluated year there was a decrease in energy consumption of approximately 15%. When divided into partial energies, the differences are visible. The energy consumption for heating fell by 14%. This is caused (and monthly data confirm this) by differently hard winters. As shown on **Figure 4** in the reference year, the energy consumption in November, December and January was significantly higher. On the other side March 2022 was quite cold [6], so the energy consumption is about 54% higher than in reference year.

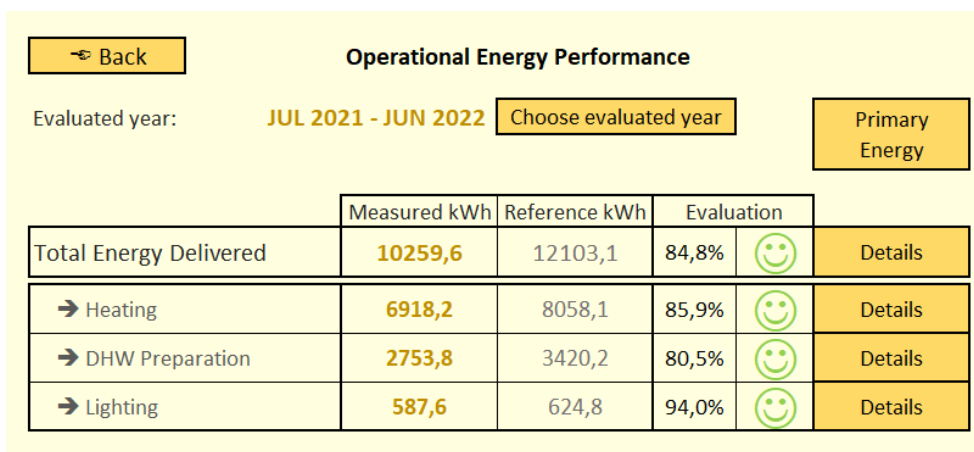


**Figure 3.** The main screen with annual evaluation of partial and total energy delivered. [7]

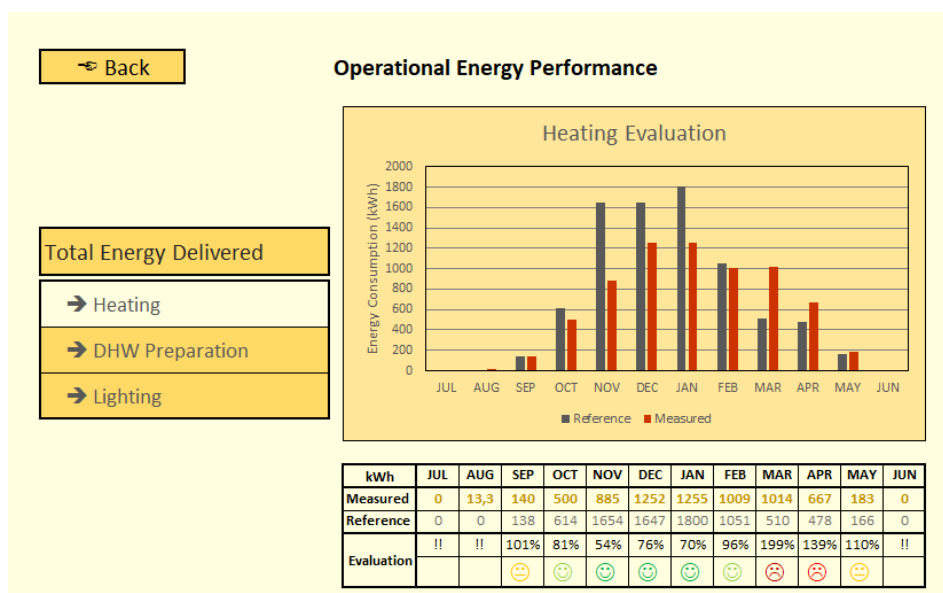


**Figure 4.** Detailed monthly analysis of energy consumption of heating. [7]

## Evaluation and outputs – Primary energy

This chapter is focused on evaluation of primary energies. The **Figure 5** shows the main screen about primary energy. The principle of evaluation is the same as on delivered energy. The screen is further supplemented with graphs dedicated to the shares of individual energy carriers.

The diagrams on **Figure 6** confirm that the building owners use piece wood more frequently in the evaluated year. It is visible mostly in November when the share of electricity dropped almost to zero (electricity covered only the consumption for lighting).

The Graph on **Figure 7** shows the electricity consumption of appliances, the increase of consumption may be caused by purchasing new appliances (for example TV and computers for kids) and a larger share of home-office due to a COVID-19 pandemic.

The appliances consume more energy than for example DHW preparation, so their consumption is not negligible and may be included in overall evaluation.

## Conclusion

The functionality “Energy Performance” has the aim to provide proper, clear information about energy flows to the building user. The interface should be user-friendly. In present time of rapidly rising energy costs, the functionality can affect the budgets of building users. However, the presence of measurements of all energy flows in the building is a basic assumption to be able to carry out the assessment.

The aim of the authors for further development (beyond the scope of the TRIO project) is to improve

the recalculation of the reference period so that the boundary conditions are as comparable as possible. For example, these are meteorological data, data on the presence of people, data on the ventilation of the interior space, etc. All this requires the installation of additional measuring sensors in the building, but at the same time it can provide even clearer information about the evaluated period in terms of energy demand.

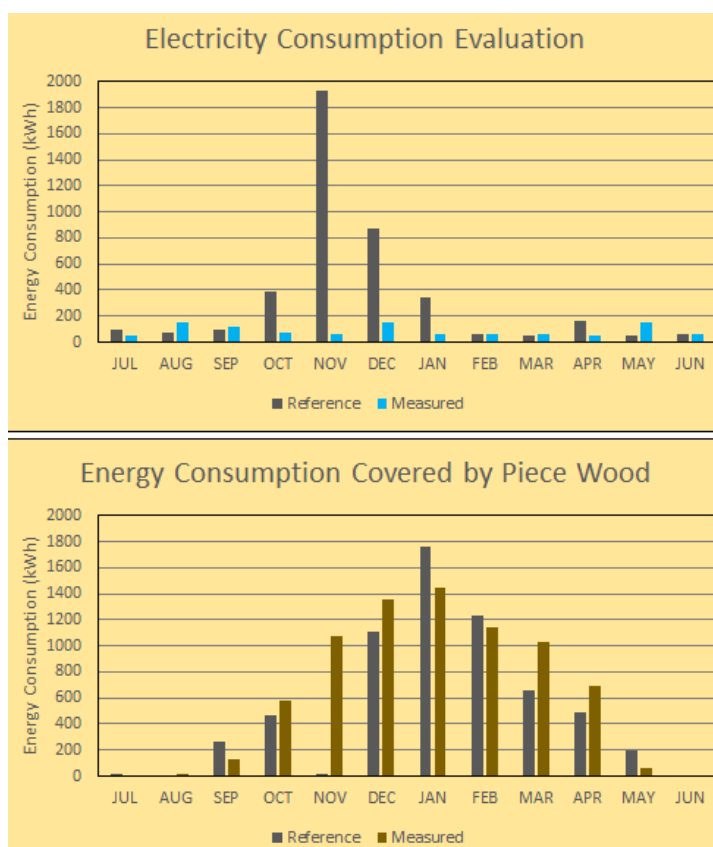


**Figure 6.** Cuttings from screens from interface showing detailed monthly consumption of electricity and heat energy covered by piece wood. [7]

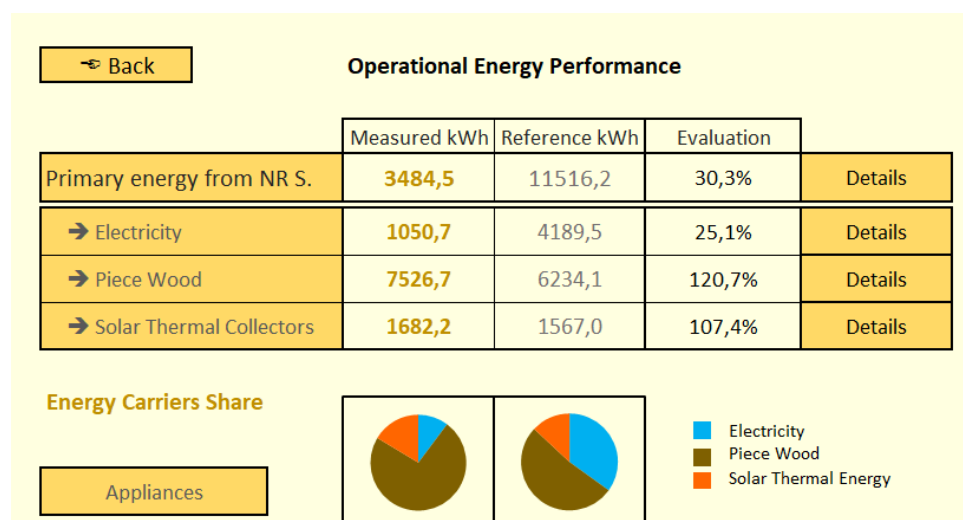


**Figure 5.** Main primary energy screen. [7]

Another goal is the ability to click energy flows down to the level of days to hours for more detailed evaluation of, for example, system failures or to optimize the operation of the building, which could lead to lower the energy consumption.

Another conclusion is that in the future it is also appropriate to focus on the consumption of electricity by appliances that are not included in the assessment according to the current legislation. In the family house, these are mainly household and office appliances. The aim of the assessment is to reduce electricity consumption and thus reduce payments. ■

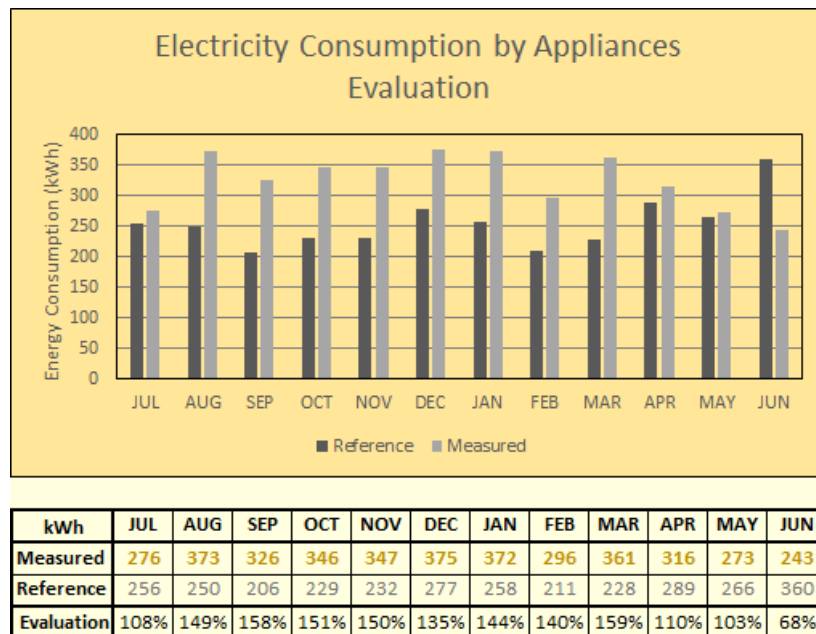


**Figure 7.** Cuttings from screen from interface evaluating electricity consumption of appliances. [7]

### Acknowledgments

This project was implemented with financial support from the state budget of the Czech Republic through the Ministry of Industry and Trade in the TRIO-FV40183 programme in cooperation with Brand-tech company.

The full paper was presented at the Indoor Climate of Buildings 2022 conference and is printed in the conference proceedings. [7]

### References

- [1] 264/2020 Sb. Vyhláška o energetické náročnosti budov. Zákony pro lidi - Sbírka zákonů ČR v aktuálním konsolidovaném znění [online]. Copyright © AION CS, s.r.o. 2010 [cit. 21.11.2022]. URL: <https://www.zakonyprolidi.cz/cs/2020-264>.
- [2] Vyhlášení čtvrté veřejné soutěže v programu TRIO | MPO. Ministerstvo průmyslu a obchodu [online]. Copyright © Copyright 2005 [cit. 18.11.2022]. URL: <https://www.mpo.cz/cz/podnikani/podpora-vyzkumu-a-vyvoje/vyhlaseni-ctvrte-verejne-souteze-v-programu-trio--239644/>.
- [3] Kabele, K.; Brůha, P.; Dvořáková, P.; Frolík, S.; Horák, O.; Kabrhel, M.; Urban, M.; Veverková, Z. et al. Modulární monitorovací systém domu s pokročilým systémem hodnocení prostředí a energetických systémů [Functional Sample] 2021.
- [4] Kabele, Urban: Grant no: te0200077 Smart Regions – buildings and settlements information modelling, technology and infrastructure for sustainable development
- [5] Horák, O.; Kabele, K. Predicted and Actual Energy Performance of Residential Buildings in Czechia. Case Study on Evaluation of Detailed Energy and IEQ Monitoring in Family House. In: Roomvent&Ventilation 2018: Excellent Indoor Climate and High Performing Ventilation. Helsinki: SIY Indoor Air Information Oy, 2018. ISBN 978-952-5236-48-4.
- [6] Portál ČHMÚ: Historická data: Počasí: Územní teploty. Portál ČHMÚ: Home [online]. URL: <https://www.chmi.cz/historicka-data/pocasi/uzemni-teploty#>.
- [7] Horák, O.; Kabele, K. Operational Building Energy Performance. In: Indoor Climate of Buildings 2022 Healthy Built Environment and Energy Security. Bratislava: Slovenská spoločnosť pre techniku prostredia, 2022. p. 196-203. ISBN 978-80-8284-004-2.

# Identification of Performance Gaps of Heat Pump Systems in Real Operation with Model-Based Data Analysis



**SEBASTIAN DRAGOSITS**

Center for Building Technology,  
Forschung Burgenland GmbH, Research  
Centre Pinkafeld, Austria  
[sebastian.dragosits@forschung-burgenland.at](mailto:sebastian.dragosits@forschung-burgenland.at)



**ROMAN STELZER**

Center for Building Technology, Forschung  
Burgenland GmbH, Research Centre  
Pinkafeld, Austria  
[roman.stelzer@forschung-burgenland.at](mailto:roman.stelzer@forschung-burgenland.at)

This paper presents an analysis model that can be used to automatically assess the efficiency of heat pumps under real operating conditions and identify performance gaps based on measured data. For the model validation historical data from a real plant from a time period that the plant is known to have operated inefficiently was used. The validation showed that the model was able to detect the corresponding inefficiencies. The model is highly scalable, i.e. the more measurement data and plant information available, the more detailed analyses and results are possible.

**Keywords:** heat pump, performance gaps, scalable model, real operation environment, data analysis, data validation

In Austria, but also in the EU (EU 27), energy consumption in the household sector has remained very steady at around 20 to 25% of total consumption in recent years. [1] In order to reduce the total energy consumption and thus to increase the overall energy efficiency, this sector can therefore be a good opportunity. Building services equipment in particular should be examined here, as incorrect design or inefficient operation often goes undetected, as long as the plant meets user requirements. Directive 2018/844/EU (EPBD) aims to counteract such undetected inefficiencies by requiring regular inspections and a monitoring system, depending on the size of the system. [2]

In the course of the “digital Twin” research project, modular and scalable inspection and diagnostic methods for the automated operational performance analysis of building services equipment and systems are

to be developed, among other things. Heat pumps are often used to provide heating and cooling in buildings, which is why the research project took a closer look at the heat pump as a building services system alongside HVAC systems (Heating, Ventilation and Air Conditioning). In this paper, the developed analysis model for heat pumps is presented in more detail.

## Methodology - structure of the analysis model

The analysis model was developed with Matlab. The chosen approach allows the evaluation of the heat pump performance in interaction with the connected devices, thus considering the surrounding system as well. Therefore, specific plant information (e.g. design power) as well as historical measurement data are combined to calculate various key performance indicators.

In order to create the broadest possible field of application for this overall model, individual analysis submodels were developed, which can be used depending on the information basis. In existing plants, the available measurement technology often does not allow detailed analyses to be carried out, which makes such an approach with a scalable analysis model attractive.

Depending on which variables are measured by a plant, other submodels can be selected, which in sum result in the overall analysis and evaluation. In general, the more information is available and the more quantities are measured, the more accurate the analysis and evaluation of the investigated plant will be. It should also be mentioned here that both reversible and non-reversible heat pumps can be investigated with this analysis model, since the input and calculation structure were defined so generally in advance.

The following submodels are present in the analysis model, which can identify various performance gaps in real operation mode and environment:

- Identification of the heating and cooling period of the heat pump
- Identification of the heat pump switch-on times
- Performance ratio

- Identification of the switch-on times of the secondary pump
- Identification of the switch-on times of the primary pump
- Analysis of heat storage tank (temperature stratification, loading errors)
- Analysis of cold storage tank (temperature stratification, loading errors)

Since the heat and cold supply is often coupled with balancing storage tanks, simple analysis options for heat and cold storage tanks.

The first three submodels each contain two different options on which information basis the analysis and calculation should be performed. For the identification of the heating and cooling period (ID H/C) of the heat pump, for example, there are the options to determine the respective periods with the help of the measured thermal power or the measured supply and return temperature, as can also be seen in **Figure 1**. In addition to the individual model options, for all sub-models except the first two (they form the basic variant for evaluating the heat pump and are therefore always executed) there is the option to skip the respective evaluation if these

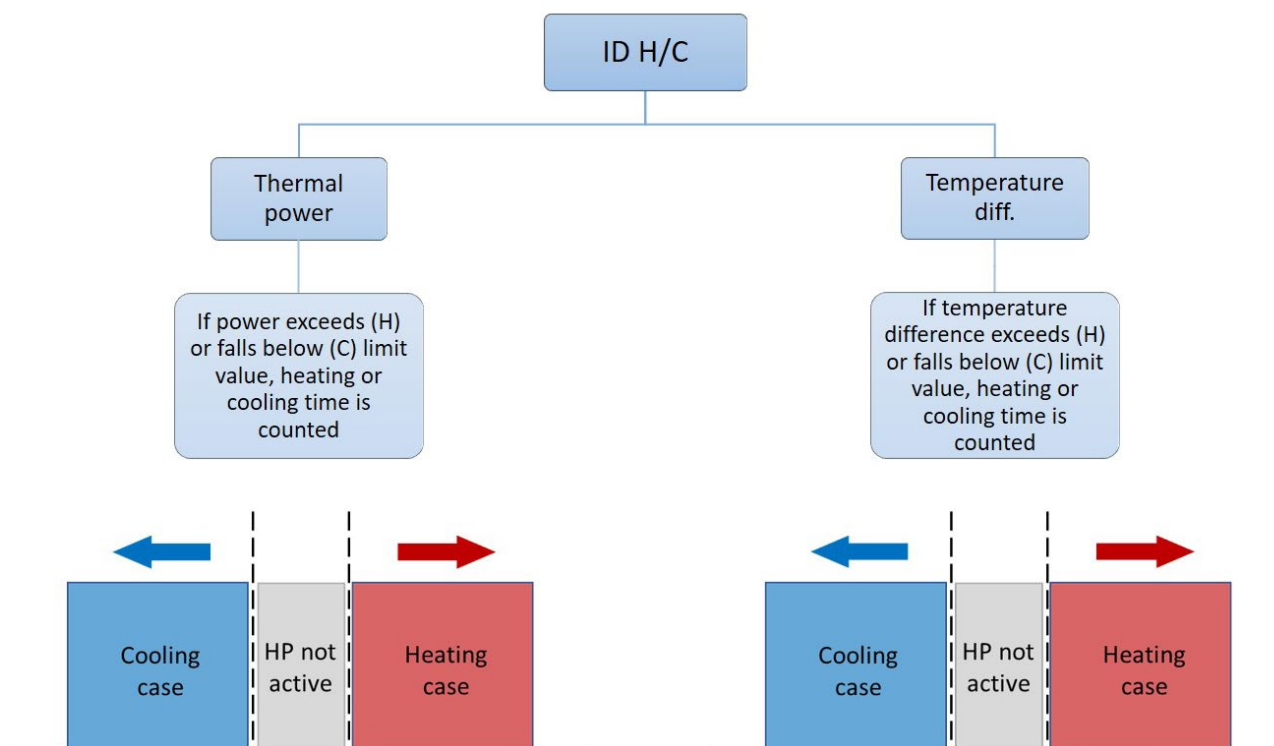


**Figure 1.** Example of a submodel structure (submodel: identification of heating and cooling period).

aspects are not to be evaluated or the information and measurement data required for this are not available.

All required inputs for all submodels together are shown in **Figure 2**. Depending on the submodels and submodel options chosen, not all of the information shown in the **Figure 2** is required.

In addition to the individual submodels, the overall analysis model also includes a resampling of the measured data, an input check of the input variables and a rough check of the data quality. For the individual calculations and evaluations in the submodels, a uniform and constant time step size of the measurement data is required. Therefore, the model includes a resampling that is performed by default each time the program is executed. Since the overall model has many submodels, an input control of the input variables was implemented. On the one hand it is checked whether all inputs were made in the necessary format and on the other hand whether the necessary information for the in each case selected models was entered before. If an input does not fit or is not existing, an error message including a correction notice will be displayed automatically. The data quality check includes statistical (number of statistical outliers, rate of change of the respective measured variable) and rule-based checks (no negative volume flows, no negative changes in cumulative measured data). If the analysis and evaluation of a plant yields unusual results, the results of the data validation can be checked to see if a faulty data set is responsible.

When all submodels are executed, the following evaluation results and ratings are returned to determine specific performance gaps:

- Switch-on times of the heat pump
- Cycle rates or cycle durations of the heat pump per operating mode (heating/cooling)
- Performance ratios
- Coefficient of Performance (COP)
- Energy Efficiency Ratio (EER)
- Seasonal Coefficient of Performance SCOP
- Seasonal Energy Efficiency Ratio (SEER)
- Comparison of the switch-on times of the heat pump with those of the feed pumps on the evaporator and condenser side
- Temperature stratification in the heat and cold storage tank
- Loading errors during heat pump operation (heat storage tank is loaded with too low or cold storage tank with too high temperature)

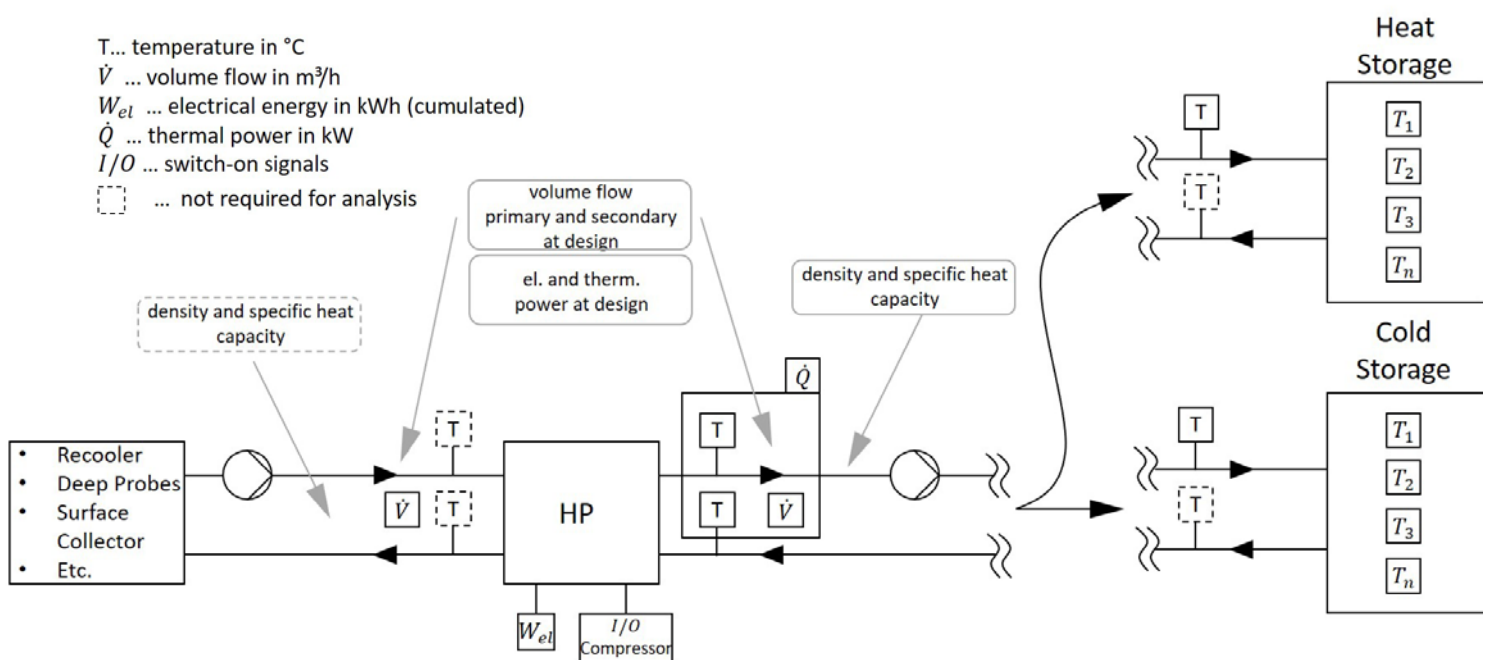


**Figure 2.** Total required inputs for all submodels together for reversible heat pumps.

The switch-on times of the heat pump are analyzed in order to compare whether it was operated in the desired or energetically optimal periods. The cycle rates or cycle durations of a heat pump quickly provide information about how efficiently the heat pump is operated and whether the control or the design are generally suitable. The performance ratios (COP, EER, SCOP, SEER) directly indicate the efficiency of the heat pump and are thus an essential result of the analysis model. The comparison of the switch-on times between the heat pump and the feed pumps provides information about the timing between these components, i.e. whether the control of the feed pumps roughly fits. Regarding the storage tanks, the difference between the highest and lowest measured temperature is evaluated to check the temperature stratification (for stratified charging storage tanks). The calculation of the loading errors is again mainly aimed at checking the control whether the respective storage tank is actually always loaded with the correct temperature.

With regard to the evaluation of the individual results, limit values can be defined in the model itself, which are then used for visualization.

## Validation

The analysis model was developed and validated using measurement data from a real plant. The investigated system is a reversible heat pump used in an office building. On both the heating and cooling sides, stratified charging storage tanks are available. However, it was mainly used to provide cooling energy. For validation, a historical annual data set was taken from a period in which inefficient operation of the plant was known.

The model determined, that the heat pump had very short cycle durations (six minutes on average), which was mainly due to the system being oversized relative to the actual cooling energy demand (**Figure 3**).

The fact that the heat pump was used almost exclusively to provide cooling was also shown by the visualization of the switch-on times, which were mainly concentrated in the summer months (**Figure 4**).

Furthermore, the SEER was somewhat low at 3.3. Regarding the feed pumps, it was found that they were active for almost the entire period, i.e. not well matched to the heat pump operation. The analysis

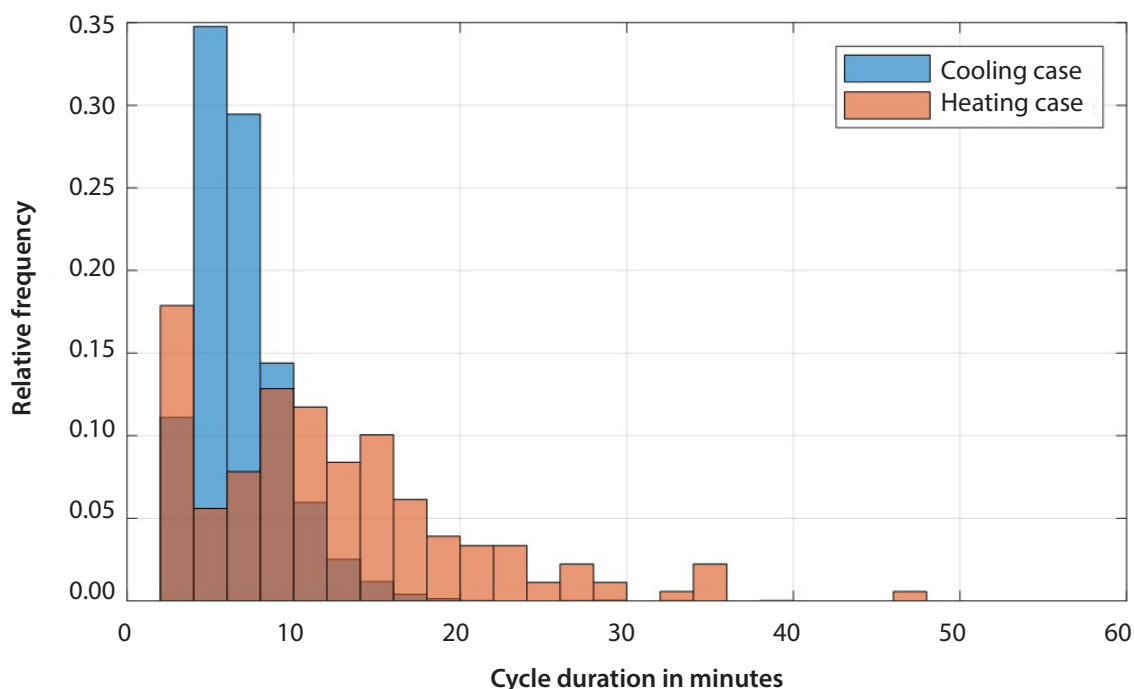


**Figure 3.** Cycle durations of the heat pump in cooling and heating case.

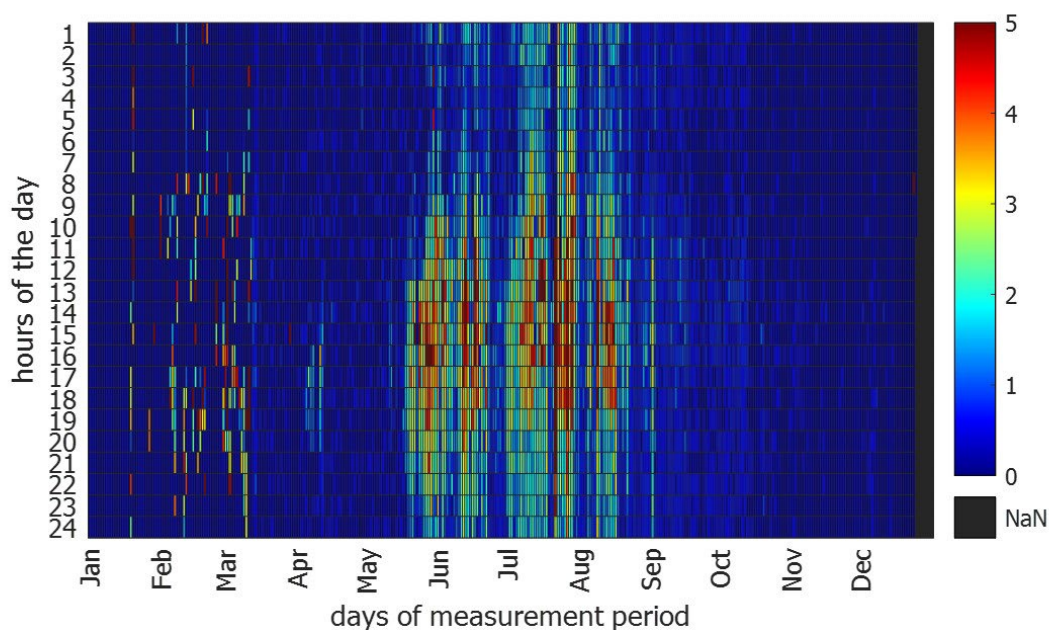


**Figure 4.** Hourly electrical power consumption of the evaluated heat pump in kW.

of the two storage tanks showed that there was no effective stratification in the cold storage tank (the temperature difference between the upper and lower sensors averaged 1 K in the cooling period). This result again coincides with the almost continuous flow of the feed pump, since the water in the cold storage tank was constantly circulated outside the heat pump operation. But also, during active cooling operation some loading errors (cold storage was loaded with too high temperature) could be identified.

## Conclusion

The validation showed that the analysis model was able to identify the expected problems and inefficiencies of the plant under investigation. The approach of a scalable analysis model is promising, since existing plants often do not have sufficient measurement technology to allow detailed analyses. With this model, it is possible to perform simple analyses with only a few

measured quantities, which is an advantage especially when investigating existing plants with few installed sensors. Furthermore, this approach of a scalable analysis model can also be applied to other building systems and components (e.g. HVAC systems).

Currently, this analysis model is decoupled from the measurement and further processing of the analysis and evaluation results. The aim of the “digital Twin” project is not only to develop such a stand-alone analysis model, but also to link it to data acquisition (using measurement data stored in a database directly for analysis) and the visualization of results in e.g. online dashboards. This would move the actual Matlab model including operation into the background and the user would thus receive information on the plant performance on the dashboards directly after the measurement has been carried out, and this with comparatively less handling effort. ■

## References

- [1] Eurostat, Energy balances, Energy Balances in the MS Excel file format (2022 edition), Available online: <https://ec.europa.eu/eurostat/web/energy/data/energy-balances> (accessed on Sep 26, 2022).
- [2] Directive (EU) 2018/844 of the European Parliament and of the Council of 30 May 2018 amending Directive 2010/31/EU on the energy performance of buildings and Directive 2012/27/EU on energy efficiency, Available online: <https://eur-lex.europa.eu/legal-content/EN/TXT/?uri=celex%3A32018L0844> (accessed on Sep 26, 2022).

# Farm Constructions in Relation to the Quality of the Environment



**JANALENDELOVÁ**

Institut of Agricultural Engineering, Faculty of Engineering Slovak University of Agriculture in Nitra, Slovakia  
[jana.lendelova@uniag.sk](mailto:jana.lendelova@uniag.sk)



**INGRID KARANDUŠOVSKÁ**

Institut of Agricultural Engineering, Faculty of Engineering Slovak University of Agriculture in Nitra, Slovakia



**MIROSLAV ŽITŇÁK**

Institut of Agricultural Engineering, Faculty of Engineering Slovak University of Agriculture in Nitra, Slovakia



**MILADA BALKOVÁ**

Institut of Agricultural Engineering, Faculty of Engineering Slovak University of Agriculture in Nitra, Slovakia

Environmental research and progress in the introduction of innovations and the construction of new facilities also offer significant structural challenges in the construction of stables in our breeding practice. The aim of the article was to verify the quality of the environment in two different types of buildings in terms of the production of harmful gases and the state of heat load indicators in a small-scale renovated building using motor ventilation and many innovative solutions - in comparison with a large-scale, excellent modern building, which by its parameters surpassed the novelty of many construction solutions on a global scale and highlighted the trend of low-energy solutions in precision breeding. The effects of a high concentration of animals in the old building predicted the emergence of unsuitable living conditions for both animals and people. But the integration of major innovations in the past transformed the old building and created much better conditions for both animals and people. On the other hand - according to the new assignment of the project as well as the high-quality execution of building structures and technological equipment of the new barn, it was assumed that in this new building, it would be possible to create much better well-being of animals in a more hygienic environment and with less heat load for the animals even without the installation of motorized ventilation. During hot summer days, there were no significant differences in the heat load indices THI and ETIC between the small-volume building with forced ventilation compared to the index values in the large-volume building with natural ventilation. In the large-volume building without motorized ventilation,  $\text{NH}_3$  and  $\text{CH}_4$  levels were lower by more than 34.2% and 41.5% ( $P < 0.01$ ), which, including other open design conditions, predicts more effective conditions to ensure the required environmental hygiene.

**Keywords:** gas concentrations; heat stress index; barn volume; technical solution

**D**airy cow farming is one of the largest sources of  $\text{NH}_3$  and  $\text{CH}_4$  within livestock production (Poteko, 2019). Their high concentration in production buildings has a negative effect on both

livestock and livestock breeders. Poor ventilation can increase the relative humidity and the concentration of harmful gases such as carbon dioxide and ammonia. The concentration of carbon dioxide depends to a large

extent on the type of building, the ventilation system and the density of the animals. A significant source of  $\text{CH}_4$  is the manure because it contains cellulose that is degraded by methane-producing bacteria (Maurer et al., 2016). Ammonia contributes to eutrophication and soil acidification, and it exerts an adverse impact on biodiversity and ecosystems (Witkowska & Sowińska, 2017). Many factors influence the concentrations of harmful gases, in especially high temperature, emitting area and emission source, etc. Due to climate change, even in temperate climates, the issue of high air temperatures and increased heat load is increasingly becoming more common and affects high producing dairy cows the most (Herbut, 2019). One option to reduce heat load in dairy cows and increase air quality is by using flow cooling through natural and forced ventilation. Natural ventilation is dependent on weather and structural design and is often not adequate in summer. Then it is required to provide cooling by forced ventilation or by a combination of several methods (evaporative cooling, shading, spraying of animals, etc.) (Fournel, 2017). To assess the quality of the environment, in scientific practice, combined methods are used - part of practical measurements and part of theoretical calculations, or the detection of production or health indicators. The worst combination is when extremes in both high concentration of pollutants and high heat load of animals occur. The article is devoted to the comparison of the state of air chemistry and the level of heat load in two structurally different types of barns.

## Material and Methods

The research was performed during the summer season in two types of dairy cattle barns, in the same farm. The barns differed in herd size, housing system, and manure management.

The new PUR panel-hall building “A” for 444 dairy cows had two internal feeding corridors, the length of the building was 85.4 m, the width of the building was 51.8 m. The total height of the 3-sector counter roof in the ridge was 18.2 m. The steel structure system with 4 longitudinal rows of columns was made in a module of 5 m. The height of the wall was  $h_s=8$  m on the south side,  $h_n=7$  m on the north side. The front walls were made of PUR-panels with a thickness of 40 mm, 8 gates for the entry of the mechanisms were made up of remote-controlled green plastic blinds. The roller shutter system was also used on the side walls, where a fully openable roller shutter 85 m long and 4.8 m high was made above the 2.2 m high fixed wall. The roof area was composed of three roof boards - the southern area made of PUR-panels 1,500 m<sup>2</sup> (with slope of 15°),

the middle area made of double-cavity polycarbonate corrugated roofing 1,865 m<sup>2</sup> with a slope of 15° and the northern roof (PUR-panel) area 1,440 m<sup>2</sup> with a slope of 24°. Two large vertical slits were made along the entire roof, which ensure the removal of air through natural ventilation. The upper continuous intermediate vertical opening in the ridge was 3.3 m high, the second vertical roof opening was high of 1.5 m.

The dimensions of massive old brick building “B” for 158 dairy cattle were 70 m in length and 11.5 m in width. The height of the side (longitudinal) wall was 4.3 m and a ridge height was 9.7 m. An outdoor feeding area with a length of 70 m and a width of 3.25 m was added to the building. The ceiling parts were removed due to the increase in the volume of the building from the original 2,329.6 m<sup>3</sup> to 5,154.1 m<sup>3</sup>. The ridge of the roof was opened to a width of 350 mm and parts of the roof covering were illuminated by five vertical strips 1 m wide. In the old building, there was an air volume of 34.3 m<sup>3</sup> per animal, a floor area of 4.85 m<sup>2</sup> per animal indoors and 6.37 m<sup>2</sup> per animal including the outdoor covered feeding area. Five basket fans were installed in the longitudinal axis above the double cubicles, each with a capacity of 16,500 m<sup>3</sup>h<sup>-1</sup> (total 82,500 m<sup>3</sup>h<sup>-1</sup>).

The concentrations of  $\text{CH}_4$ ,  $\text{NH}_3$ ,  $\text{N}_2\text{O}$ , and  $\text{CO}_2$  were measured using a photo-acoustic multi-gas analyser 1309 (Inova, Denmark). Gas concentrations were measured at 4 indoor locations in the object A and 4 indoor locations in the object B and 1 outdoor location. Air was sampled from the various locations using 10–30 m long polytetrafluoroethylene (PTFE) tubes with an inner diameter of 3.2 mm. The air temperature and relative humidity were measured every 5 min using datalogger Comet. The two types of indexes were used to evaluate the heat load of animals. The temperature humidity index (THI) combines the air temperature and relative humidity into one value to estimate the heat load. We assessed heat stress according to the levels set as follows: mild heat stress  $72 < \text{THI} < 79$ , moderate stress  $80 < \text{THI} < 89$  and severe heat stress  $\text{THI} > 89$  (Armstrong, 1994; Hoffmann et al., 2019). The Equivalent Temperature Index for dairy Cattle (ETIC - calculated according to Wang et al., 2018) takes into account - in addition to temperature and relative air humidity - air velocity and solar radiation (Hempel et al. 2019). We valued ETIC according 4 categories: mild category  $18 \leq \text{ETIC} < 20$ , moderate category  $20 \leq \text{ETIC} < 25$ , severe category  $25 \leq \text{ETIC} < 31$ , emergency category  $31 \leq \text{ETIC}$  (Hempel et al. 2019). The quality of the workers’ working environment was evaluated according to Law No 355/2007 and DECREE No 99/2016.

The aim of this study was to compare the concentrations of harmful gases and microclimatic properties of indoor air in two different building and benefits of construction types of dairy housing in the summer season with an emphasis on the evaluation of the effect of structural innovation on air chemistry and animal heat load indexes, as well as parameters of the quality of the employees' environment.

Data on climatic parameters, gas concentrations in two barns with different housing systems were processed statistically. Since all variables had a normal distribution, single factor ANOVA was performed. The significance of differences between the mean values of gas concentrations in barns was determined by Tukey's test. All calculations were made using Statistica 10 for Windows (StatSoft, CZ).

## Result and Discussion

During the assessment of indoor climate parameters, no significant differences were found between objects A and B ( $p > 0.05$ ), however, the pre-ventilation fans were not operating in building A during the research as per the methodology. The intention of the breeder was to provide the new building with a large-cubicle space with low-energy, quiet and low-emission operation.

The optimum temperature in dairy cow housing is 8–16°C (Kołacz and Dobrzański, 2019). As expected - in neither building was the optimal temperature ensured. In the location of Central Europe, this is almost impossible during the day in summer. Moreover, the methodology of the experiment was aimed at monitoring situations during days with

extremely high outdoor air temperatures, so that air chemistry and heat load were assessed for critical cases. The climatic data were recorded during the period with outdoor air temperature  $30^{\circ}\text{C} < T_{\text{ext}} < 32^{\circ}\text{C}$ , relative humidity  $47\% < \text{RH}_{\text{ext}} < 53\%$  and airflow velocity  $0.2 \text{ m}\cdot\text{s}^{-1} < v_{\text{ext}} < 1.2 \text{ m}\cdot\text{s}^{-1}$ . The average values from climatic measurements at 65 indoor points in the building A without the use of motor ventilation were:  $T_{\text{int,AVG}}=32,61\pm 0,71^{\circ}\text{C}$ ,  $\text{RH}_{\text{int,AVG}}=50,94\pm 2,86\%$ ,  $v_{\text{int,AVG}}=0,47\pm 0,28\text{m}\cdot\text{s}^{-1}$ . According the two heat indexes were not found a significant differences in that values; the  $\text{THI}_{\text{A,AVG}}=82,09\pm 0,89$  and  $\text{ETIC}_{\text{A,AVG}}=26,12\pm 0,71$  (Figure 1). Heat stress level was not significantly different ( $P > 0,05$ ) compared these two buildings - it was moderate (for THI) and severe (for ETIC) category, but there were different possibilities to modify this level. For old one - very limited possibilities, for new one there were a lot of technical solutions.

According to results of the evaluation of on-farm climatic measurements at the 16 indoor points in the building B using motor ventilation we found, that the average values were:  $T_{\text{int,AVG}}=32,22\pm 0,45^{\circ}\text{C}$ ,  $\text{RH}_{\text{int,AVG}}=52,92\pm 2,14\%$ ,  $v_{\text{int,AVG}}=0,37\pm 0,23\text{m}\cdot\text{s}^{-1}$ . The Temperature-Humidity Index was higher that limit level with value of  $\text{THI}_{\text{B,AVG}}=81,93\pm 0,87$  and Equivalent Temperature index for Dairy Cow was  $\text{ETIC}_{\text{B,AVG}}=26,07\pm 0,71$ , which is about the limit level (Figure 2).

Mean concentrations of greenhouse gases and ammonia differed significantly ( $P < 0.01$ ) between facilities. Building A (new) was characterized by lower ( $P < 0.01$ ) mean concentrations of GHGs and ammonia compared to building B (Figure 3). The detected amounts of all gases were lower than

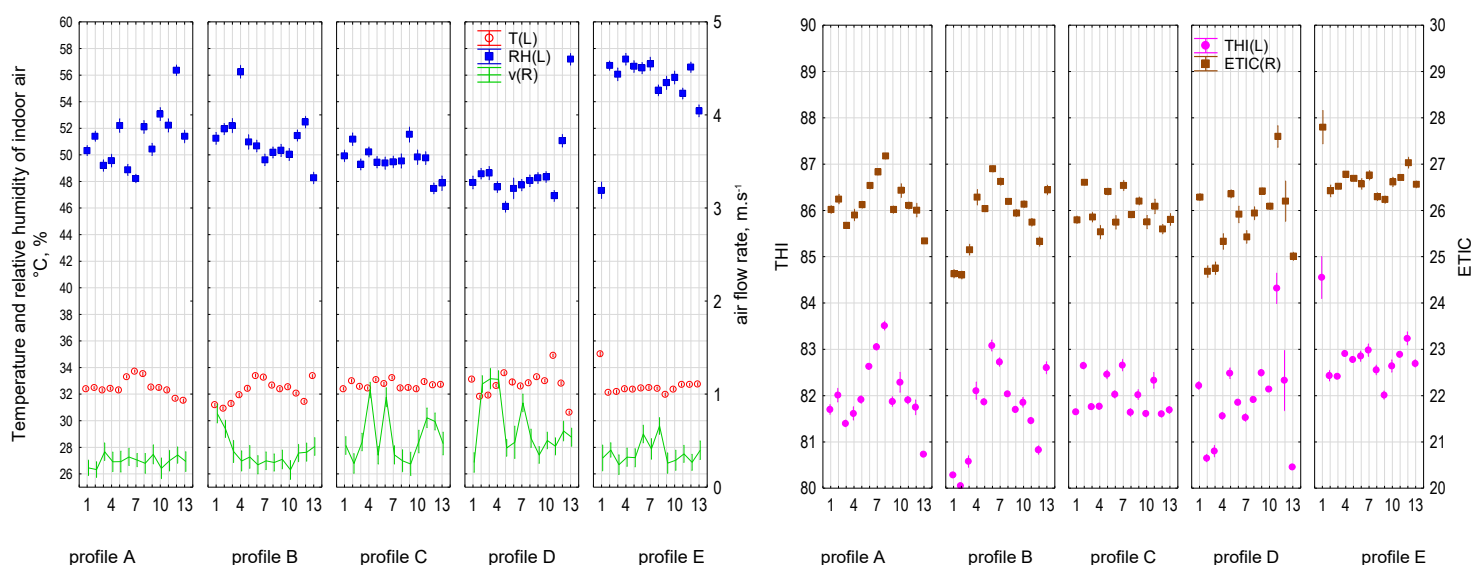


Figure 1. Results of microclimate conditions in low-volume new barn A.

the recommended environmental limits for workers and animals during the experiment.

The average  $\text{CO}_2$  concentration in the new barn (A) was 9.8% lower than in barn B. The most significant improvement in view of chemistry was observed for  $\text{NH}_3$ , which was 34.2% lower in the new facility, and

$\text{CH}_4$  concentrations were 41.5% lower than in the old facility.

Microclimatic parameters are an important physical factor of the working environment, which in Slovakia is subject to Act No. 355/2007 and decree no. 99/2016 Coll.

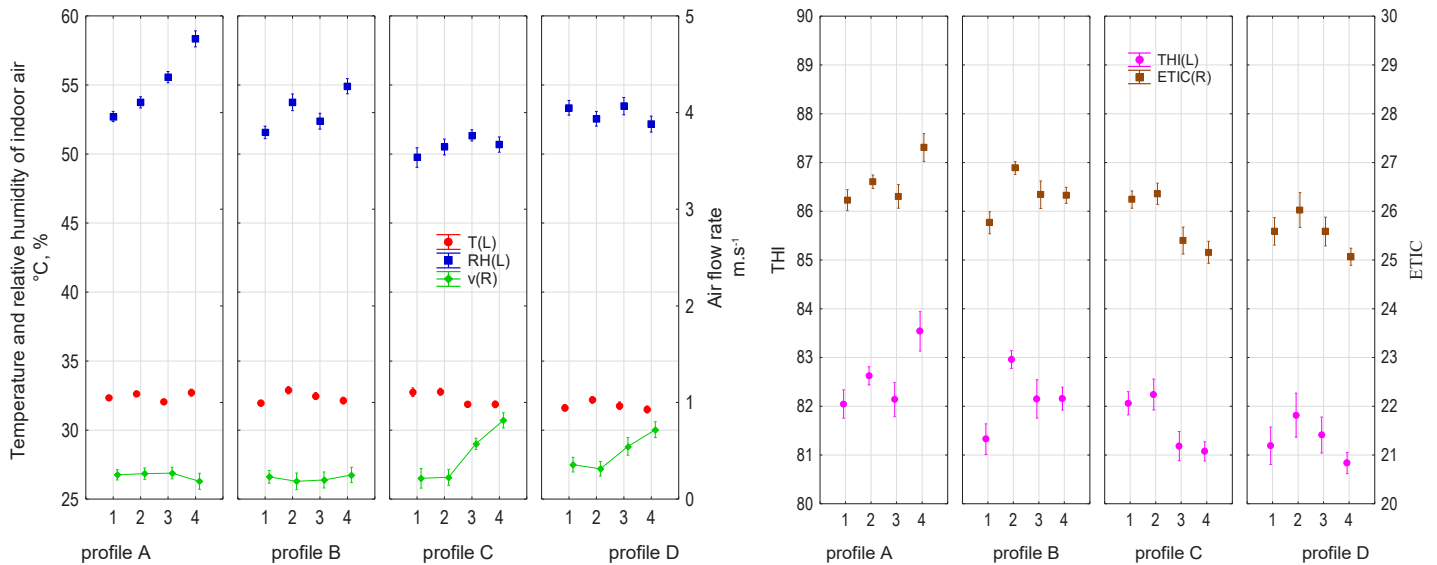


**Figure 2.** Results of microclimate conditions in large-volume old - reconstructed barn B.

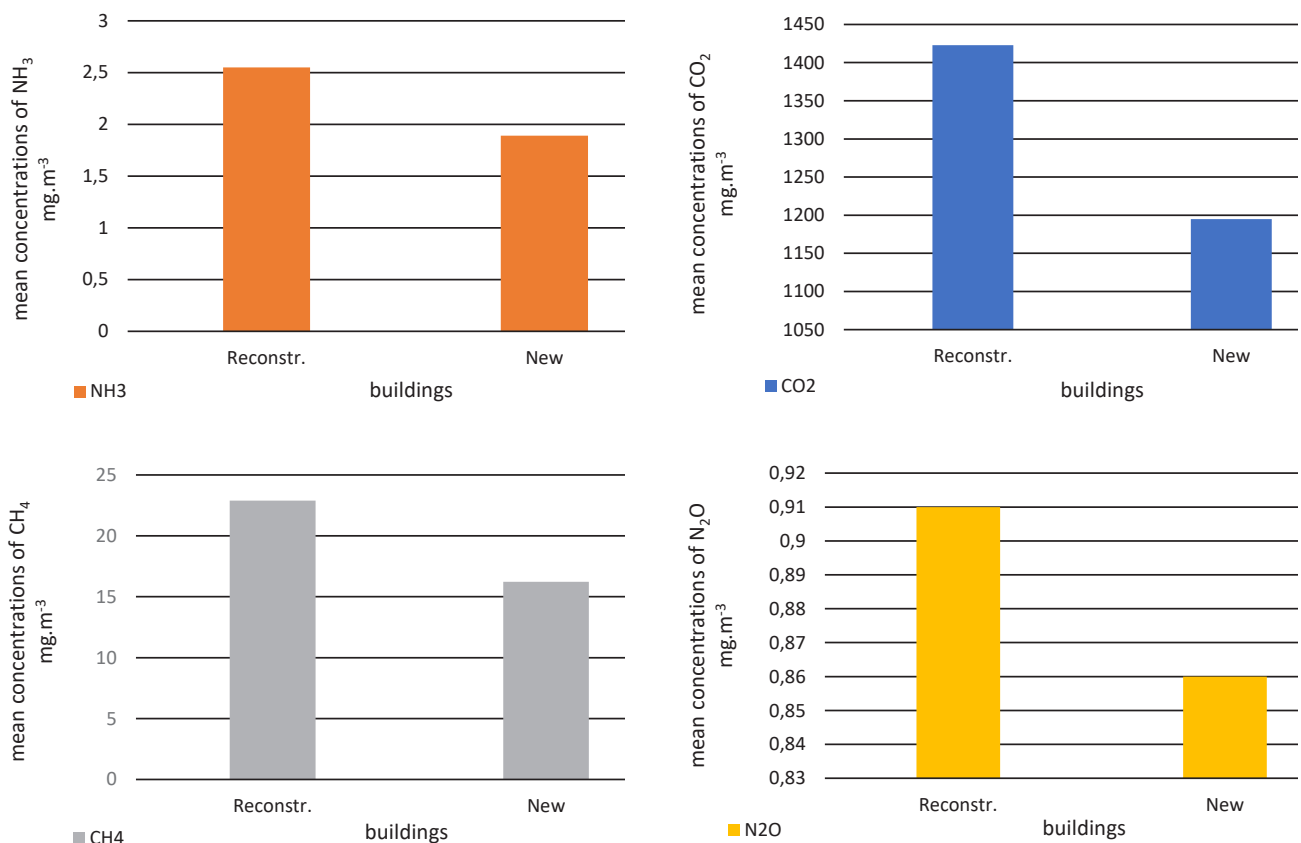


**Figure 3.** Results of mean concentrations of ammonia and greenhouse gases measured in reconstructed and new barn.

For working class “1b”, the optimum temperature is  $T_{op}=22-25^{\circ}\text{C}$ , permissible relative humidity  $RH=30-70\%$  and permissible air velocity  $v \leq 0.3 \text{ m}\cdot\text{s}^{-1}$ .

A new structural barn design and innovative housing technology have increased the comfort of the housed animals and the air quality in terms of ammonia production, greenhouse gases as well as microclimatic parameters which are also supported by the findings of other researchers (Witkowska, 2017; Dimov et al. (2019). The productivity of labour has also increased, the cubic volume of the environment has increased from the original  $V_B=34.3\text{m}^3$  to the new  $V_A=82.5 \text{ m}^3$  per cow.

The design of ventilation openings in buildings with natural ventilation is also an important element subject to beneficial innovative changes Li et al. (2020). In accordance with his testing, the design of the side walls of barn A of our experimental farm stands out, where the wall openings occupied the area ( $AR_w$ ), protected by a controllable roller shutter system,  $AR_w=882 \text{ m}^2$ .

The vertical openings between the roof slabs ( $AR_r$ ) with the area of the upper opening  $AR_{r,1}=280 \text{ m}^2$  and the lower vertical opening  $AR_{r,2}=127 \text{ m}^2$  effectively helped the flow regime. In total, there were  $2.7 \text{ m}^2$  of structural openings per animal in barn A which positively influenced lower concentrations of harmful gases.

## Conclusions

Large-cubature buildings prevent quick changes in the environment and large openings are a guarantee to the possibility of rapid air exchange. If the roof covering is thermally insulated and sufficiently protects the overheating of the structures, the larger air volumes around the animals, act as a buffering factor for the cleaning period of the buildings even in cases of midday solar radiation. More detailed research is needed to assess the overall decline in production parameters attributable to the occurrence of extreme summer heat situations at a particular farm location and the balance of benefits of using motor ventilation. ■

## Acknowledgement

The research presented in this scientific paper is supported by the Ministry of Education, Science, Research and Sport of the Slovak republic, by the project VEGA 1/0709/21: “Scientifically justified proposals for technological solutions of housing facilities ensuring optimal microclimatic conditions for livestock and their practical verification”.

## References

- [1] Armstrong, D. (1994). Heat stress interaction with shade and cooling. *J Dairy Sci* 77(7), 2044–2050.
- [2] Dimov, D., Marinov, I., Penev, T., Miteva, Ch. & Gergovska, Z. (2019). Animal hygienic assessment of air carbon dioxide concentration in semi-open freestall barns for dairy cows. *Bulgarian Journal of Agricultural Science*, 25(2), 354–362.
- [3] Fournel, S., Rousseau, A.N., Laberge, B. (2017). Rethinking environment control strategy of confined animal housing systems through precision livestock farming. In: *ö*, 155, 96–123.
- [4] Hempel, S., Menz, C., Pinto, S., Galan, E., Janke, D., Estelles, F., Müschner-Siemens, T., Wang, X., Heinicke, J., Zhang, G., Amon, B., del Prado, A., Amon, T. (2019). Heat stress risk in European dairy cattle husbandry under different climate change scenarios - uncertainties and potential impacts. *Earth Syst. Dynam. Discuss*, 1–38.
- [5] Herbut, P., Angrecka, S., Godyn, D., Hoffmann, G. (2019). The physiological and productivity effects of heat stress in cattle - a review. *Ann. Anim. Sci.* 19, 579–593.
- [6] Hoffmann, G., Herbut, P., Severino, P., Heinicke, J., Kuhla, B., Amon, T. (2019). Animal-related, non-invasive indicators for determining heat stress in dairy cows. *Biosystems Engineering*, 199, 83–96.
- [7] Kolacz, R., Dobrzanski, Z. (2019). Animal hygiene and welfare. Univerzity of Environmental and Life Sciences, Wroclaw, Poland, pp. 41, 78–79.
- [8] Maurer, D., Koziel, J.A., Harmon, J.D., Hoff, S.J., Rieck - Hinz, A.M., Andersen, D.S. (2016). Summary of performance data for technologies to control gaseous, odor, and particulate emissions from livestock operations: *Air Management Practices Assessment Tool (AMPAT)*.
- [9] Poteko, J., Zähler, M. & Schrade, S. (2019). Effects of housing system, floor type and temperature on ammonia and methane emissions from dairy farming: A meta-analysis. *Biosystems Engineering*, 182, 16–28.
- [10] Wang, X., Gao, H., Gebremedhin, K. G., Bjerg, B. S., Van OS, J., Tucker, C. B., Zhang, G. (2018). A predictive model of equivalent temperature index for dairy cattle (ETIC). *Journal of Thermal Biology*, 76, 165–170.
- [11] Witkowska, D. & Sowinska, J. (2017). Identification of microbial and gaseous contaminants in poultry farms and developing methods for contamination prevention at the source. *Poultry Science*, London: IntechOpen.

# Indoor Climate After Energy Renovation of Family house



**ANNA PREDAJNIANSKA**

Ing., Department of Building Services, Slovak University of Technology in Bratislava, Faculty of Civil Engineering, Bratislava, Slovakia  
[predajnianska.anna@gmail.com](mailto:predajnianska.anna@gmail.com)



**EVA ŠVARCOVÁ**

Ing., Department of Building Services, Slovak University of Technology in Bratislava, Faculty of Civil Engineering, Bratislava, Slovakia



**DUŠAN PETRÁŠ**

Prof. Ing., PhD, Department of Building Services, Slovak University of Technology in Bratislava, Faculty of Civil Engineering, Bratislava, Slovakia

The model renovation of typical family houses in Slovakia can help everyone who want to indulge in modern 21st century living with a healthy indoor environment even in an older house. This project is not only a source of inspiration. In addition to proven tips and practical advice from experts, it will also provide complete instructions for the reconstruction of a family home with an emphasis on healthy living.

**Keywords:** energy, renovation; family house; indoor climate, energy evaluation

The results of an international study entitled Healthy Home Barometer 2017 showed that every sixth Slovak is not satisfied with their housing. Slovaks are troubled by insufficient light conditions or excessive humidity causing mold. Up to 21% of Slovak households are not economically able to heat their house or apartment to a comfortable temperature. The speed of the renovation process in Slovakia is also insufficient. According to available statistics, there are more than 950 000 family houses in Slovakia, of which only 35% have been renovated. The renovation project of typical family houses has them ambition to change this unfavorable statistic. The model renovation for healthy living is intended to inspire Slovaks how they can renovate their house in a financially optimal way. At the end of the entire process, they will receive modern and healthy housing

that takes into account parameters in three fundamental categories – quality of housing, impact on the environment and operating costs.

## Family House Renovation

Family houses built between 1950s and 1970s had a typical square floor plan and material composition. At present, many of them are inhabited, but they do not meet today's strict thermal technical requirements. Exterior walls were built without thermal insulation. The interior and exterior finishing of the walls, ceilings, and floors are in unsatisfactory conditions. Single or double windows with simple glazing were used in these houses. The ceilings were made of wooden beams. In many cases, the roof system is degraded by time, especially due to weather conditions.

The project documentation of these house was drawn by hand, as no drawing software was used at that time (Predajnianska et al. 2021, 2022; Švarcová et al 2021). The original state of family house is showed in the **Figure 1**. Renovation of building structures is very important. However, it is not the only parameter that improves the energy efficiency of the building. A large share in the energy efficiency of building also plays building services. The new heat source in the renovated family house is a gas condensing boiler, which represents an excellent price-quality ratio. For domestic hot water preparation was used storage heat system with volume of 120 l. Heating in the building is provided by radiators. Renovated family house is showed in the **Figure 2**.

### Energy Evaluation

At the beginning of the project, several reconstruction variants were created for the family house. Each variant included different thicknesses of thermal insulation,



**Figure 1.** Original state of family house in Šaľa. [Authors]



**Figure 2.** Renovated family house in Šaľa. [Authors]

or different heat sources. A detailed description of the various renovations will not be given. However, an energy evaluation was created for the various renovations which is given in **Table 1** and **Figure 3**. The aim of the energy evaluation is to compare the energy needed for the family house in different variants and after the renovation. As a part of the energy evaluation, the building is classified into classes based on the energy need for heating, energy need for domestic hot water preparation, energy need for ventilation or forced air extraction, total needed energy, primary energy and emission CO<sub>2</sub>. The renovations were designed in such a way that it was possible to create a passive building that corresponds to class A1 in the classification system. The most demanding renovation was designed in such a way that it was possible to create a nearly zero energy building, which corresponds to class A0 in the classification system. The criteria to specific total energy use for different types and global indicator classification of buildings are defined in Regulation No. 364/2010 (Decree No. 625; Standard STN EN 15603/NA: 2012).

The results of the energy evaluation are summarized also in the following graph, in which it is possible to compare the individual energy needs within the various variants of the reconstruction of a family house. The graph clearly shows the huge difference between the energy required for a family house in its original state and the energy need for a family house after any proposed renovation.

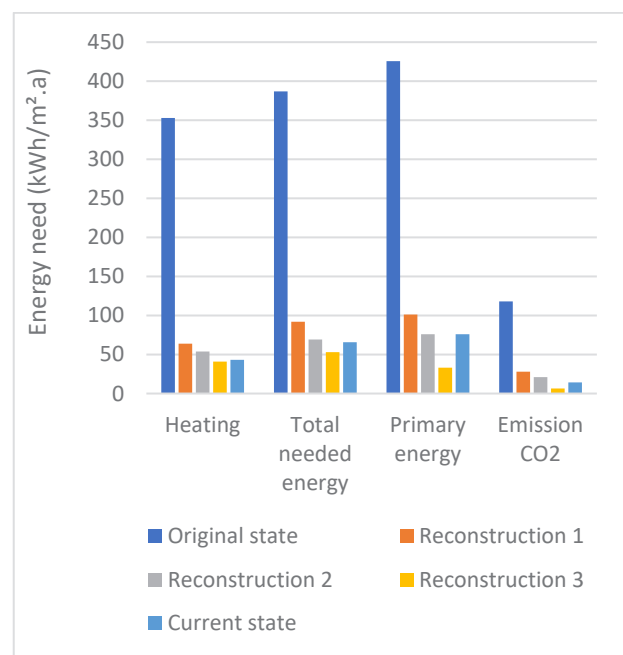


**Figure 3.** Energy needed based on energy evaluation. [Authors]

## Indoor Climate Measurements

The model renovation for healthy living is intended to inspire Slovaks how they can renovate their house in a financially optimal way. The main criteria of the renovation project is the house that provides comfortable and healthy living which is affordable and repeatable. At the end of the entire process of the reconstruction of the family house, there is an increase on the living space to 115 m<sup>2</sup>, an increase in energy savings of up to 80%, but above all a healthy living full of daylight and fresh air. Renovated family house has been occupied by a young family of four since September 2019. At the beginning of 2022, the stage of gathering

experience with operation, monitoring and measuring key parameters began. These current measurements are ensured by the Department of Building Services at the Slovak University of Technology in Bratislava. With the consent of the family, measuring devices are currently installed in the family house, which record the interior temperature, CO<sub>2</sub> concentration and air humidity in every room. The measuring devices placed in the family house are COMET U3430. The datalogger measures and records the values in its internal memory. **Figure 4** shows the floor plan of the first floor, where an entrance hall, a bathroom, a kitchen a living room and a children's playroom are located.



**Figure 4.** Measuring device's location in first floor. [Authors]

**Table 1.** Energy evaluation of different types of renovation. [Authors]

Variant	Energy need for heating	Energy need for DHW preparation	Energy need for ventilation	Total needed energy	Primary energy	Emission CO <sub>2</sub>
	kWh/(m <sup>2</sup> .a)	kWh/(m <sup>2</sup> .a)	kWh/(m <sup>2</sup> .a)	kWh/(m <sup>2</sup> .a)	kWh/(m <sup>2</sup> .a)	kg/(m <sup>2</sup> .a)
Original state	353,0	34,0	0	387,0	425,7	117,92
	G (>258)	C (25-36)	Not evaluated	G (>258)	D (325-432)	-
Renovation 1	63,9	28,1	0	92,0	101,2	28,03
	B (43-86)	C (25-36)	Not evaluated	B (55-110)	A1 (55-108)	-
Renovation 2	53,7	15,4	0	69,1	76,01	21,05
	B (43-86)	B (13-24)	Not evaluated	B (55-110)	A1 (55-108)	-
Renovation 3	40,8	12,2	0	53,0	33,17	6,37
	A (<42)	A (<13)	Not evaluated	A (<54)	A0 (<54)	-
Current state	40,5	11,4	0	51,9	29,29	18,36
	A (<42)	A (<12)	Not evaluated	A (<54)	A0 (<54)	-

In addition to the corridor, there is a datalogger in each room, which records the mentioned values. The ideal location of datalogger is in the middle of the room, but this is not possible in all cases. The location of the dataloggers is adapted to the location of the furniture in the interior. It was also more than necessary to take into account the fact that the house is inhabited by a young family with children and the dataloggers should not disturb the comfort of residents.

On the second floor there is a bathroom, parent's bedroom and children's room. In these rooms, the comfort of the residents and the placement of furniture in the rooms were also taken into account. The location of the dataloggers is shown in **Figure 5**.

## Results of Indoor Climate Measurements

The aim of the experimental measurements is to record the temperature, humidity and CO<sub>2</sub> concentration in the interior of a renovated family house and evaluate them. Measurement started in February 2022 and will run for two years. The values are recorded in the internal memory of the dataloggers COMET U3430. The recording interval is once per four hours. For the ongoing evaluation of the data, the measured quantities were taken from the memory of the dataloggers in the interval from February 2, 2022 to July 28, 2022. A two-week period from March 7, 2022 to March 21, 2022 was selected for the ongoing evaluation of the measured data. **Figure 6** shows the progress of air temperatures in each measured room. The indoor air

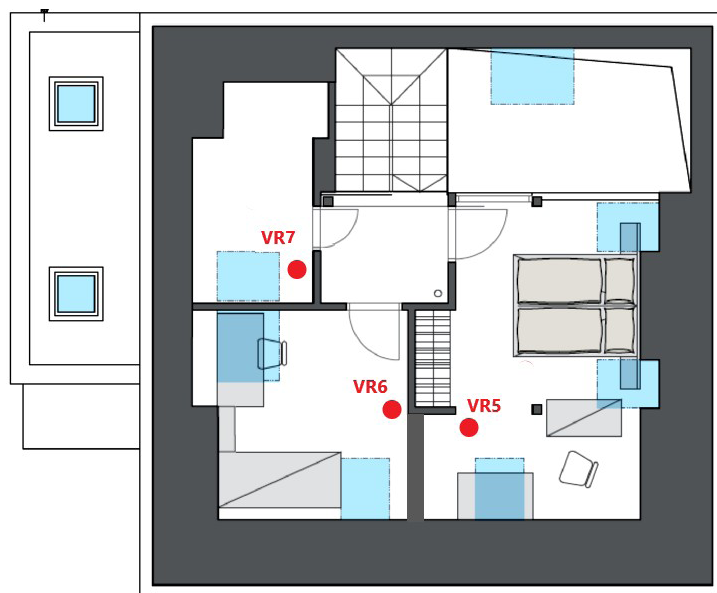


**Figure 5.** Measuring devices location in first floor. [Author]

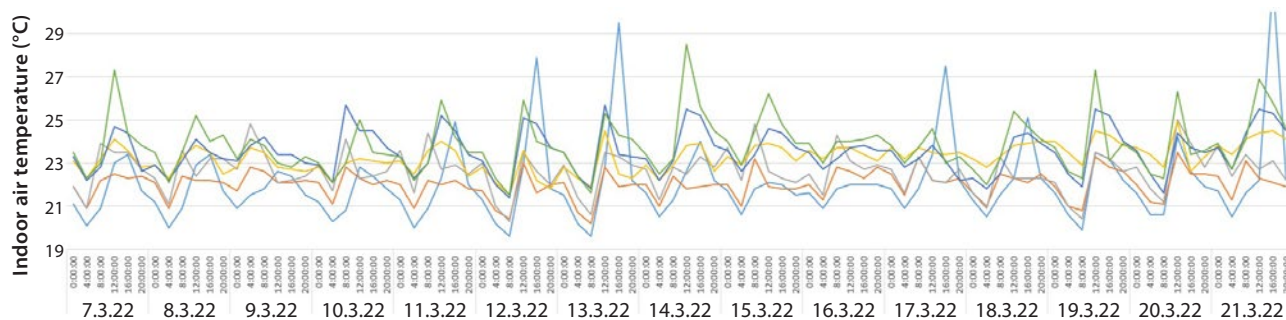


**Figure 6.** Indoor air temperature in each measured room. [Authors]

temperature ranged from 19 to 30°C. The drop in temperature to a lower value corresponds to the time when the room was naturally ventilated.

This corresponds also to the concentration of CO<sub>2</sub> at the given time, which is shown in **Figure 7**. It is clear that the object was regularly naturally ventilated, which corresponds to a regular decrease in CO<sub>2</sub> concentration. The last **Figure 8** shows the progress of air humidity in the interior of each measured room.

The following **Table 2** summarizes the minimum, average and maximum temperature, CO<sub>2</sub> concentration and air humidity in each room.

The datalogger VR2 in the children's playroom did not work after two days from the start of the measurement. Therefore, data on temperature, humidity and CO<sub>2</sub> concentration in this room are unknown. After talking with the owners of the family house, information was found that this room is used very rarely.

**Table 2.** Summary average temperature, CO<sub>2</sub> concentration and humidity [Author]

Room	Device	Temperature (°C)			CO <sub>2</sub> concentration (ppm)			Humidity (%)		
		Min	Avg.	Max	Min	Avg.	Max	Min	Avg.	Max
Kitchen	VR1	19,6	22,1	31,4	475	746	1113	12,8	34,8	46,8
Playroom	VR2	-	-	-	-	-	-	-	-	-
Livingroom	VR3	20,2	22,0	23,5	488	810	1399	26,8	34,8	43,9
Bathroom 1NP	VR4	20,3	22,6	25,0	494	706	1035	24,1	35,2	41,2
Bedroom	VR5	21,5	23,2	24,9	500	1141	1955	18,2	34,5	41,3
Children bedroom	VR6	21,4	23,5	25,7	445	869	1272	14,9	31,5	37,5
Bathroom 2NP	VR7	21,5	23,8	28,5	457	729	1162	20,3	31,5	43,8

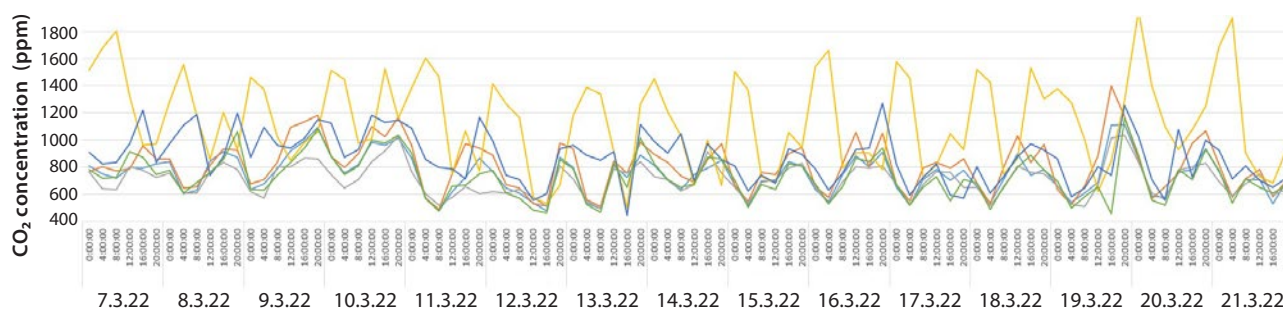


**Figure 7.** CO<sub>2</sub> concentration in each measured room. [Authors]

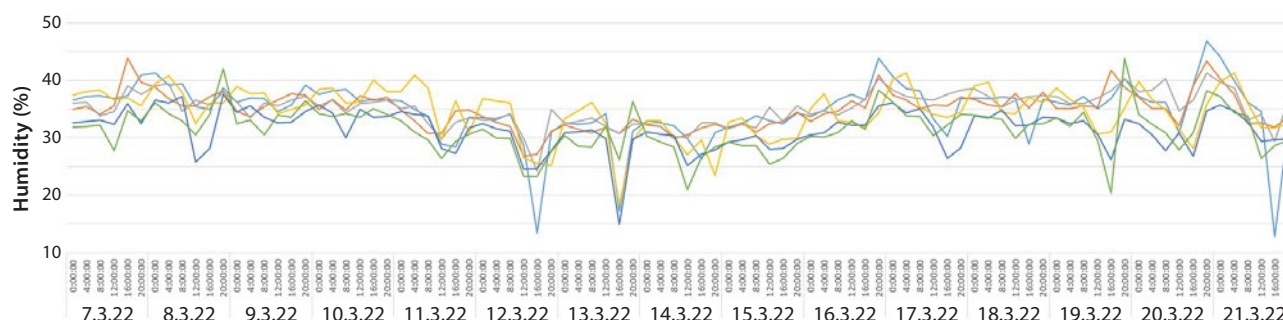


**Figure 8.** Humidity in each measured room. [Authors]

## Conclusion

The original family house was in a desolate state and uninhabited for many years. Therefore, in such a case like this one, it is not possible to speak about a satisfactory indoor climate. Renovation of a family house should ensure satisfactory conditions for living in terms of indoor climate. Not only the renovation of building structures and technical equipment, but also the operation of the building has a great impact on the comfort in the building. Therefore, it is more than important that even the owners of the family home care about its quality. This is mainly connected with the ventilation of the building. In cooperation with the Department of Building Services at Slovak University of Technology in Bratislava, measurements of the indoor climate of the building are carried out. The interim

results showed that thanks to the renovation of the building, the required indoor climate for the residents is ensured in terms of temperature, air humidity and CO<sub>2</sub> concentration.

You can find a square family house in almost every Slovak village. Most often in original condition. The owners are attracted by reconstruction, but they don't know where to start. The RenovActive model renovation will help everyone who wants to indulge in modern 21st century living with a healthy indoor environment even in an older house. Owners of typical square family houses, such as the one in Šaľa, can find the complete instruction on how to renovate the house and transform it into healthy and modern living. ■

## Acknowledgment

This work has been supported by the Ministry of Education, Science, Research and Sport of the Slovak Republic through the grant VEGA 1/0303/2021, VEGA 1/0304/2021 and KEGA č. 005STU-4/2021.

Thanks to the Velux company which established cooperation with the Department of Building Services at Slovak University of Technology in Bratislava and made it possible to be a part of the RenovActive project.

## References

Decree No. 625 of the Ministry of Construction and Regional Development of the Slovak Republic dated November 22, 2006, implementing the Law No. 555/2005 Coll. on the energy efficiency of buildings and on the amendment of some laws.

Standard STN EN 15603/NA: 2012 on Energy efficiency of Buildings. Total energy demand and definition of energy assessment. National Annex.

PREDAJNIANSKA, Anna - ŠVARCOVÁ, Eva - SÁNKA, Imrich - PETRÁŠ, Dušan. Nearly zero energy buildings as a standard of 21st century - Velux RenovActive. In CLIMA 2022 [elektronický zdroj]: proceedings of the 14th REHVA HVAC World Congress, 22-25 May 2022, Rotterdam. 1. vyd. Delft: TU Delft OPEN Publishing, 2022, online, s. 35-40. ISBN 978-94-6366-564-3. V databáze: DOI: 10.34641/mg.33.

PREDAJNIANSKA, Anna - PETRÁŠ, Dušan - KRAJČÍK, Michal - SÁNKA, Imrich. Energy Efficiency Trends for Houses in Slovakia. In AEE World Energy Conference and Expo 2021 [elektronický zdroj]. 1. vyd. New Orleans: [s.n.], 2021, USB klúč, s. 1706. ISBN 978-17-13838-65-4.

ŠVARCOVÁ, Eva - SÁNKA, Imrich - PREDAJNIANSKA, Anna - PETRÁŠ, Dušan. Renovation of a Family House with Achievement of a Nearly Zero Energy Building Requirement. In ISHVAC 2021 and 2021 KIAEBS Autumn Conference [elektronický zdroj]: Healthy, Smart and Interactive Built Environment. November 24 to 26, 2021, Virtual (Seoul, Korea). 1. vyd. Seoul: Korean Institute of Architectural Sustainable Environment and Building Systems.

# SMART Solutions for Energy Saving and Better Indoor Environment



**JIŘÍ HIRŠ**

Prof. Ing. PhD, Brno University of Technology, Czech Republic  
[hirs.j@vutbr.cz](mailto:hirs.j@vutbr.cz)



**ALI BADAI**

Ir., MSc., Kraaijvanger Architects, Rotterdam, The Netherlands

This article contains partial results of a case study in the urban area of Brno - Nový Lískovec in the Czech Republic and partial results of a dynamic analysis of energy use in a case study setting in the Netherlands. Future research tasks, municipal visions and goals are discussed in order to fulfil the vision of the SMART Region concept in these locations. The article contains a brief presentation of some outputs and application of experiences from the National Centre of Competence project focused on energy flows in buildings, regions and distribution networks with a focus on heat/cooling supply, efficient use of RES, improvement of environmental quality and user comfort.

**Keywords:** Smart region, Buildings Refurbishment, Energy simulation, Indoor climate, Monitoring, Web map application

In Project [1], solved out from 2014 to 2019 in the Czech Republic, a multidisciplinary and interdisciplinary system of cooperation between companies and research organizations for the development of energy-efficient and environmentally friendly technological systems, equipment, components, methods and strategies for buildings in smart regions was analysed.

The outputs of the project have led to the establishment of a basis for a resilient approach in the pilot sites to address the energy and environmental situation of a set of buildings and the surrounding area/environment. A typical site is the urban district of Nový Lískovec with a detailed design of prefabricated residential, educational, office and civil buildings as well as a central and decentralized heat supply system and the use of renewable energy. Energy management was introduced in this area in 2000 and is still in operation today. Another example of smart solutions for the region is the analysis of energy flows and indoor environment and the solution of sub-issues in the Spa Piešťany site,

which includes the efficient use of heat from the water of the healing springs and a study of natural lighting with a focus on the colours of interior wall surfaces and interior furnishings, leading to a reduction in energy consumption for lighting. A dynamic analysis of unused thermal energy sources in the region is a topic being worked on by a PhD student in the Netherlands. It deals with the usable energy flows between buildings that are in permanent cooling mode all year round (supermarkets, food warehouses, medicine stores) and other buildings that need heating in winter. The analysis also addresses the dynamics of the mismatch between energy supply and consumption (heat and cold) and the use of solar energy storage in the asphalt roads in the region.

The last sub-part of the smart region concept presented in this paper focuses on the possibility of using wind energy for power generation. It solves the CFD simulation of wind flow over the roofs of buildings. This issue has also been researched by a PhD student in recent years.

### SMART city district BRNO – NOVÝ LÍSKOVEC

The Brno - Nový Lískovec district is located in the South Moravian Region of the Czech Republic. Currently, the area of this locality is 1.66 km<sup>2</sup> with 11 500 inhabitants. At the end of the 1990s, the Brno - Nový Lískovec municipal district launched an ambitious plan to revitalize the prefabricated apartment buildings in its ownership. Since the late 1990s, the municipality has introduced a building energy management system in its own housing stock to obtain valuable data on the energy behaviour of the buildings. Now, 22 years of intensive long-term monitoring of building energy consumption (heating and DHW) has provided and continues to provide decision-makers with valuable data and information when implementing renovation strategies and concepts and helps to facilitate important decisions in the future. Since 2014, indoor climate and indoor air quality (IAQ) has been monitored in selected apartments and municipal offices. Selected indoor climate and IAQ parameters such as air temperature, relative humidity and carbon dioxide (CO<sub>2</sub>) concentration have been measured. A comparison of the energy performance of the pilot building type T06B before and after renovation is shown in **Figure 1**. The heating energy consumption in the selected years shows a significant decrease of 67% in 2004 and 78% in 2014 compared to the building energy consumption before retrofit. The energy consumption for hot water preparation shows only a gradual decrease in the selected measurement period.

The values of the heating system heat consumption obtained by implementing energy management with a weekly interval and related to the outdoor temperature plotted in the so-called E-T curve for the selected regenerated apartment building are shown in **Figure 2**. Research in this location in recent years has been focused on the use of IoT technologies for efficient energy use in controlling the operation of school buildings.

### SMART region SPA PIEŠŤANY

The world-famous Piešťany Spa is located in the western part of the Slovak Republic, in the Trnava region, in the valley of the lower reaches of the longest Slovak river Váh. It is located on a spa island of 60 hectares at an altitude of 162 m. The spa island is one of the largest and most exceptional spa complexes in Europe. Its reputation is mainly due to its unique natural springs with thermal mineral water, which springing from cracks in the tectonic plates at a depth of 60 to 200 meters underground. The water on the surface reaches a very high temperature of 67–69°C, so it is first cooled before being used in the spa. Thermal mineral water is unique for its high sulphur and hydrogen sulphide content. The natural healing water pumped from the boreholes is piped into a storage station. Part of the natural healing water from the springs flows directly into the distributor, from where it flows into the balneotherapy department, the other part flows into the graphite heat exchanger

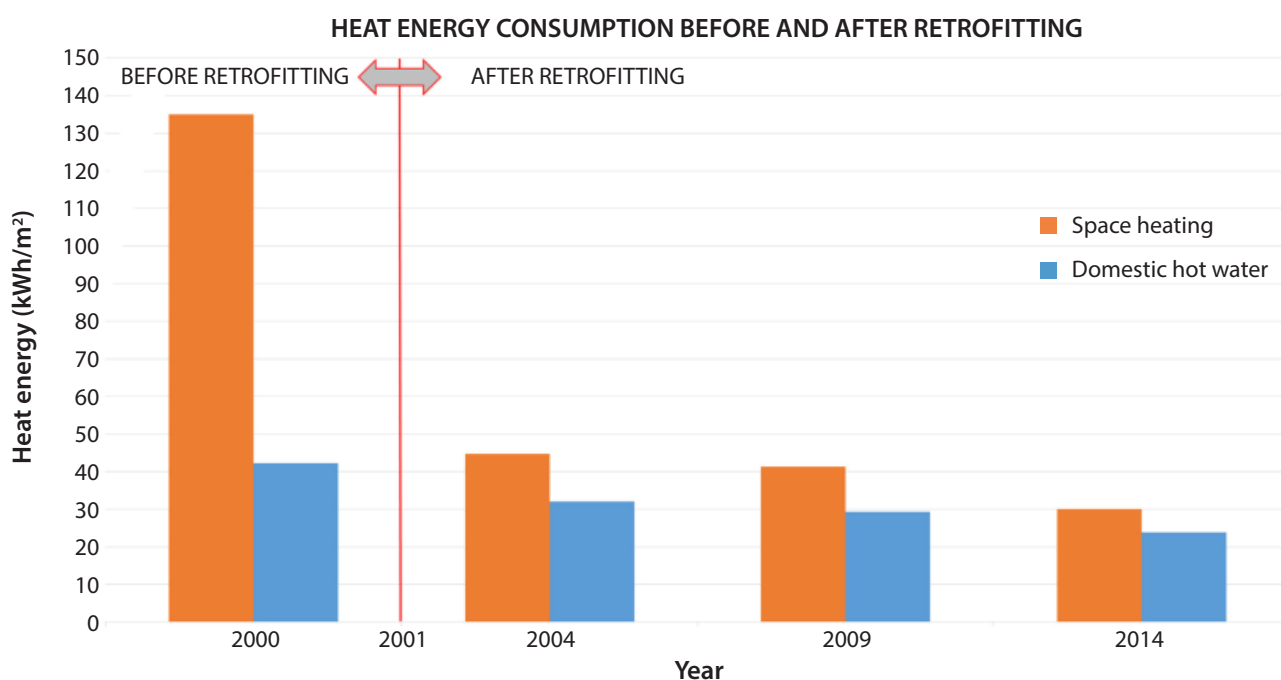


**Figure 1.** Comparison of the pre- and post-retrofitting results.

block, where it is cooled to a temperature of about 24°C and flows into the cooled water distributor, from where it flows into the balneotherapy department. The hot natural healing water distributor separates a partial quantity of this water into hot natural healing water storage tanks, where it is stored at a temperature of approximately 67°C and a pressure of 180 kPa. The cold natural medicinal water distributor separates a partial quantity of the cooled natural medicinal water into storage tanks of cooled natural medicinal water, where it is stored at a temperature of about 24°C and a pressure of 240 kPa. The pressure in the tanks is maintained by air compressors. In the event of greater water demand, this stored water can be used in the distribution system. The idea of implementing the SMART region principle in the Piešťany Spa was based on a detailed dynamic analysis of the temperature conditions of natural healing water in the distribution system and in the source wells with relation to the requirements of the healing processes and the management of the used healing water. The following measures have been developed and implemented: extension and improvement of the monitoring system of energy flows and water temperature parameters, systematic evaluation of information and data on the operation and use of natural medicinal water, efficient use of warm natural medicinal water in swimming pools, optimization of the technology of the accumulation station, dynamic analysis of the generation of natural medicinal water from the source and the requirements and utilization of natural healing water for therapeutic processes, design and implementation of a new heat exchanger for cooling of natural medicinal water based on experimental measurements and simulation model, and analysis of interior daylighting as a function of interior colour and with impact on electricity consumption for artificial lighting.

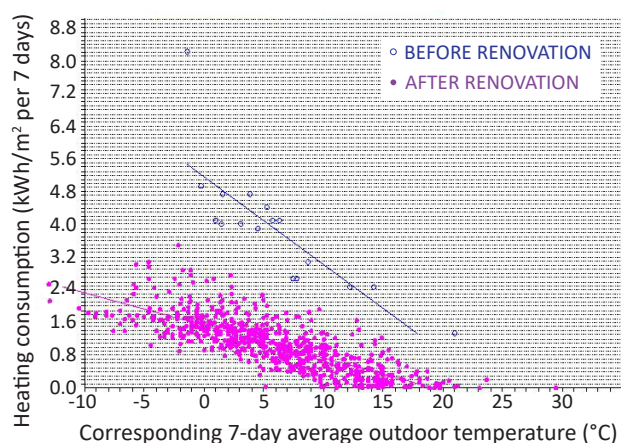


**Figure 2.** E-T curve for heating of prefabricated apartment building T06B (from 2000 year).

## SMART region in Netherland

A pilot analysis of energy flows was carried out on a case study in the Netherlands. In the selected location, the combination of energy systems in a supermarket, an adjacent asphalt road, single-family and apartment buildings and truck traffic to supply the supermarket was analysed. To reduce the carbon footprint from truck traffic, the location of the greenhouse adjacent to the supermarket was chosen. The location of the collector in the road was investigated in terms of solar energy use. For residential and single-family homes, the option of ground energy accumulation was investigated, and for the supermarket, the objective was to analyse mainly the residual heat from refrigeration. The role of the four partners in the thermal energy exchange network was defined from dynamic simulations and the evolution of the time dependence of the energy flows. The **Figure 4** show the cooperation schemes in energy use between the partners.

## WIND in SMART region

One of the scientific papers related to the SMART region concept deals with the use of wind flow over a building to provide information to determine the energy potential for a small wind power plant. A detailed 3D CFD simulation model including the surrounding terrain in two variants was used to analyse the wind flow over the roof of the FAST BUT science centre building. The variants differed in the use of boundary conditions for the building surroundings. The resulting findings, in particular the processed images of the wind flow fields, can be used to optimize the location of the wind turbine on the roof of the building and contribute to expanding the use of renewable energy potential in the region and in the building.

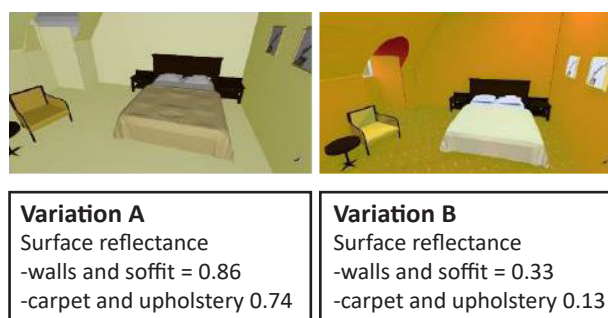


**Figure 3.** Room interior, in variation A and B (DIALux simulations).

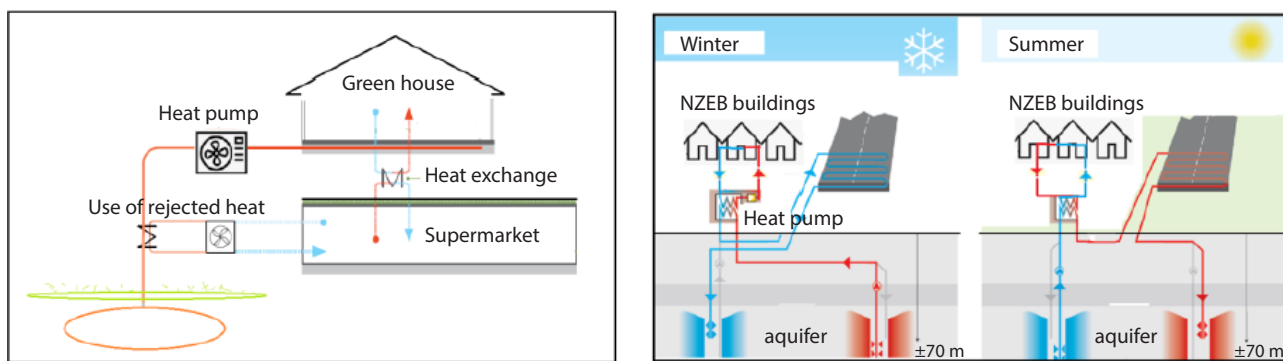


**Figure 4.** Collaboration between road and dwellings and between supermarket – greenhouse.

## Conclusion

Creating a model and implementing the vision of a SMART region is a long-term activity that, thanks to modern technologies, enables efficient operation not only of energy systems, but also the use of data and information for further decision-making processes. The concept of the SMART Region can be built gradually, by developing partial solutions that build on each other and are compatible with each other. In the paper some solutions in recent years in several

locations have been presented. The methodology and the form of the elaboration allows to repeat the application in other regions. ■

## Acknowledgment

This article has been worked out under the project Competence Centre TE02000077 supported by the Technological Agency of the Czech Republic.

## References

- [1] Project TE02000077, "Smart Regions - Buildings and Settlements Information Modelling, Technology and Infrastructure for Sustainable Development", (2014-2019), Technology Agency of the Czech Republic - Centre of Competence.
- [2] J. Hirš, S. Dermeková, R. Wawerka, T. Volařík, J. Mohelníková, "Information modelling process based on integrated data acquisition", *Energy and Buildings*, Volume 130, 2016, Pages 122-130, ISSN 0378-7788.
- [3] A. Badai, "Environmental benefits through Storage, Exchange of thermal energy in smart city", *Journal of Engineering*, 27(3), pp. 130–142, 2021, ISSN 1726-4073.
- [4] P. Komínek, J. Hirš, "The Use of a Mathematical Model for the Management and Distribution of Heat", *Applied Mechanics and Materials*, ISSN: 1662-7482, Vol. 824, p. 299-306, 2016, Trans Tech Publications, Switzerland.
- [5] D. Miček, J. Hirš, "Energy, economic and environmental analysis of opened natural healing water source". In *E3S Web of Conferences*. Francie: EDP Sciences, 2019. p. 1-8. ISSN: 2555-0403.
- [6] J. Hirš, J. Mohelníková, D. Miček, S. Floreková, "Daylighting Simulation Analysis for Historical Hotel Rooms. International Conference on Innovative Applied Energy/IAPE 2019, Oxford, United Kingdom, ISBN: 978-1-912532-05-6.
- [7] J. Hirš, Z. Auer, "E-T curves for energy management". In VIII. symposium GREEN WAY 2017. Společnost pro techniku prostředí (STP), Praha, 2017, p. 50-51. ISBN: 978-80-02-02731-7.
- [8] E. Tůmová, S. Pokorná, J. Hirš. "Wind flow CFD simulation over the building rooftop." *World Multidisciplinary Civil Engineering – Architecture - Urban Planning Symposium (WMCAUS) 2022*, Prague.

# Laboratory for testing of heating/cooling radiant systems



**MARTIN ŠIMKO**

Department of Building Services, Faculty of Civil Engineering, Slovak University of Technology, Bratislava, Slovakia  
[martin.simko@stuba.sk](mailto:martin.simko@stuba.sk)



**DUŠAN PETRÁŠ**

Department of Building Services, Faculty of Civil Engineering, Slovak University of Technology, Bratislava, Slovakia



**DANIEL SZABÓ**

Department of Building Construction, Faculty of Civil Engineering, Slovak University of Technology, Bratislava, Slovakia

The aim of this study is to describe the laboratory for testing of the floor, ceiling and wall radiant systems. The laboratory consists of three identical rooms located to the east, with a floor radiant system integrated in the first room, a ceiling radiant system in the second room and a wall mounted radiant system in the third room. The laboratory is part of an administrative building owned by the Faculty of Civil Engineering in Bratislava. The heat/cooling source is an air-to-water heat pump located on the roof of the building.

**Keywords:** laboratory, radiant floor system, radiant ceiling system, radiant wall system, heating/cooling

**W**e live in a time when climate change is increasingly forcing us to deal with the question of the right choice of heating or cooling system for living spaces. Due to global warming, we are experiencing milder winter seasons and then, without a pleasant transitional period of spring, we find ourselves in hot summer days. The question of how to cool residential buildings during hot summer days therefore comes to the fore.

There are different choices of heating or cooling systems. One option for both heating and cooling design is the use of water-based radiant systems.

Radiant systems are particularly suitable for combination with renewable sources, provide high sensible output and can be used for both heating and cooling [1,2,3].

Compared to other systems, large-area radiant systems provide a fundamentally more even distribution of temperatures indoors. In terms of design, radiant heating/cooling systems can be integrated into the wall, ceiling or floor. The common advantage of all three technical solutions is that they can be implemented as part of retrofitting, so they can be used in building renovation [4,5,6,7,8].

## Laboratory for testing heating/cooling systems

The laboratory consists of 3 office rooms of a north-east facing office building, with the same boundary conditions (**Figure 1**).

In the first office room number 202.1, a Siccus dry radiant floor system was installed in two circuits with 150 mm pipe spacing, using Comfort Pipe PLUS 14 × 2.0 mm, with a radiant area of 15 m<sup>2</sup>. In the second room number 202.2, a Uponor Renovis dry radiant ceiling system using Uponor PE-Xa pipe 9.9 × 1.1 mm with 8 Uponor Renovis panels (2000 × 625 mm) was installed with a radiant area of 10 m<sup>2</sup>. In the third office room number 203 a Uponor Renovis wall-mounted radiant system with Uponor PE-Xa 9.9 × 1.1 mm pipes with 8 Uponor Renovis panels (2000 × 625 mm) and a radiant area of 10 m<sup>2</sup> was installed. The heat and cooling source was an air-to-water heat pump F2040-6.

### Radiant floor system

In **Figure 2**, is shown the floorplan of the office room number 202.1, where the radiant floor system was investigated.

Numbers 2, 14, 15, 18, 19, 20, 47, 49, 50, 51, 52 in **Figure 2** represent the sensors type PT100 CRZ-2005-100-A-1-Ni and number 55 represents the heat flux sensor type FQA017CSI with accuracy within ±5% of the measured value. In the **Figure 2**, you can see also the installation of the Uponor Siccus dry floor system. The **Figure 2** shows the building of the

Uponor Siccus system board, the installation of the sensors, the installation of the Uponor comfort pipe plus 14 × 2,0 mm, the installation of the PE foil, the floor dry-screed board BRIO represented final layer of the radiant floor system and measured devices: globe thermometer, heat flux sensor, sensor of the surface temperature and data logger.

### Radiant ceiling system

In **Figure 3**, on the right side, you can see the office room number 202.2, where the radiant ceiling system was investigated and on the left side in **Figure 3** you can see the Uponor Renovis dry ceiling system. The placement of the sensors is shown on the right side in **Figure 3**. Numbers 3, 6, 7, 11, 12, 13, 41, 43, 44, 45, 46 represent the sensors type PT100 CRZ-2005-100-A-1-Ni and number 53 represents the heat flux sensor type FQA017C with accuracy within ±5% of the measured value.

In **Figure 3**, is shown the installation of Uponor Renovis radiant ceiling system.. The Uponor Renovis ceiling system is a dry ceiling system. The Uponor Renovis ceiling system consists from CD profiles for Uponor Renovis Panels with Uponor PE-Xa 9.9 × 1.1 mm pipes. We can also see the Tichelman loop with supply and return pipe for the Uponor Renovis Panels. In **Figure 3**, is shown the installation of the sensors (type PT100 CRZ-2005-100-A-1-Ni). In **Figure 3**, is shown the building of the final structure of the Uponor Renovis dry ceiling system. The Uponor



**Figure 1.** Office building with laboratory for testing radiant systems. (Author: Martin Šimko)

Renovis ceiling system is a dry ceiling system and this system consists from 8 Uponor Renovis panels (2000 × 625 mm). The radiant area of the ceiling

system is 10 m<sup>2</sup>. The **Figure 3** on the right shows the measurement equipment: globe thermometer, heat flux sensor, sensors of surface temperatures.

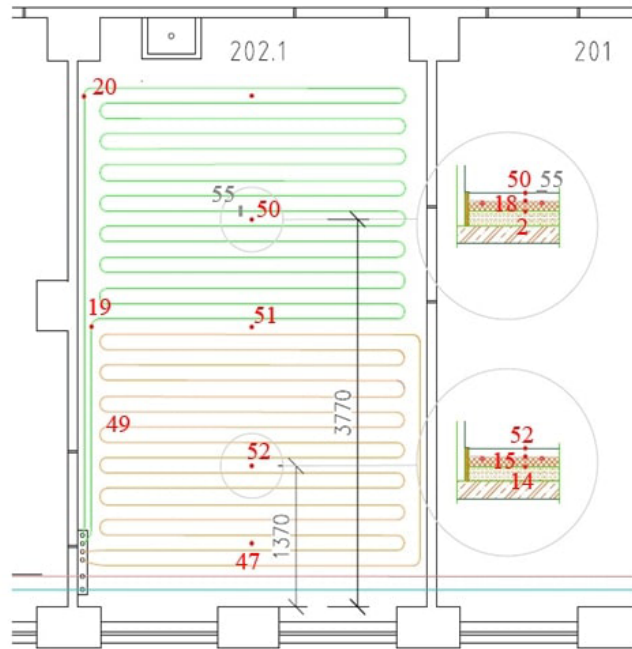


**Figure 2.** Floorplan of the room 202.1 with radiant floor system and placement of sensors. (Author: Martin Šimko, Uponor, s.r.o.)

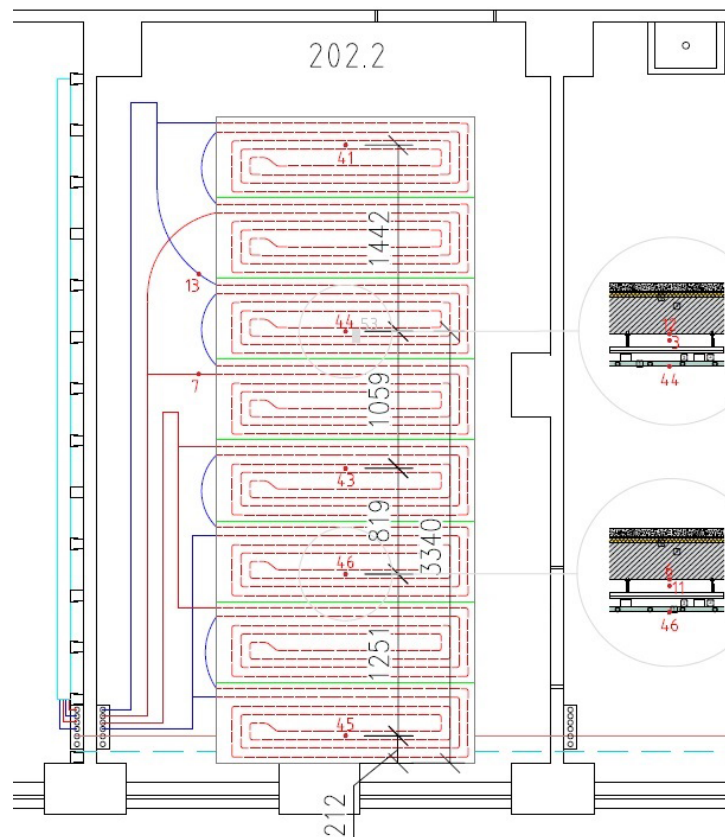


**Figure 3.** Floorplan of the room 202.2 with radiant ceiling system and placement of sensors (Author: Martin Šimko, Uponor, s.r.o.)

## Radiant wall system

In **Figure 4**, is shown the section through the office room number 203, where the radiant wall system was investigated. On the right side in **Figure 4** is shown the Uponor Renovis dry wall system. In **Figure 4**, is shown also placement of the sensors. Numbers 37, 38, 39, 40, 42 represent the sensors type PT100 CRZ-2005-100-A-1-Ni and number 54 represents the heat flux sensor type FQA017C with accuracy within  $\pm 5\%$  of the measured value. In **Figure 4**, is shown also the building of the Uponor Renovis wall system. The Uponor Renovis wall system is dry wall system and this system consist from 8 Uponor Renovis panels (2000 × 625 mm). The radiant area of the wall system is 10 m<sup>2</sup>. The **Figure 4** from the left shows the Tichelmann loop with supply and return pipe for the Uponor Renovis Panels. The final structure of the Uponor Renovis wall radiant system consists of CD profiles with Uponor Renovis Panels.

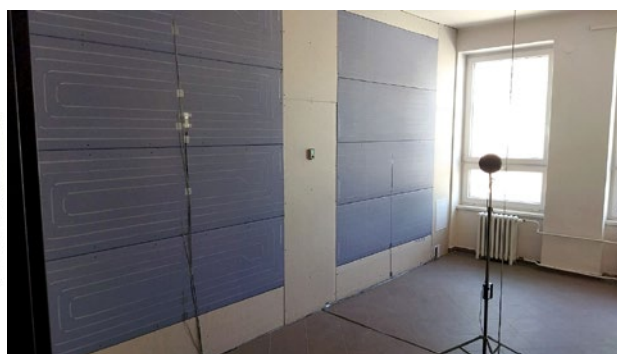
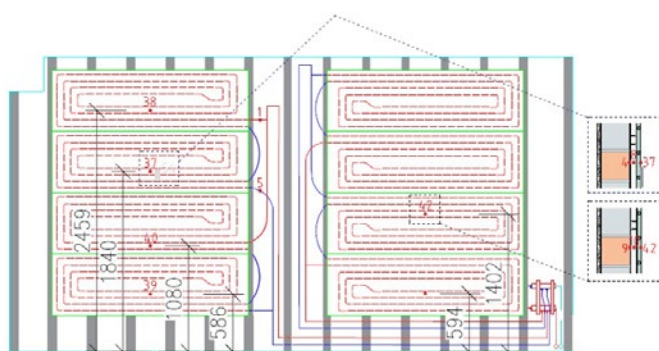


**Figure 4.** Radiant wall system and placement of sensors. (Author: Martin Šimko, Uponor, s.r.o.)

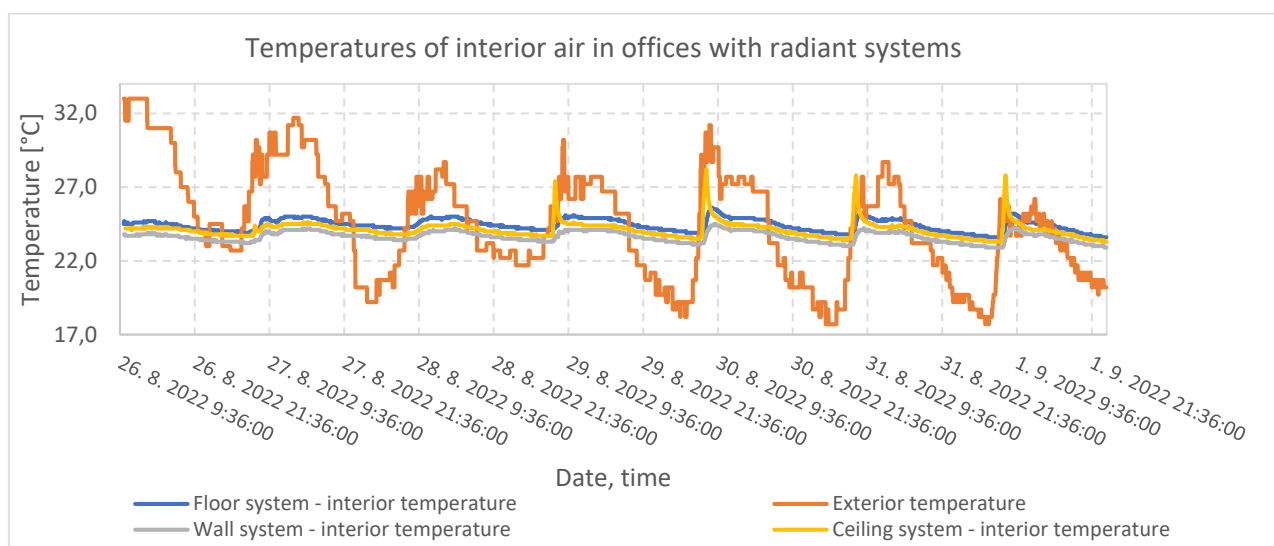


**Figure 5.** Relation between indoor and outdoor air temperature (Author: Martin Šimko)

In **Figure 4**, we can see the final structure of the Uponor Renovis dry wall system and measurement equipment: globe thermometer, heat flux sensor, sensors of surface temperatures and data loggers

## Experimental verification of radiant systems in cooling mode

From 26.08.2022 to 01.09.2022 three radiant systems in cooling mode were verified. We verified the effect of radiant systems on the indoor climate. We investigated radiant dry floor system in office room 201.1, radiant ceiling system in office room 202.2 and radian dry wall system in office room 203. The effect of three radiant systems on the interior air were investigated for one week from 26.08.2022 to 02.09.2022. The thermal gradient was 15/19°C.

**Figure 5** shows relation between indoor and outdoor air temperature in three office rooms with radiant

systems from 26.08.2022 to 02.09.2022. We verified effects of the three radiant systems on the indoor climate (interior air) in three offices. The measurements of interior air were recorded with data loggers COMET U3430 and COMET S3120. The red curve represents the course of the outdoor air temperature, the blue curve represents the course of the indoor air temperature in the room 201.1 with radiant floor system, the yellow curve represents the course of the indoor air temperature in room 202.2 with radiant ceiling system, and the gray curve represents the course of the indoor air temperature in room 203 with radiant wall system. The results of the indoor air were measured using data loggers Comet U3430 in office rooms 201.1, 202.2 and the results of the indoor air in office room 203 were measured using data loggers Comet S3120. The maximum value of the outdoor air was measured on 26.08.2022 at 13:00, at that time the temperature of indoor air in office room 201.1 with radiant floor system was 24.6°C, the temperature of indoor air in office room 202.2 with radiant ceiling system was 23.8°C and the temperature of indoor air in office room 203 with radiant wall system was 24.2°C.

The effect of the three radiant systems in cooling mode on the indoor climate of these offices in summer was sufficient. These results show that radiant systems can create a pleasant thermal comfort even in summer.

### Conclusion

The paper shows the laboratory for testing of radiant floor, ceiling and wall systems. We explored the effect of three radiant systems in cooling mode on the indoor climate in summer. There is a significant potential of these three radiant systems to create a pleasing thermal comfort in summer. In terms of thermal comfort in cooling mode, radiant floor system was weaker than radiant wall or radiant ceiling. In future research it would be good to verify these three radiant systems: in terms of performance in both cooling and heating mode, how much energy does each radiant system consume individually, the temperature profile of each office in both cooling and heating mode, the surface temperatures of the radiant systems and the effect of the shading elements on the cooling performance of the three systems. ■

### Acknowledgment

This research was supported by the Slovak Research and Development Agency under contract No. APVV-21-0144 and Ministry of Education, Science, Research, and Sport grants VEGA 1/0303/21 and 1/0304/21.

### References

- [1] J. Babiak, B.W. Olesen, D. Petráš. *Low temperature heating and high temperature cooling*. REHVA Guidebook No 7. 3rd revised ed. Brussels, Belgium: REHVA (2013).
- [2] M. Krajčík, M. Arıcı, O. Šikula, M. Šimko, Review of water-based wall systems: Heating, cooling, and thermal barriers, *Energy and Buildings*. vol. 253 (2021).
- [3] M. Krajčík, M. Šimko, O. Šikula, D. Szabó, D. Petráš, Thermal performance of a radiant wall heating and cooling system with pipes attached to thermally insulating bricks, *Energy and Buildings*. vol. 246 (2021).
- [4] U. Akbulut, O. Kincay, Z. Utlu. *Analysis of a wall cooling system using a heat pump*. *Renew Energ* **85** (2016).
- [5] D. Petráš, M. Krajčík, J. Bugáň, E. Ďurišová. *Indoor Environment and Energy Performance of Office Buildings Equipped with a Low Temperature Heating / High Temperature Cooling System*. *Adv Mater Res* **899** (2014).
- [6] X. Wu, L. Fang, B.W. Olesen, J. Zhao, F. Wang. *Comparison of indoor air distribution and thermal environment for different combinations of radiant heating systems with mechanical ventilation systems*. *Building Serv. Eng. Res. Technol.* **39** (2018).
- [7] Á. Lakatos. *Comprehensive thermal transmittance investigations carried out on opaque aerogel insulation blanket*. *Mater. Struct.* **50** (2017).
- [8] EN ISO 11855-2:2012. Building environment design - Design, dimensioning, installation and control of embedded radiant heating and cooling systems - Part 2: Determination of the design heating and cooling capacity.

# Comparison of Daylighting in Different Climatic Conditions



**IVETA SKOTNICOVÁ**

Assoc. Prof.  
iveta.skotnicova@vsb.cz



**VOJTĚCH KOLARČÍK**

Ph.D., Eng.



**ONDŘEJ FADRNÝ**

Eng.

This article compares daylighting in administrative building located in different climatic zones. Depending on the simultaneous identical changes in window geometry and wall reflectance, the changes of distribution and values of daylight factor were monitored and compared in each case of localization of the building.

**Keywords:** daylighting, daylight factor, administrative building, Czech Republic, Sweden, Greece

Daylight has been used as the main source of light in interiors for centuries and has always been an integral part of architecture since buildings have existed. Not only does it replace electric lighting during the day, reducing electricity consumption, but it also affects heating and cooling, making it an important parameter in energy efficient design. Research has shown that daylighting is of great benefit to the health and comfort of occupants [1]. Nowadays, in the context of a significant increase in energy prices, the contribution of daylight to the interior of buildings is becoming increasingly important. Many studies have shown that the right daylighting space can improve occupant productivity, reduce electricity consumption, and thus contribute to sustainable design. The dynamic nature of daylighting presents many challenges when considering the metrics that define good and efficient daylighting design [2,3]. In the following work, the evaluation of daylighting in different climatic conditions of the Czech Republic, Sweden and Greece is investigated. The research focuses on the calculation and evaluation of daylighting in a residence room (spaces that may be regularly occupied by people) in a multi-storey building located in Ostrava (Czech Republic), as well as in Stockholm (Sweden) and Athens (Greece). The choice of countries is characterized by different latitudes and thus different median diffuse horizontal skylight illuminance. A static simulation method in Building Design was used to determine the daylight illuminance in the room under evaluation.

## Considered input values

The considered input values, which were used for modelling in the Building Design simulation program, were taken from ČSN EN 17037 [4], Table A3. These are the median diffuse skylight horizontal illuminance, and the requirements for the value of the daylight factor in the residence room in each case.

## Data about the compared room

The assessment room is located in a multi-storey building. Residence room number 104 on the first floor of the building under evaluation was selected. The room is oriented southeast and located in the corner of the building. It is a children's playroom. The dimensions of the room are 4,000 × 5,000 mm and its clear height is 2,600 mm. A regular set of points with a spacing of 571 × 600 mm has been placed in the room, which is set back a minimum of 500 mm

**Table 1.** Considered input values and requirements of daylighting.

	Czech Rep.	Sweden	Greece
City	Ostrava	Stockholm	Athens
Latitude	50.10°	59.65°	37.90°
Median diffuse horizontal skylight illuminance	14,900 lx	12,100 lx	19,400 lx
D over 100 lx	0.7%	0.8%	0.5%
D over 300 lx	2.0%	2.5%	1.5%

from the walls of the room. The point array was placed at a height of 800 mm above the floor of the room under assessment. The simulation was carried out for 2 model situations in which simultaneous changes in window geometry and wall reflectance of the room took place. The changes were considered the same in all cases (Czech Republic, Greece, Sweden).

### Description of model situations

In the model situation No.1 the following windows dimensions were considered: width – 1,750 mm, height – 1,500 mm, sill height – 900 mm. Clear, double glazing with a transmission coefficient of 0.92 (for each glazing) was considered. Both windows in the room have identical dimensions and glazing properties. The simulation was performed with the considered reflectivity of the walls surrounding the room – 0.5. The floor reflectivity was chosen to be 0.3 and the ceiling reflectivity 0.7.

In the model situation No.2 the following windows dimensions were considered:

Window 1: width – 1,750 mm, height – 1,500 mm, sill height – 900 mm. Clear glazing with double glazing with a transmission coefficient of 0.92 (for each glazing) was considered.

Window No. 2: width – 2,500 mm, height – 1,500 mm, sill height – 900 mm. Clear, double glazing with a transmission coefficient of 0.92 was considered. The simulation was carried out with the considered reflectivity of the walls surrounding the room – 0.77. The floor reflectance was chosen to be 0.3 and the ceiling reflectance 0.7.

The ISO-line were then used to show the levels where the daylighting requirements of ČSN EN 17037 [4] are met. The isolines show the level at which the value of the daylight factor is constant.

### Simulations and results

#### Czech Republic

The minimum value of the daylight factor (0.7%) must be met on at least 95% of the room area according to the legislative requirement. The required value of the daylight factor (2.0%) shall be met by a minimum of 50% of the room area as required by legislation.

By simulation in the Building Design software and subsequent calculation for model situation 1 was found, that the minimum value of the daylight factor (0.7%) is met in 100% of the room area. The required daylight factor value (2.0%) is met for 54% of the room area. The boundary where the required value is met is shown in ISO-line green.

By simulation in Building Design and subsequent calculation for model situation 2 was found, that the minimum value of the daylight factor. (0.7%) is met in 100% of the room area. The required daylight factor value (2.0%) is met for 83% of the room area. The boundary where the required value is met is shown in ISO-line green.

#### Sweden

The minimum value of the daylight factor (0.8%) must be met in at least 95% of the room area according to the legislative requirement. The required value of the daylight factor (2.5%) shall be met by a minimum of 50% of the room area as required by legislation.

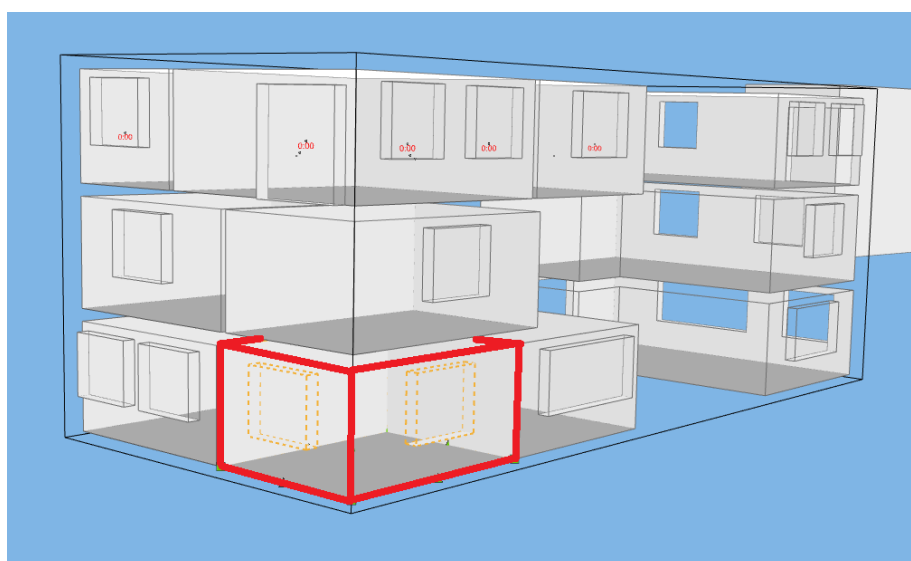


Figure 1. The location of the rated room in the building.

**Table 2.** Data considered for the calculation of daylighting in Czech Republic.

	Czech Rep.
City	Ostrava
Latitude	50.10°
Median diffuse horizontal skylight illuminance	14,900 lx
D over 100 lx	0.7%
D over 300 lx	2.0%

**Table 3.** Data considered for the calculation of daylighting in Sweden.

	Sweden
City	Stockholm
Latitude	59.65°
Median diffuse horizontal skylight illuminance	12,100 lx
D over 100 lx	0.8%
D over 300 lx	2.5%

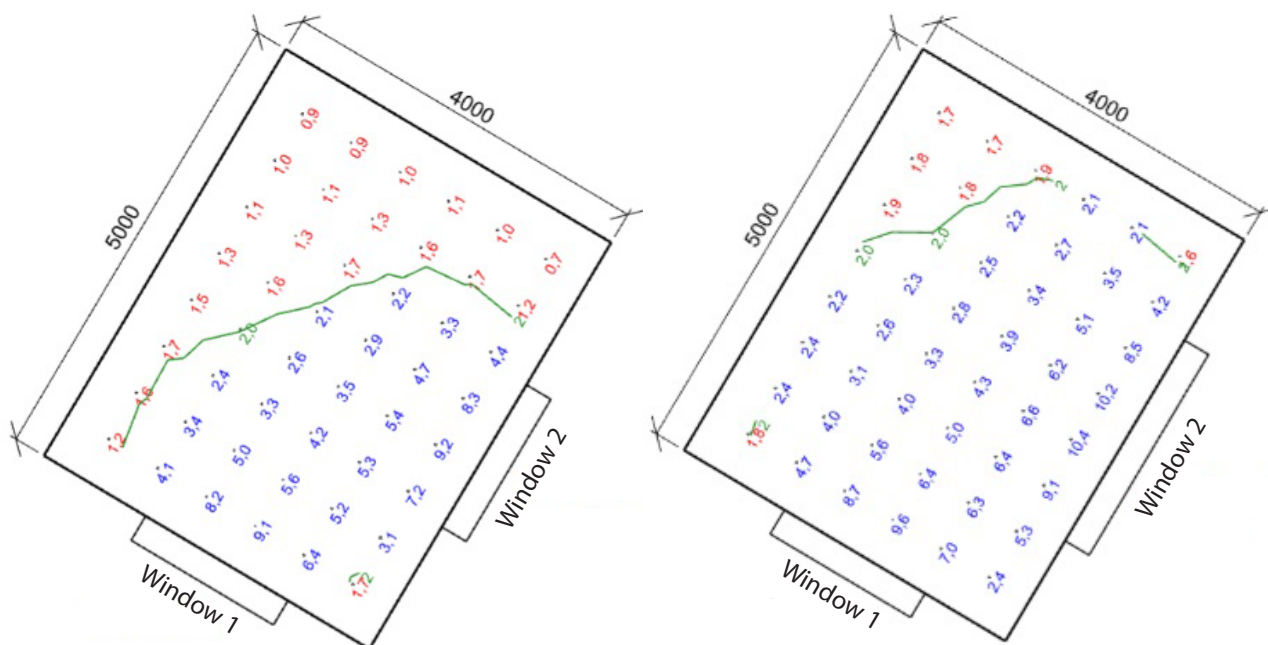


**Figure 2.** Distribution of the daylight factor in the treatment room for the first and second model situation in Czech Republic.

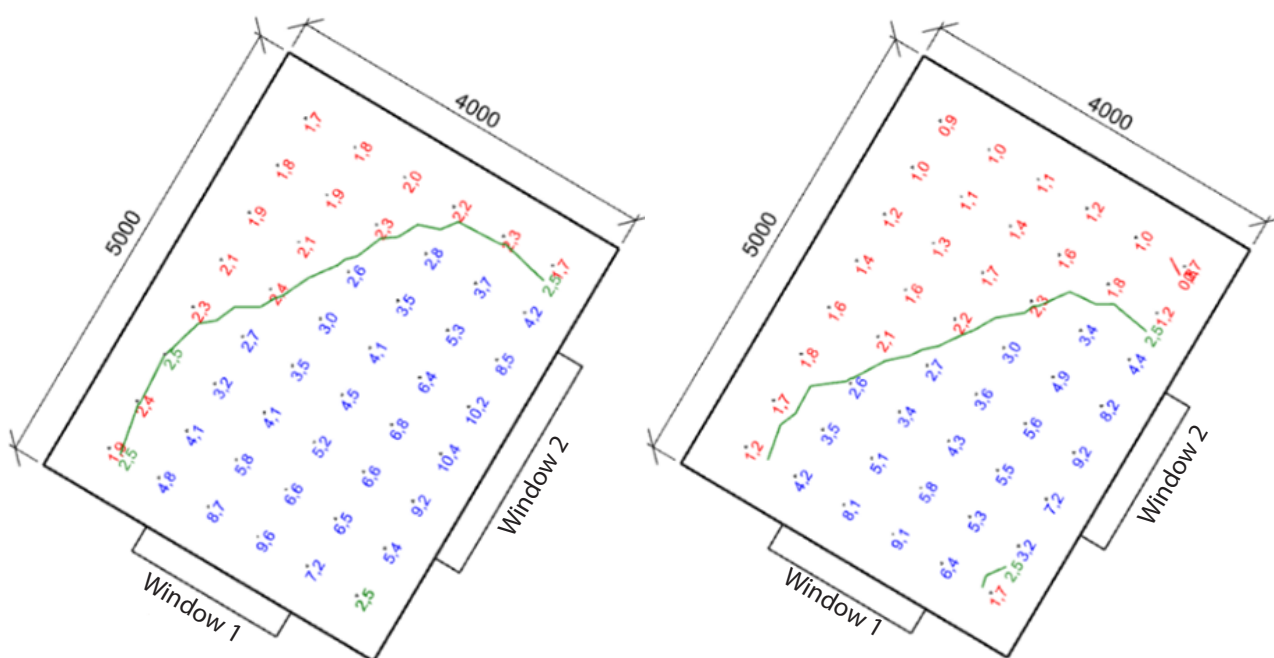


**Figure 3.** Distribution of the daylight factor in the treatment room for the first and second model situation in Sweden.

By simulation in the Building Design software and subsequent calculation for model situation 1 was found, that the minimum value of the daylight factor (0.8%) is met in 98% of the room area. The required value of the daylight factor (2.5%) is met in 48% of the room area. The boundary where the required value is met is shown in ISO-line green.

By simulation in Building Design and subsequent calculation for model situation 2 was found, that the minimum value of the daylight factor (0.8%) is met in 100% of the room area. The required value of the daylight factor (2.5%) is met on 67% of the room area. The boundary where the required value is met is shown in ISO-line green.

### Greece

The minimum value of the daylight factor (0.5%) must be met in at least 95% of the room area according to the legislative requirement. The required value of the

daylight factor (1.5%) shall, according to the legislative requirement, be met at least for 50% of the room area.

By simulation in the Building Design software and subsequent calculation for model situation 1 was found, that the minimum value of the daylight factor (0.5%) is met in 100% of the room area. The required value of the daylight factor (1.5%) is met in 71% of the room area. The boundary where the required value is met is shown in ISO-line green.

By simulation in Building Design and subsequent calculation for model situation 2 was found, that the minimum value of the daylight factor (0.5%) is met in 100% of the room area. The required value of the daylight factor (1.5%) is met for 100% of the room area. The boundary where the required value is met is shown in ISO-line green.

### Conclusion

Based on the modelling, simulation and subsequent calculation for each model situation, the following was evaluated: In the baseline model situation, the daylighting requirements were met in the case of the Czech Republic and in the case of Greece. In the case of Sweden, the minimum target daylight factor requirement was not met, which was only met for 48% of the assessment room area (the standard requirement is 50% of the assessment room area). The requirement for the target daylight factor was met. After the changes made to the window geometry and wall reflectance in the assessment room, the daylighting requirements

**Table 4.** Data considered for the calculation of daylighting in Greece.

	Greece
City	Athens
Latitude	37.90°
Median diffuse horizontal skylight illuminance	19,400 lx
D over 100 lx	0.5%
D over 300 lx	1.5%

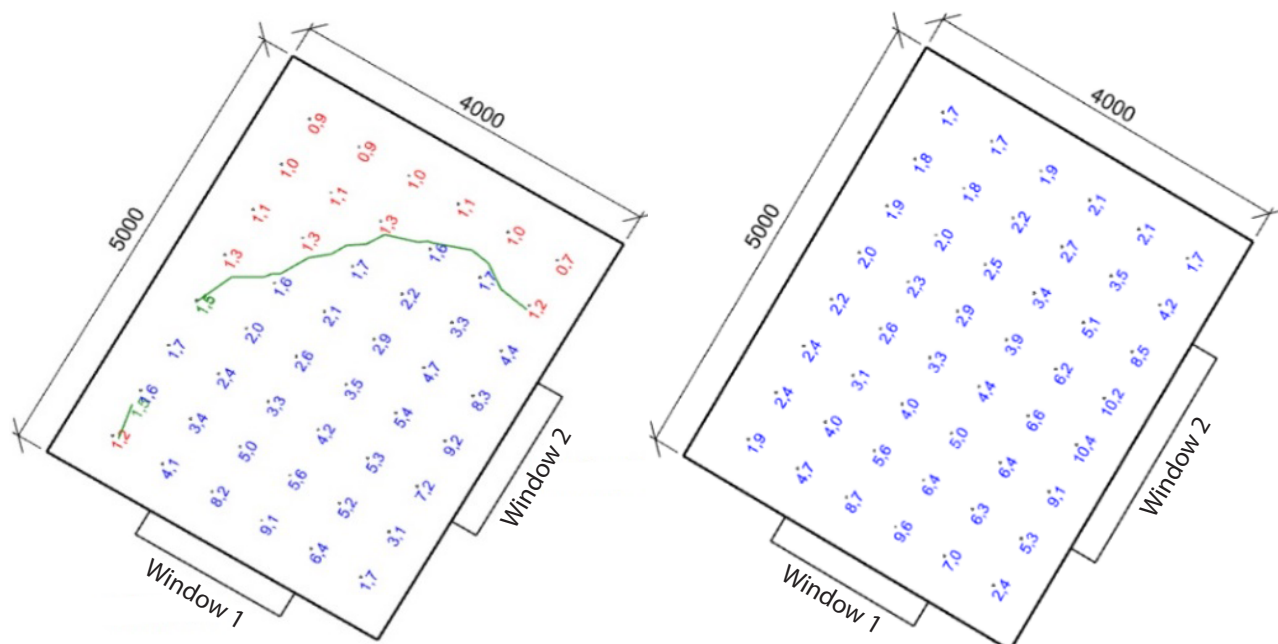


**Figure 4.** Distribution of the daylight factor in the treatment room for the first and second model situation in Greece.

have already been met, even for the building location in Sweden.

As can be seen from the simulations and calculations carried out, the change in window geometry and wall reflectance will be the most significant in terms of daylighting in the case of Greece. This is due to both the requirement for a target daylight factor of 1.5% (lowest) and the median horizontal sky illuminance, which is highest in Greece (19,400 lx). On the other hand, in the case of Sweden, the change in the geometry of the lining and the reflectivity of the walls

is the least affected, given that the median horizontal sky illuminance is the lowest in the case of Sweden (12,100 lx).

It has been found that in the case of the Swedish building location, larger window openings or higher wall reflectance than in Greece or the Czech Republic have to be considered in order to meet the daylighting requirements. This is due to the fact that the median horizontal sky illuminance decreases with increasing latitude, while at the same time the minimum and required daylight factor in the living room increases. ■

### Acknowledgment

Authors want to thank the Ministry of Education, Youth and Sports for financial support in the framework of the Student Research Grant Competition of the Technical University of Ostrava under identification number SP2022/128.

### References

- [1] NOVÁKOVÁ, Petra, VAJKAY, František. Factors influencing the value of daylight factor. In MATEC Web of Conferences. MATEC Web of Conferences. 10th International Scientific Conference Building Defects (Building Defects 2018). CEDEX A, France: E D P SCIENCES, 2019. ISSN: 2261-236X.
- [2] ABU-DAKKA, Moana Ghazi. The Use of Useful Daylight Illuminance (UDI) to Test New Designs for Improving Daylight Performance of Office Buildings in Dubai-UAE. Dubai, 2009. Master Thesis. Faculty of Engineering, The British University in Dubai. Prof. Bassam Abu-Hijleh.
- [3] BHAVANI, R. G. and KHAN, M. A., (2006) Present Trends and Future Direction of Lighting Control in Dubai. Middle East Economic Survey (MEES) 2007, vol. 50, no. 30, pp 23-24.
- [4] ČSN EN 17037+A1, Daylight in buildings (EN 17037:2018+A1:2021).

## REHVA EUROPEAN GUIDEBOOKS

### Energy Efficient Renovation of Existing Buildings for HVAC professionals

No.32

Energy Efficient Renovation of Existing Buildings for HVAC professionals.

This REHVA Guidebook shows the baseline for specific energy efficiency and other renovation measures in existing buildings for which the HVAC systems play an important role. It presents the best available techniques and solutions that can be used as part of the energy modernization of the HVAC systems.

REHVA  40 RUE WASHINGTON 1050 BRUSSELS, BELGIUM  
 +32-2-5141171  INFO@REHVA.EU  WWW.REHVA.EU



# Study of the Pressure Resistance of Odour Traps



**MARTIN SOKOL**

Department of Building Services,  
Faculty of Civil Engineering, Slovak  
University of Technology, Bratislava,  
Slovakia  
martin.sokol@stuba.sk



**JANA PERÁČKOVÁ**

Department of Building Services,  
Faculty of Civil Engineering, Slovak  
University of Technology, Bratislava,  
Slovakia

The paper deals with the study of the pressure resistance of odour traps, which are the only ones that protect the interior from the spread of unpleasant smells and viruses from the building's drainage system. The study was carried out on two reference types of odour traps based on earlier research and our simulation in Ansys.

**Keywords:** pressure fluctuations, drainage system, sanitary appliances, odour traps, viruses, smells

Odour traps are the only protection against the spread of unpleasant odors and viruses from the building's drainage system. The issue of pressure fluctuations in the foul water stacks and its effect on the water level in the odour traps is not new, but the pandemic situation associated with SARS-CoV-2 has brought it up to date once again. There has been a lot of research in recent years that confirms the presence of this virus in the building's sewer system. When the function of the odour traps is lost, this virus can get out and endanger the health

of the building occupants [1, 2]. Overpressure occurs most often over stack direction changes as a result of hydraulic jump, **Figure 1b**. At lower overpressure values, water bubbles in the traps, and at higher values, water is ejected or knocked out from sanitary appliances. Negative pressure occurs in the stack at the connection points of the branch pipes with the flow or below the change of direction of the stack where the air core of the stack closes, **Figure 1a, c**. When the negative pressure limits are exceeded, water is sucked out of the odour trap [3].

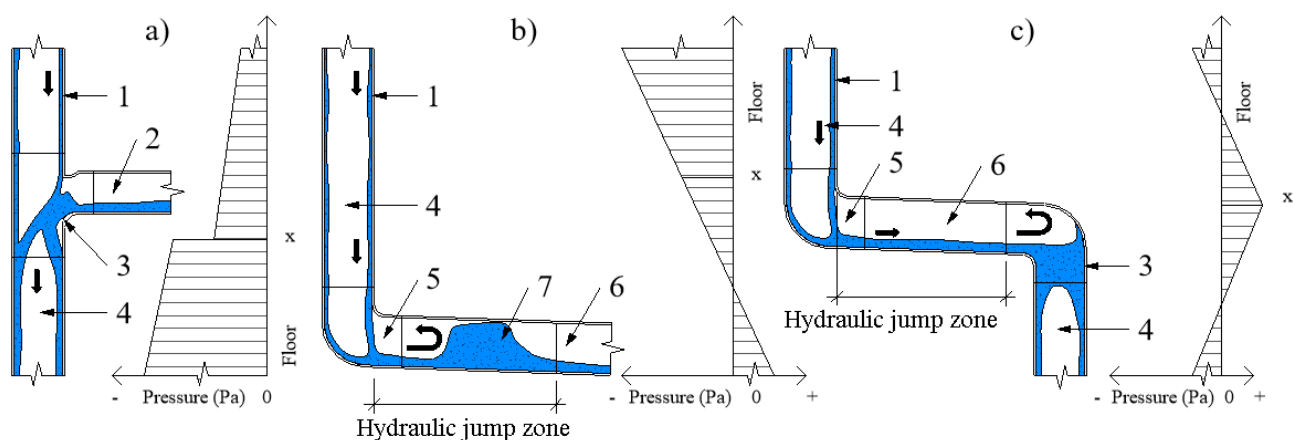


**Figure 1.** Water flow and pressure fluctuations in the waste pipe. a) at the point of connection of the branch pipe to the stack, b) at the point of transition of the stack to the drain, c) at the point of stack offset, 1 – annular flow, 2 – water flow from the branch pipe, 3 – piston effect, 4 – air core, 5 - water impact on the wall of the arc, 6 – steady state flow regime, 7 – hydraulic jump.

## Pressure resistance of odour traps

According to EN 12056 [6] and Slovak national standard STN 73 6760 [7], the minimum water level in the trap at the connection to a foul water pipe is  $h_{tot} = 50$  mm, and at the connection to the rainwater pipe, it is  $h_{tot} = 80$  mm. The pressure resistance of odour traps at different water level heights is shown graphically in **Figure 2**. The pressure resistances were calculated based on formulas that were developed in the 1980s and are still in use today [4]. However, these formulas have one major drawback in that they do not take into account the shape of the odour traps, which has a major impact on its pressure resistance. Currently, there are a large number of 50 mm odour

traps on the market that have a pressure resistance of around 400 Pa or quite a bit higher, which does not correspond to these calculations. This information is also not found in the manufacturers' datasheets, which would greatly reduce the error rate of the designs.

## Mathematical simulation of the pressure resistance of an odour trap

Our simulation observed the effect of pressure fluctuations in a stack on the water level in the trap. Two reference traps, which are most commonly used for sinks or basins and toilets, were used, **Figure 3a, b**. Pressure ranging from  $-550$  Pa to  $+1500$  Pa was

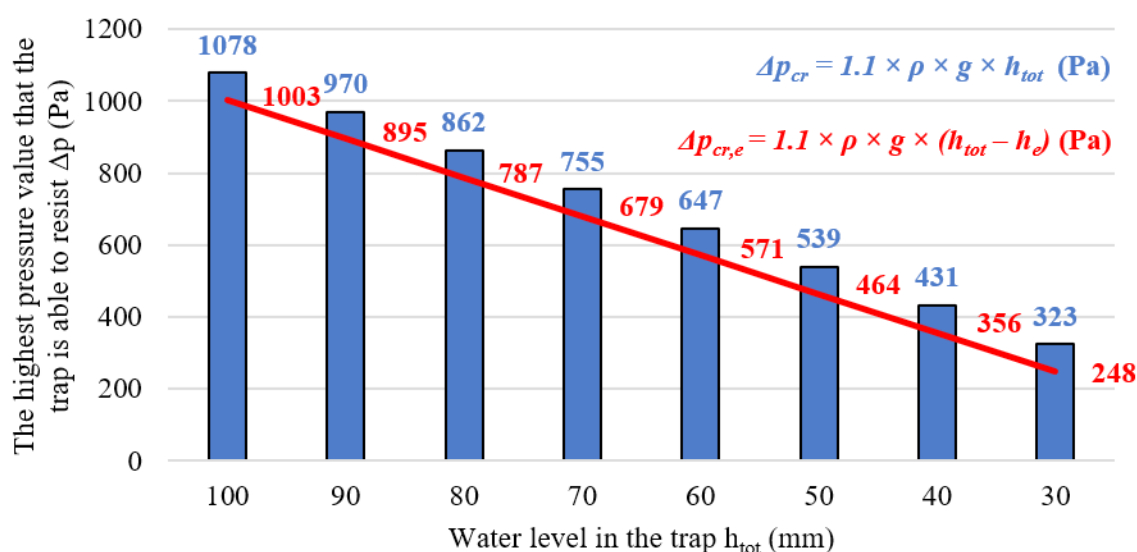


**Figure 2.** Resistance of the trap to pressure according to the water level. ■ without taking into account evaporation according to Formula (1), ■ taking into account the evaporation after 14 days of not using the sanitary appliance (evaporation 0,5 mm/day),  $\Delta p_{cr}$  – the maximum pressure that the trap can resist (Pa),  $\rho$  – water density ( $\text{kg}/\text{m}^3$ ),  $g$  – gravitational acceleration ( $\text{m}/\text{s}^2$ ),  $h_{tot}$  – the height of water in the trap (m),  $h_e$  – decrease of water in the trap due to evaporation (m).

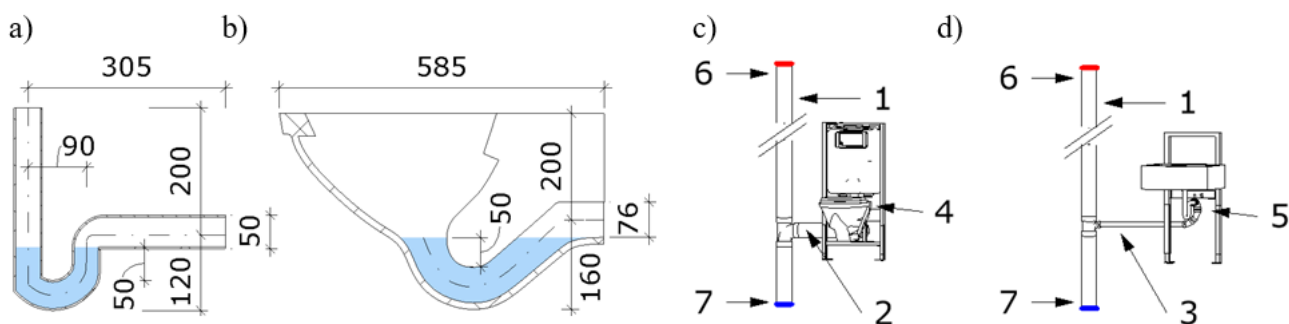


**Figure 3.** Traps used for simulation. a) trap for sink or basin with 50 mm height of the water, b) trap for WC with 50 mm height of the water, c) WC connection to the stack, d) connection of the sink or basin to the stack, 1 – DN 100 stack, 2 – DN 100 branch pipes with a length of 1 m, 3 – DN 50 branch pipes with a length of 1 m, 4 – the trap for WC with a water seal height of 50 mm, 5 – the trap for the sink or basin with a water seal height of 50 mm, 6 – pressure outlet (atmosphere), 7 – pressure inlet ( $-550$  to  $+1500$  Pa).

simulated in the stack. The range of values was chosen based on various experimental measurements outside of Slovakia, where similar ranges of pressures were measured [4, 5]. The boundary conditions of the simulation are shown in **Figure 3c, d**. The following inputs and settings were used for the simulation:

- the trap contained water with a density of  $999.1 \text{ kg/m}^3$ ,
- air with a density of  $1.225 \text{ kg/m}^3$  was present in the stack and branch pipe,
- pressure values ranging from  $-550 \text{ Pa}$  to  $+1500 \text{ Pa}$  were generated in the stack [4, 5],
- calculations were performed with 1000 time steps, a time step length of  $0.005 \text{ s}$ , and a number of iterations per time step of 40.

The following water level conditions were monitored in the trap:

- water level fluctuations due to overpressure or negative pressure (without compromising the functioning),
- the suction of part of the water due to negative pressure (without compromising the function/ with compromising the functioning),
- complete suctioning of the water due to negative pressure (loss of function),

- water bubbling due to overpressure (loss of function),
- ejection of water due to overpressure (loss of function).

### Effect of negative pressure on the water level in the trap

The traps from **Figures 3a, c**, were tested for negative pressures ranging from 0 to  $550 \text{ Pa}$ . The above-mentioned water level conditions were observed in the trap. The toilet trap, which could withstand a negative pressure of  $p_n = 525 \text{ Pa}$  without any loss of function, achieved the best results in this test. The trap for the basin or sink withstood a negative pressure of  $p_n = 475 \text{ Pa}$ . The detailed simulation results are shown in **Table 1** and **Table 2**.

From the point of view of safety, the lowest risk of sucking water out of the water seal is the negative pressure  $p_n \leq 300 \text{ Pa}$ . At these values, the water drop in the trap is minimal, **Figure 4a**. The safest design method is to assess the stacks for a negative pressure  $p_n \leq 300 \text{ Pa}$ . There was more water suction from the trap and a negative pressure from 300 to  $450 \text{ Pa}$ , but the functioning of the trap was not compromised. The maximum recorded water drop in the trap was  $25 \text{ mm}$ , **Figure 4b**. Considering issues of safety and

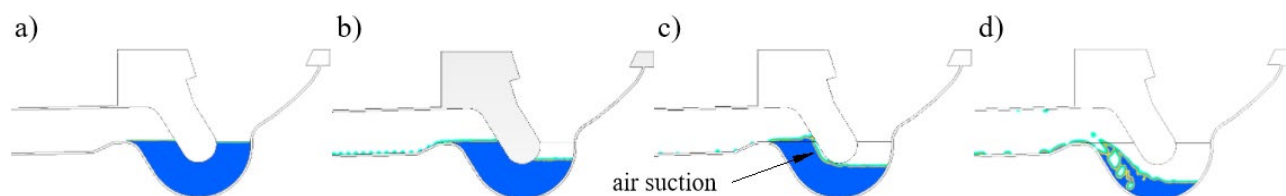


**Figure 4.** Effect of negative pressure on the water level in the trap. a) no impact on the water level, b) water level losses (without compromising its functioning) c) water level losses with air intake from the interior (compromising its function) d) complete suction of water from the odour trap (loss of functioning).

**Table 1.** Effect of negative pressure on the water level in the sink trap.

Negative pressure $p_n$ (Pa)	Effect on the water level
$\leq 300$	without compromising its functioning, drop in water minimal
300 to 450	without compromising its functioning, drop in water up to $25 \text{ mm}$
450 to 475	compromising its function, drop in water up to $30 \text{ mm}$ , suctioning of air from the interior
$> 475$	loss of functioning, complete suction of water from the trap

**Table 2.** Effect of negative pressure on the water level in the WC trap.

Negative pressure $p_n$ (Pa)	Effect on the water level
$\leq 300$	without compromising its functioning, drop in water minimal
300 to 450	without compromising its functioning, drop in water up to $25 \text{ mm}$
450 to 525	compromising its function, drop in water up to $35 \text{ mm}$ , suctioning of air from the interior
$> 525$	loss of functioning, complete suction of water from the trap

costs, assessing stacks to a negative pressure  $p_n \leq 450$  Pa is an economical solution and is still relatively safe.

### Effect of overpressure on the water level in the trap

The traps from **Figures 3a, c**, were tested for overpressures ranging from 0 to 1500 Pa. The high overpressure range was chosen based on experimental measurements from outside of Slovakia when the overpressure of 1500 Pa was measured. The overpressure was measured at the incorrectly chosen technical solution of the stack offset in a 9 – story building [5]. The above-mentioned water level conditions were observed in the trap. The best results in this test were achieved by the toilet trap that could withstand an overpressure  $p_o = 875$  Pa without any loss of functioning. The trap for the basin and sink withstood an overpressure  $p_o = 725$  Pa. The detailed simulation results are shown in **Table 3** and **Table 4**.

From a safety point of view, an overpressure of  $p_o \leq 725$  Pa (sink, basin) and  $p_o \leq 875$  Pa (WC) runs the lowest risk of the water bubbling or the ejection of water from the sanitary appliance. At these values, the water level in the trap only fluctuates, without any undesirable processes occurring, **Figure 5b**.

The problems with the high overpressure values cannot be solved by the correct design of the stack's dimensions. An incorrectly resolved change in the direction of the stack can cause overpressure above 1000 Pa even in low buildings (10 floors). Nowadays, there are various accessories for stacks, including positive pressure attenuators, which can sufficiently eliminate such high values.

### Summary of results

Based on the simulation of the effect of pressure on the water in a trap, it can be stated:

- the safest solution is to assess the stacks for a negative pressure of  $p_n \leq 300$  Pa, which has a minimal effect on the water level in the trap,
- after taking into account the costs and safety, it is acceptable to design stacks for
- a negative pressure of  $p_n \leq 450$  Pa when there is a drop in the water in the trap, which does not endanger its functioning,
- at a negative pressure of  $p_n > 450$  Pa, the functioning of traps is compromised due to the suctioning of air from the interior; and when  $p_n > 475$  Pa, the functioning of the trap ceases due to the suctioning of the water seal,

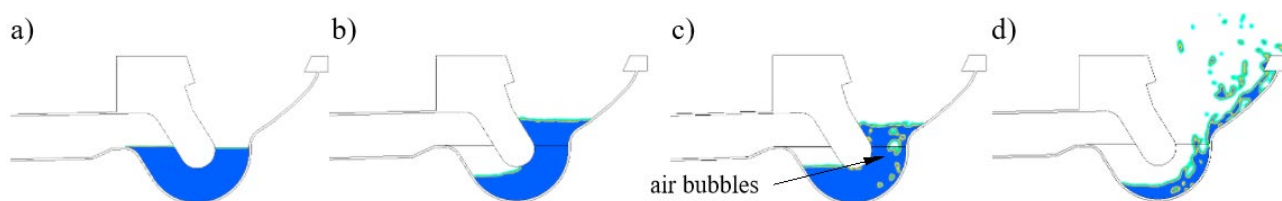


**Figure 5.** Effect of overpressure on the water level in the trap. a) no impact on the water level, b) water level fluctuations (without compromising its functioning), c) water bubbling (loss of function), d) complete ejection of water (loss of function).

**Table 3.** Effect of overpressure on the water level in the sink or basin trap.

Overpressure $p_o$ (Pa)	Effect on the water level
$\leq 725$	without compromising functioning, water level fluctuations
725 to 1025	loss of function, water bubbling
$> 1025$	loss of function, complete ejection of water

**Table 4.** Effect of overpressure on the water level in the WC trap.

Overpressure $p_o$ (Pa)	Effect on the water level
$\leq 875$	without compromising functioning, water level fluctuations
875 to 1025	loss of function, water bubbling
$> 1025$	loss of function, complete ejection of water

- when the overpressure of  $p_o > 725$  Pa, water bubbles in traps, which leads to the spread of annoying smells in the building,
- when the overpressure of  $p_o > 1025$  Pa, the water is ejected from sanitary appliances,
- the shape of a trap affects its pressure resistance.

All results will be verified by experimental measurement in the future.

## Conclusion

The proper design of foul water stacks is crucial, particularly in high-rise buildings. To avoid undesirable effects that may arise when water is sucked or ejected from the traps, it is necessary to assess them

for the correct limit values. The most important part of assessing stacks is assessing the maximum negative pressure because the overpressure can only be influenced by the correct design of the stack offset. Consideration must be given to direct vent stacks, which may exceed the maximum negative pressure if adequately designed according to the standards. The assessment of the stacks at a negative pressure of  $p_n \leq 450$  Pa represents a safe and cost-effective route based on the simulation and the assumption of a 50 mm high water seal. However, this value should be very well considered in spite of these results, and any odour traps that are planned to be used on the stack should be analysed. It would be a great help if manufacturers would just add this information to their datasheets, as this information must be available to them before they can be placed on the market. ■

## Acknowledgments

This work was supported by the Ministry of Education, Science, Research, and Sports of the Slovak Republic through the Scientific Grant Agency VEGA 1/0303/21 and KEGA 005STU-4/2021.

## References

- [1] GORMLEY, M., ASPRAY, T., KELLY, D. Building Drainage System Design for Tall Buildings: Current Limitations and Public Health Implications. In: Buildings. 2020, 11 (2). Available at [https://doi.org/10.1016/S2214-109X\(20\)30112-1](https://doi.org/10.1016/S2214-109X(20)30112-1).
- [2] HUNG, H. C., CHAN D. W., LAW, L. K., CHAN, E. H., WONG, E. S. Industrial Experience and Research into the Causes of SARS Virus Transmission in a High-Rise Residential Housing Estate in Hong Kong. In: Building Serv. Eng. Res. Tech. 2006, 27(2), s. 91–102. Available at: <https://doi.org/10.1191/0143624406bt145oa>.
- [3] POMOGAEVA, V., MATECHKO, L., PROKOFIEV, D., NAREZHNYAYA, T. Investigation of the motion processes of wastewater in sewerage of high-rise buildings. In: E3S Wew of Conferences. 2018, s. 1 – 9. Available at: <https://doi.org/10.1051/e3sconf/20183302013>.
- [4] VALÁŠEK, J. Vodovody a kanalizácia vo vysokých budovách (Water supply and drainage in high-rise buildings). Bratislava: Alfa, 1982, Slovakia, s. 131-157. ISBN 63-021-82.
- [5] YABE, S., OTSUKA, M., KAWAGUCHI, T., SUGIMOTO, R. Experimental Investigation of the Influence of Different Offset Piping Methods on the Drainage Performance of a Drainage Stack. In: CIB W062 Symposium. 2015, s. 30 - 55. Available at: [https://www.irbnet.de/daten/iconda/CIB\\_DC30620.pdf](https://www.irbnet.de/daten/iconda/CIB_DC30620.pdf).
- [6] EN 12056:2002 Gravity drainage systems inside buildings.
- [7] STN 73 6760:2009 Kanalizácia v budovách (Drainage in budlings).

# Mycoaerosol in historic places – calculated ill health potential



**ELENA PIECKOVÁ**

Faculty of Medicine,  
Slovak Medical  
University, Bratislava,  
Slovakia  
elena.pieckova@szu.sk



**RENÁTA LEHOTSKÁ**

Faculty of Medicine,  
Slovak Medical  
University, Bratislava,  
Slovakia  
renata.lehotska@szu.sk



**SOŇA WIMMEROVÁ**

Faculty of Public  
Health, Slovak Medical  
University, Bratislava,  
Slovakia  
sona.wimmerova@szu.sk

Statistically processed quantitative analysis of airborne mycobiota at the depositaries of conserved human remains led to extrapolation of mycoaerosol inhalation risk for specialists and visitors. Indoor sources of the aerosolized fungal propagules and no seasonal impact on their quantity were proven at the locations with glass-covered undergrounds without air circulation.

**Keywords:** organic materials; aeroscopy; microbial cultivation; fungal load; inhalation

Visually clean air contains denser bioaerosol than the dirty one as bigger propagules sediment faster. Airborne fungi are commonly forming conglomerates similar to fine fog (10 – 20 µm in diameter) [1].

Employees dealing with material rich in nutrients and prone to fungal colonization due to damp conditions might be exposed to extreme fungal concentrations ( $10^9$  colony forming units, cfu/m<sup>3</sup>) – condition known as “particle burst”, and plenty of mycotoxins. Inhalation of pathogen / toxicant / irritant may result in health damage at 100-times lower loads than after ingestion, due to the crossing over even haemo-encephalic barrier [2]. Inhalation exposition to mycoaerosol is not a part of routine analysis of indoors yet [3, 4].

The study on quantitative aeromyco-analysis of places with relevant historical artefacts with estimation of possible fungal load to the individuals is presented.

## Material and Methods

Nine localities of running research works with human remains or of their public expositions in Slovakia and Hungary are observed from 2012 onward. Indoor and related outdoor air in mausoleums, depositaries, crypts, reliquaries, museums and an archive, as given in the **Figure 1**, was sampled by mean of an impactor. The DG18 agar (HiMedia, Mumbai, India) was employed as the isolation medium for 67 complex air samples, incubated at 25 and 37 °C 3 – 7 days as recommended by the IUMS Committee on Environmental Mycology. The average cultivable fungal load in cfu/m<sup>3</sup> was calculated and statistically processed by the pair t-test.

## Results and Discussion

Experts working at the sampling places and visitors are groups of interest from the mycoaerosol exposition point of view. Esp. the later ones might be in health conditions when being more sensitive to health damage due to fungal bioaerosol, incl., fungal toxic products, e. g. allergic, elderly or polymorbid persons. Quantities of cultivable aeromycobiota are summarized in the **Figure 1**.

Presence of internal sources of fungal contamination in glass covered undergrounds without air circulation is documented in the **Table 1**. According to the WHO recommendation [5], the indoor fungal concentration must not exceed the outdoor one. The qualitative composition of both fungal aerosols must cope with each other. And no pathogenic and toxic fungal species are allowed indoors. If, even, one of the given conditions is missing, the indoors is classified as the sick one.

**Table 1.** Identification of indoor fungal sources in the localities with historical objects. Legend:  $c_i$  – indoor air concentration of fungi (average);  $c_o$  – related outdoor air concentration of fungi (average);  $c_i/c_o > 1$  – no indoor fungal source present,  $c_i/c_o < 1$  – indoor fungal source likely.

Locality		$c_i$ [cfu/m <sup>3</sup> ]	$c_o$	$c_i/c_o$
Sladkovicovo		441	201	2.2
Okolicne	Summer	187	36	5.2
	Spring	190	453	0.4
Zofia Serediova		11	45	0.2
Kovarce		483	979.5	0.5
Bratislava	Chapel St. James	30	33	0.9
	Castle	543	22.5	24.1

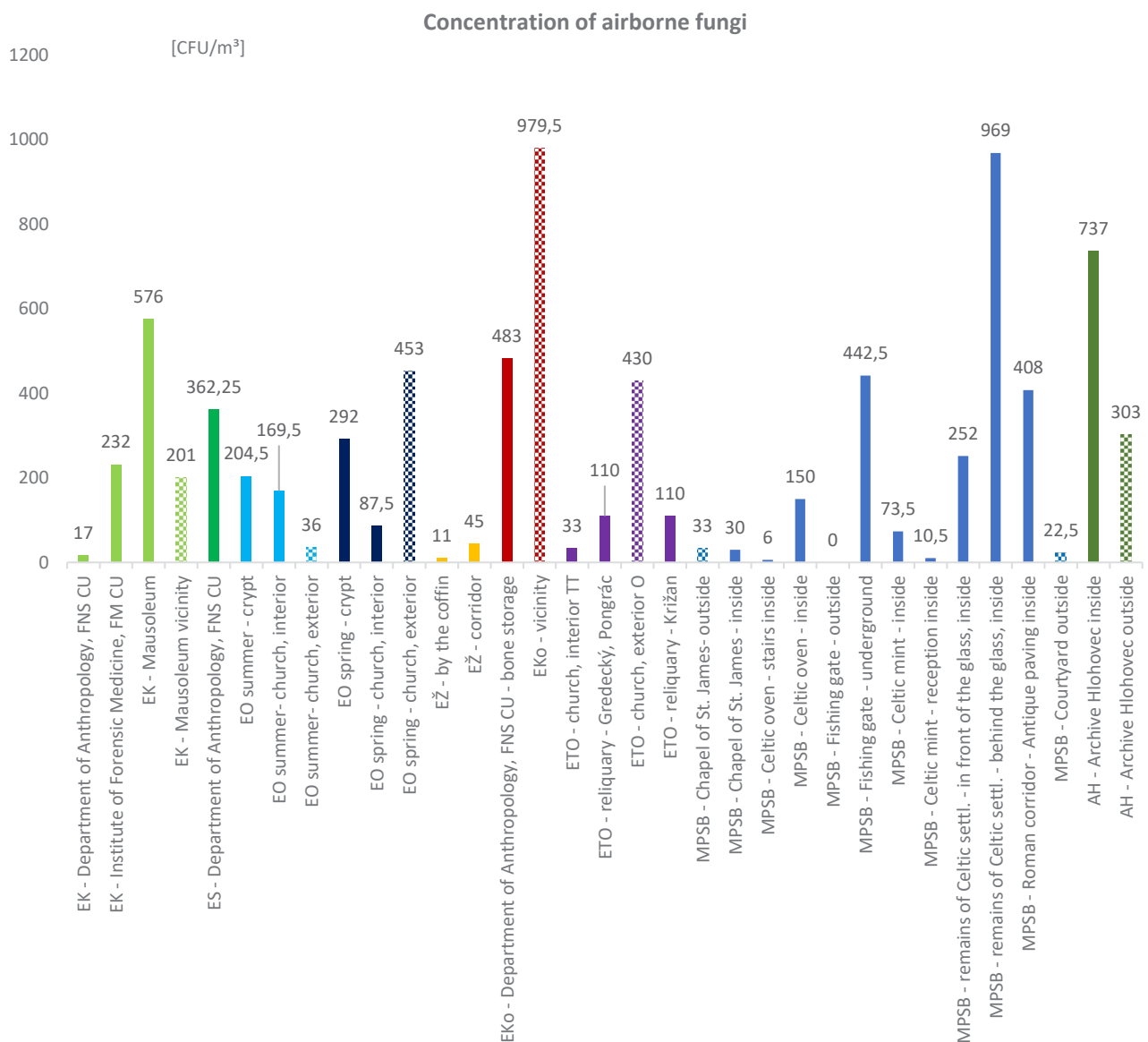


**Figure 1.** Quantification of cultivable airborne fungi in localities with different sampling sites. Legend: EK – Sladkovicovo, ES – Solosnica, EO – Okolicne, EŽ – Zofia Serediova, Eko – Kovarce, ETO – Trnava and Esztergom, MPSB – Bratislava, AH - Archive Hlohovec.

From the hygienic conditions in terms of airborne fungal content, the mausoleum yielded very high concentration, while specialized departments conducting research on the same mortal remains (the university) presented loads lower. Apparently, due to regular decontamination of the environment and handling tools. Total fungal count in the indoor air of the archive did not exceed its outdoor concentration with statistical relevance.

Awad et al. [6] evaluated total indoor environment in a museum in Giza, Egypt. They found 175 - 40,250 cfu/m<sup>3</sup> of airborne fungi. Ratio indoor/ outdoor air showed the outdoor environment was the main source of fungi isolated indoors. Concentrations of aerial mycobiota in our study fit the interval 6 – 979.5 cfu/m<sup>3</sup>. There is always a dynamic exchange between indoor and outdoor fungal bio-aerosol as proved by genetic analysis [1].

### Inhalatory exposition to aeromycobiota

The exposition was calculated as total number of inhaled propagules in one or eight hours at a normal ventilation rate of 5 – 8 litres of air per min: 5 is the value in steady state person (visitor, inhaled volume 0.3 m<sup>3</sup>) and 8 during a work shift (8 hrs, 3.84 m<sup>3</sup>) [7].

Formula:

$$V \times C = X$$

$V$  – inhaled air volume over an hour or 8 hrs [m<sup>3</sup>]

$C$  – average concentration of airborne fungi [cfu/m<sup>3</sup>]

$X$  – whole number of inhaled fungal propagules in the particular exposition course [cfu]

**Table 2** shows the calculated fungal load in cfu inhaled over 1 hour (visitor) or 8 hours (staff member).

**Table 2.** Sampling locality and inhaled fungal cfu per 1 hr (visitor) or 8 hrs (worker).

Locality		C value [cfu/m <sup>3</sup> ]	cfu/1 hr	cfu/8 hrs
Sladkovicovo	Mausoleum	576	173	2,212
	Comenius University	98	29	375
Solosnica		362	109	1,391
Okolicne	Summer	229	69	880
	Spring	193	58	74.5
Zofia Seredivova		25	7	94.5
Kovarce		483	145	1,855
Trnava		84	25	324
Ostrihom		110	33	422
Bratislava		260	78	999
Hlohovec		303	91	1,163.5

Inhaled particles of any origin are primarily released from a healthy organism by mucociliary effect. The basic factor affecting its effectivity is the inhaled particle size. During physiological ventilation, ca 1/3 of particles (the biggest) is entrapped in the upper airways and is released first. The same portion of inhaled propagules (the smallest, < 2 µm, mostly fungal hyphal fragments) might penetrate into the low airways and enter the blood stream and the skull cavity. It is not possible to extrapolate the number of cfu eliminated from the respiratory tract just according to the total inhaled fungal load.

Chen et al. [9] monitored number of visitors in the Museum of Terracota Army of the Emperor Qin in China. Max indoor fungal cfu/m<sup>3</sup> detected were 90 and was clearly related to the peaking number of tourists present in the museum.

### Statistical analysis of air fungal concentrations in sampling localities

Concentrations of fungal isolates were analysed by pair t-test with the significance level  $\alpha = 0.05$

Between paired localities, there were no statistically relevant differences in quantities of air fungi ( $p > 0.05$ ), exc. of very complex nutrient samples from Sladkovicovo (mummies, osseous remains, rests

of cloths and bandages) vs. dominating paper in the archive ( $p = 0.031$ ).

Performed quantitative analysis of indoor aeromycobiota pointed out:

- high concentrations of fungi might lead to ill health of persons staying in places, where esp. mycosis outbreaks remain the less described – an infectious dose of (opportunistic) pathogenic moulds is unknown in general (even one propagule perhaps), with remarkable amounts of fungal propagules inhaled by the staff working on site for 8 hrs;
- the settled aerosolized fungi might damage historically valuable objects irreversibly and some indoor fungi (zygomycota) are early indicators of microclimatic conditions favourable to biodeterioration.

### Conclusion

There is ongoing lack of standardized sampling methods as well as of set hygienic exposition limits to humans. The high complex bioaerosol composition and very individualized responses of human organisms being exposed might be a crucial complication. Combination of several principles in sampling is highly recommended to describe the aeromycobiome and its harming potential with the supreme objectivity. ■

### References

- [1] Pieckova E. Indoor microbial aerosol and its health effects: Microbial exposure in public buildings – viruses, bacteria, and fungi. In: C. Viegas, et al. (Eds.): Exposure to microbiological agents in indoor and occupational environments. Springer, Cham, (2017) 237 – 252. ISBN 978-3-319-61688-9.
- [2] Pieckova E. Mycotoxins and Their Inhalatory Intake Risk. In: K. Singh, N. Srivastava (Eds.): Recent Trends in Human and Animal Mycology. Part II: Mycotoxins in Relation to Human and Animal Health. Springer (2019), pp. 195 – 202. ISBN 978-981-13-9434-8.
- [3] Malta-Vacas J., Viegas S., Sabino R., et al. Fungal and microbial volatile organic compounds exposure assessment in a waste sorting plant. Journal of Toxicology and Environmental Health, Part A. 75 (2012) 1410 – 1417. ISSN 1528-7394.
- [4] Viegas S., Pinheiro C., Sabino R., et al. Environmental mycology in public health. Fungi and mycotoxins risk assessment and management. Elsevier-AP, London (2015) pp. 234. ISBN-13: 978-0124114715.
- [5] WHO Regional Office for Europe: WHO guidelines for indoor air quality: dampness and mould. Geneva: WHO 2009, pp. 228.
- [6] Awad A., Saeed Y., Shakour A., et al. Indoor air fungal pollution of a historical museum, Egypt: a case study. Aerobiologia. 36 (2020) 197 – 209. doi: 10.1007/s10453-019-09623-w.
- [7] [https://en.wikipedia.org/wiki/Minute\\_ventilation](https://en.wikipedia.org/wiki/Minute_ventilation). Online. 09/05/022.
- [8] Chen Y.P., Cui Y., Dong J.G. Variation of airborne bacteria and fungi at Emperor Qin's Terra-Cotta Museum, Xi'an, China, during the "Oct. 1" gold week period of 2006. Environ Sci Pollut Res Int. 17(2) (2010) 478-485. doi: 10.1007/s11356-009-0161-1.

# Estimation of Cross-Ventilation Through Roof Windows in Attics



**VALÉRIE LEPRINCE**  
PLEIAQ  
84 C Avenue de la  
Libération  
69330 Meyzieu, France  
valérie.leprince@pleiaq.net



**NOLWENN HUREL**  
PLEIAQ  
Avenue de Mérande  
73 000 Chambéry,  
France



**CHRISTOFFER PLESNER**  
VELUX A/S  
Ådalsvej 99  
DK-2970 Hørsholm

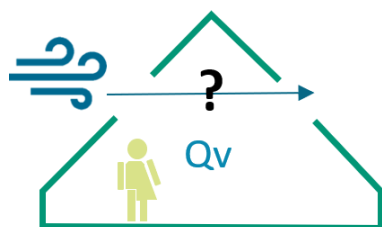
EN 16798-7:2017 considers that windows on roofs that have a pitch below  $60^\circ$  are not included on the windward side whatever their orientation. It means that roof windows are accounted for, but only on the leeward side when using the existing standard for calculation of air flows, EN 16798-7:2017 [1].

Therefore, in the specific case of a room only equipped with roof windows (e.g. an attic) and aerally independent from the rest of the building, whatever the orientation of the roof windows, only the simplified “single-sided” calculation method of EN 16798-7:2017 is applicable.

However, this study has shown that, for a building with low buildings surrounding it, the simplified single-sided method from EN 16798-7:2017 was underestimating the airflow rate by up to 77%.

**Keywords:** Cross-ventilation, roof window, attic, EN 16798-7:2017, calculation method

According to EN 16798-7:2017, roof windows always have a negative  $C_p$ . **So, the existing simplified cross-ventilation method from EN 16798-7:2017 cannot be used in the case of this attic.** Therefore, when using the existing standard, the simplified single-sided equation shall be used to calculate the airflow rate in this attic, as there are no other options.



Attic independent from  
the rest of the building

The existing simplified single-sided method from EN 16798-7:2017 will be used as reference to be compared with the new developed method.

Theoretically, it is actually possible that an airflow rate due to cross-ventilation occurs through 2 roof windows.

According to the literature, a roof window may indeed have a positive wind pressure coefficient when the wind is attacking straight onto the roof, contrary to facade windows for which the coefficient is almost always negative when the wind angle is  $45^\circ$  (see **Figure 1**).

In this study, it is assumed that  $C_p$  coefficients are constant for a roof pitch between  $30$ – $60$  degrees. In the following example, a roof with a pitch of  $45$  degrees has been considered as illustrated in **Figure 2**. A linear extrapolation was used on  $C_p$  coefficient from **Figure 1** (see green markings in **Figure 1** for the line “Roof >  $30^\circ$  pitch”) for wind angles between  $0^\circ$  and  $45^\circ$ .

As the  $C_p$  depends on the surrounding of the building, if the building is surrounded by obstructions equal to:

- half the height of the building (left table), then  $C_p$  is positive for wind angles between  $-30^\circ$  and  $+30^\circ$
- the height of the building (right table), then  $C_p$  is positive for wind angles between  $-12^\circ$  and  $+12^\circ$ .

[1] More information on the calculation method proposed in EN 16798-7:2017, including the validation of simplified formula with a pressure code, can be found in (Leprince, Valérie; Carrié, François-Rémi, 2016) and (Larsen et al. 2018).

**Figure 2** compares wind directions that induce positive  $C_p$  coefficients for roof windows and facade windows. It highlights that the wind angle that induces positive  $C_p$  coefficient is narrower for roof windows than for facade windows. Moreover the range is reduced by roughly 60% if the building is surrounded by buildings with the about same height rather than half the height.

As EN 16798-7:2017 only divides the building into 4 orientations, it considers that  $C_p$  coefficients for roof windows are always negative. Therefore, according to EN 16798-7:2017,

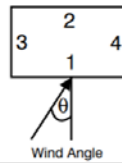
cross-ventilation cannot occur when there are only roof windows in a ventilation zone (e.g. in an attic).

**Objective and method**

The objective of this study is to test a new method, based on a EN 16798-7:2017 method (called the “adapted cross-ventilation method”), to take into account cross-ventilation occurring through roof windows and find the impact on estimated ventilation airflow rate. The principle of this new method is, when

**Table A2.5 Wind Pressure Coefficient Data**

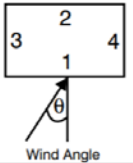
Low-rise buildings (up to 3 storeys)  
 Length to width ratio: 2:1  
 Shielding condition: Surrounded by obstructions equivalent to half the height of the building  
 Wind speed reference level: Building height



Location	Wind Angle							
	0°	45°	90°	135°	180°	225°	270°	315°
Face 1	0.25	0.06	-0.35	-0.6	-0.5	-0.6	-0.35	0.06
Face 2	-0.5	-0.6	-0.35	0.06	0.25	0.06	-0.35	-0.6
Face 3	-0.6	0.2	0.4	0.2	-0.6	-0.5	-0.3	-0.5
Face 4	-0.6	-0.5	-0.3	-0.5	-0.6	0.5	0.4	0.2
Roof (<10° pitch)	Front	-0.6	-0.6	-0.6	-0.6	-0.6	-0.6	-0.6
	Rear	-0.6	-0.6	-0.6	-0.6	-0.6	-0.6	-0.6
Average	-0.6	-0.6	-0.6	-0.6	-0.6	-0.6	-0.6	-0.6
Roof (11-30° pitch)	Front	-0.6	-0.6	-0.55	-0.55	-0.45	-0.55	-0.55
	Rear	-0.45	-0.55	-0.55	-0.6	-0.6	-0.55	-0.55
Average	-0.5	-0.6	-0.55	-0.6	-0.5	-0.6	-0.55	-0.6
Roof (>30° pitch)	Front	0.15	-0.08	-0.4	-0.75	-0.6	-0.75	-0.4
	Rear	-0.6	-0.75	-0.4	-0.08	0.15	-0.08	-0.4
Average	-0.2	-0.4	-0.4	-0.4	-0.2	-0.4	-0.4	-0.4

**Table A2.6 Wind Pressure Coefficient Data**

Low-rise buildings (up to 3 storeys)  
 Length to width ratio: 2:1  
 Shielding condition: Surrounded by obstructions equal to the height of the building  
 Wind speed reference level: Building height



Location	Wind Angle							
	0°	45°	90°	135°	180°	225°	270°	315°
Face 1	0.06	-0.12	-0.2	-0.38	-0.3	-0.38	-0.2	0.12
Face 2	-0.3	-0.38	-0.2	-0.12	0.06	-0.12	-0.2	-0.38
Face 3	-0.3	0.15	0.18	0.15	-0.3	-0.32	-0.2	-0.32
Face 4	-0.3	-0.32	-0.2	-0.32	-0.3	0.15	0.18	0.15
Roof (<10° pitch)	Front	-0.49	-0.46	-0.41	-0.46	-0.49	-0.46	-0.46
	Rear	-0.49	-0.46	-0.41	-0.46	-0.49	-0.46	-0.41
Average	-0.49	-0.46	-0.41	-0.46	-0.49	-0.46	-0.41	-0.46
Roof (11-30° pitch)	Front	-0.49	-0.46	-0.41	-0.46	-0.4	-0.46	-0.41
	Rear	-0.4	-0.46	-0.41	-0.46	-0.49	-0.46	-0.41
Average	-0.45	-0.46	-0.41	-0.46	-0.45	-0.46	-0.41	-0.46
Roof (>30° pitch)	Front	0.06	-0.15	-0.23	-0.6	-0.42	-0.6	-0.15
	Rear	-0.42	-0.6	-0.23	-0.15	-0.06	-0.15	-0.23
Average	-0.18	-0.4	-0.23	-0.4	-0.18	-0.4	-0.23	-0.4

**Figure 1.** Wind pressure coefficient data from (Liddament 1996) for a rectangular building for 2 different shielding conditions.

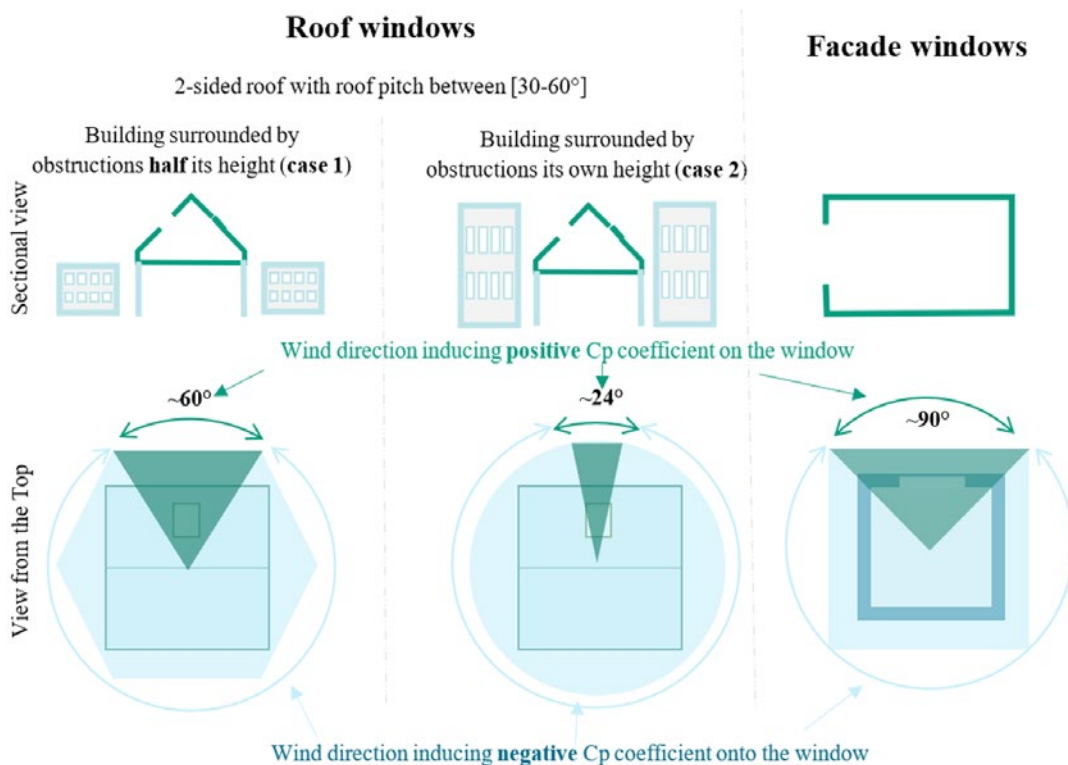


**Figure 2.** Wind directions that induce positive pressure coefficients on roof and facade windows.

a zone with only roof windows is simulated, instead of dividing the plan into 4 zones, to divide the plane into:

- 6 orientations ( $=360^\circ/60^\circ$ , where  $60^\circ$  is the range for positive  $C_p$  values) when the zone is surrounded by obstructions half its height (case 1)
- 15 orientations ( $=360^\circ/24^\circ$ , where  $24^\circ$  is the range for positive  $C_p$  values) when the zone is surrounded by obstructions of the same height (case 2).

**Test Case**

The test case is an attic aerally independent from the rest of the building. The roof is a two-sided roof with a pitch of  $45^\circ$  and equipped with one roof window on each side of the room.

The hypotheses used are detailed in **Table 1**.

The following configurations have been considered for the test case (**Table 2**):

**EN 16798-7:2017 method for cross-ventilation**

Simplified formulas for cross-ventilation cannot be used in our test cases as there are no facade windows, however, this is the method that has been used to develop the “adapted method”.

To calculate the airflow rate coming in and out of a ventilation zone when cross-ventilation occurs, EN 16798-7:2017 proposes a simplified method based on **Eq.1**.

$$Eq.1 \quad q_{V,arg;in} = 3600 \times \frac{\rho_{a;ref}}{\rho_{a,e}} \cdot \max \left( C_{D,w} \cdot A_{w,cros} \cdot \min (u_{10,site}; u_{10,site,max}) \cdot (\Delta C_p)^{0,5}; \frac{A_{w,tot}}{2} \cdot (C_{st} \cdot h_{w,st} \cdot abs(T_z - T_e))^{0,5} \right)$$



**Figure 3.** Illustration of the test case.

**Table 1.** Hypotheses of the calculation.

Reference air density	$\rho_{a,ref}$	1.2	kg/m <sup>3</sup>
External air density	$\rho_{a,e}$	1.2	kg/m <sup>3</sup>
Discharge coefficient	$C_{D,w}$	0.67	-
Coefficient taking into account stack effect in airing calculations	$C_{st}$	0.0035	m/s/(m.K)
Useful height for stack effect for airing: height difference between the bottom and the top of the windows	$h_{w,st}$	0.8	m
Coefficient taking into account wind speed in airing calculations	$C_{wnd}$	0.001	1/(m/s)
Temperature difference between inside and outside	$\Delta T$		°C
Wind pressure coefficient	$C_p$		-
Wind speed at 10 meter high	$u_{10,site}$		m/s

**Table 2.** Configurations considered for the test case.

Assumption on	Configurations considered
Temperature difference between inside and outside (°C)	0; 2; 5; 8; 10; 15; 20
Wind speed, u (m/s)	0; 1; 2; 3; 4; 5
Free window area: $A_{w;1}=A_{w;2}$ (m <sup>2</sup> )	0.15; 0.25; 0.35; 0.5
Difference of wind pressure coefficients between windward and leeward sides ( $\Delta C_p$ ) see <b>Table 1</b> .	
Case 1: building surrounded by obstructions equivalent to half the height of the building	0.75 (case 1)
Case 2: building surrounded by obstructions equal to height of the building	0.48 (case 2)

Where the calculation of  $A_{w,cross}$ , representing the equivalent cross ventilation area, is made through an algorithm that divides the building into four orientations and calculate the window opening area in each (see EN 16798-7:2017).

The calculation of the airflow rate due to wind takes into account roof windows only on the leeward side (never on the windward side).

### Adapted cross ventilation method for roof windows

To take into account the fact that cross-ventilation may occur through roof-windows located as described in our example, in this study, instead of dividing the plane into 4 angles of 90° each, it will be divided into:

- Case 1: 6 angles of 60° ( $N_{ang} = 6$ )
- Case 2: 15 angles of 24° ( $N_{ang} = 15$ )

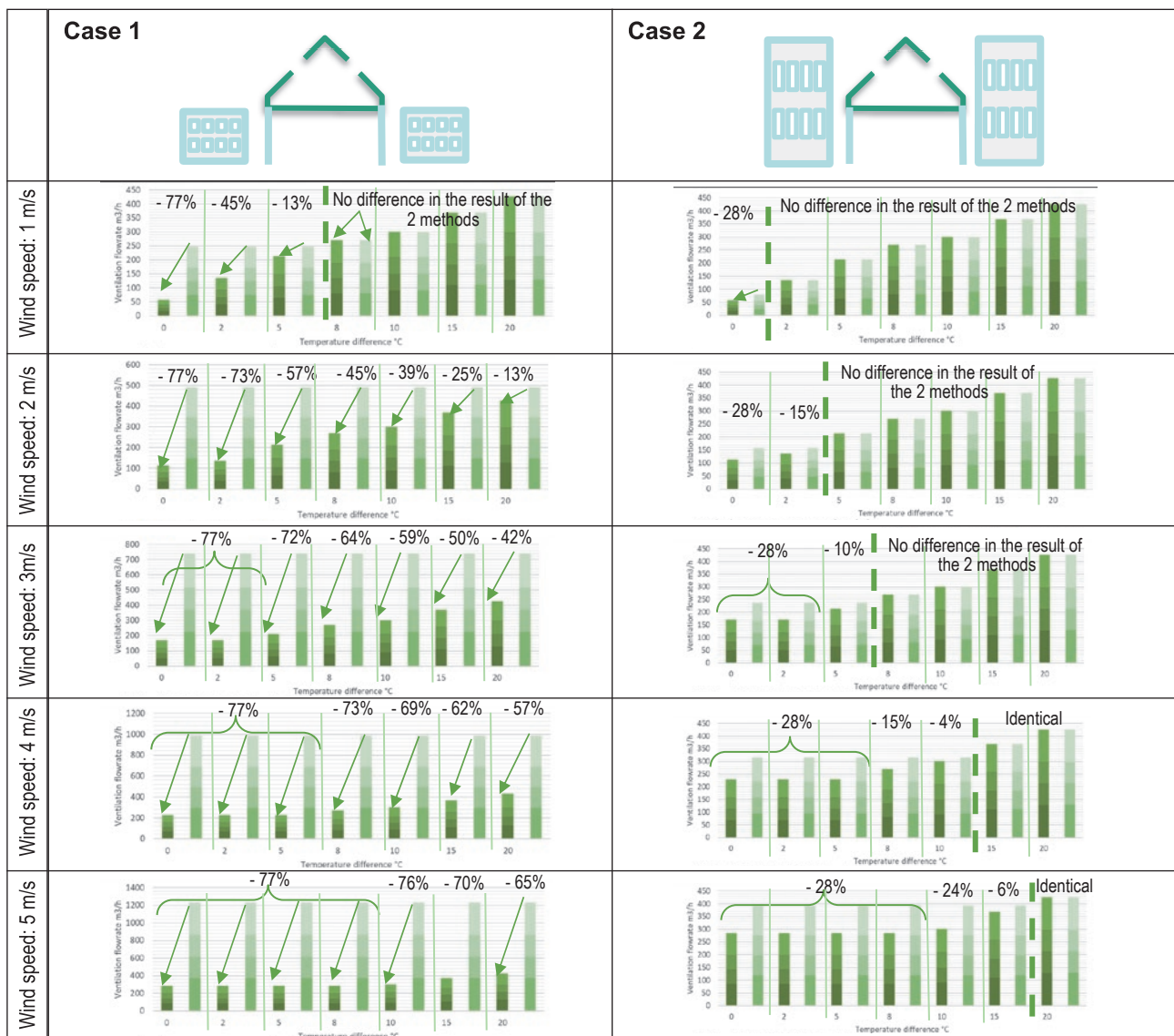
Results from this equation will be named “Adapted cross-ventilation method from EN 16798-7:2017” and will be compared to the simplified single-sided method.

More information on the calculation method proposed in EN 16798-7:2017, including the validation of simplified formula with a pressure code, can be found in (Leprince, Valérie; Carrié, François-Rémi, 2016) and (Larsen et al. 2018).

### Results

The graphs in **Table 3** compare the ventilation airflow rates calculated with the simplified single-sided method

**Table 3.** Results for the simulations for case 1 and case 2.



Method EN 16798-7:2017 single-sided  
 ■ Window area 0.15m² ■ Window area 0.25m² ■ Window area 0.35m² ■ Window area 0.5m²  
 Adapted cross ventilation method from EN 16798-7:2017  
 ■ Window area 0.15m² ■ Window area 0.25m² ■ Window area 0.35m² ■ Window area 0.5m²

from EN 16798-7:2017 (dark green bars) and the ventilation airflow rate calculated with the “adapted” cross-ventilation method (which takes into account cross ventilation that can occur in a zone or room with two roof windows) illustrated in light green bars.

Results for wind speed from 1 to 5 m/s show an important difference between case 1 and case 2 (see table 3):

- when the building is surrounded by buildings of its own height (case 2) there are little differences between the simplified single-sided method of EN 16798-7:2017 and the adapted cross-ventilation method. For 25 out of the 42 cases studied, results are the same and the maximum difference is 28% when wind is the main driver (hence small temperature difference and high wind speed)
- when the building is surrounded by building equivalent to half its height, the difference is significant: only 11 out of the 42 configurations studied provide the same results, the maximum difference reaches 77% and is observed for 11 configurations.

For case 1, with the adapted cross-ventilation method, the wind is the main driver for ventilation from 2 m/s

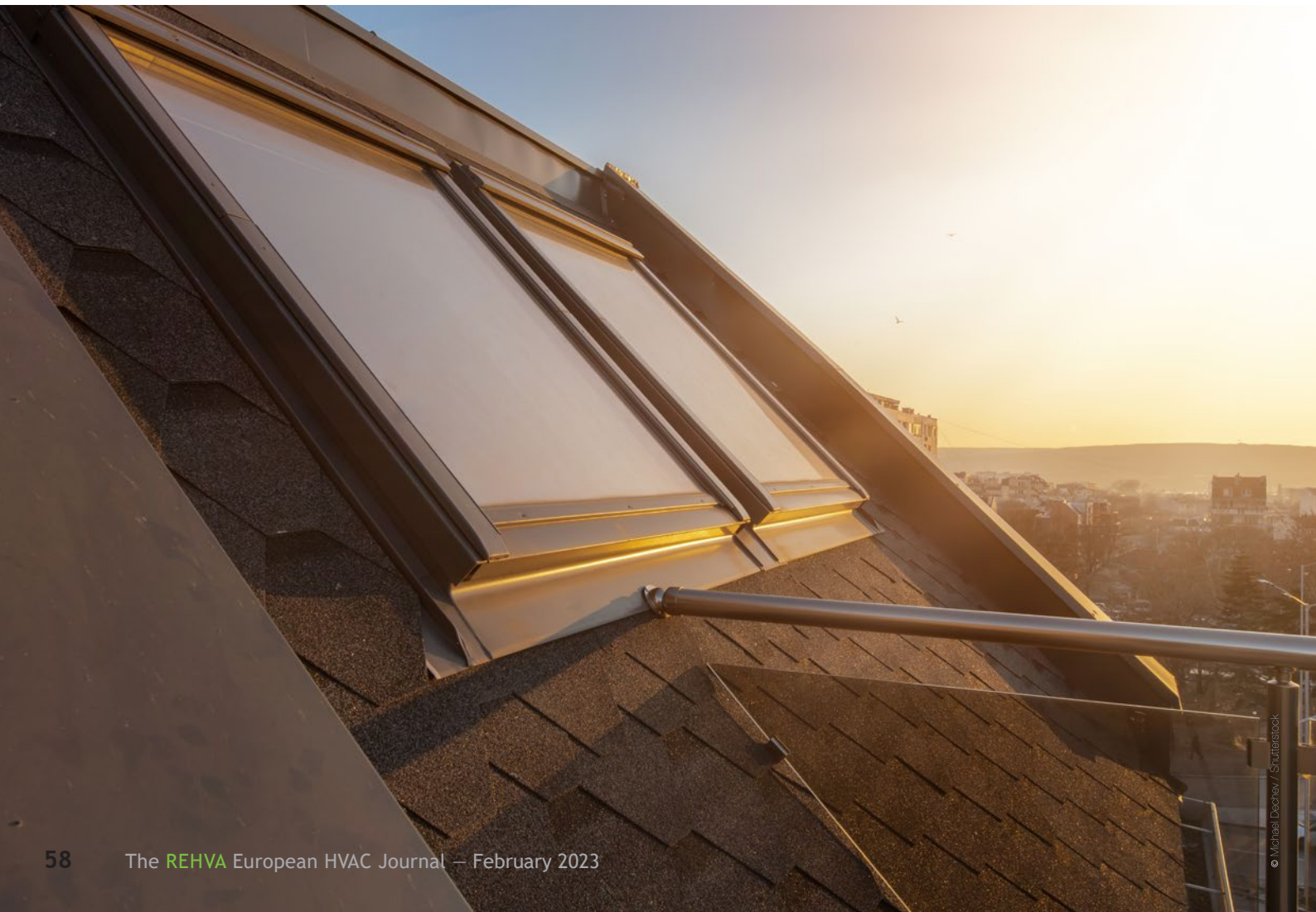
as long as the temperature difference remains below 20°C. This is shown by the airflow rates seen in the light green bars being constant (for a given wind speed above 2 m/s, they are all having the same height whatever the temperature difference).

The results also show that, for a given case, wind speed and temperature difference, differences in percentage between the 2 methods do not depend on the free window area (as in both methods the flowrate is proportional to the free window area).

## Conclusions

The objectives of this study were:

- to develop a more precise calculation method adapted to roof windows to take into account cross-ventilation that may occur through them (even when there are no facade windows in the zone)
- to compare results obtained with this method to the simplified single-sided method from EN 16798-7:2017



The “adapted” calculation method developed is consistent with the one proposed in EN 16798-7:2017, but simply further divides the horizontal plane to better take into account the specific cases of roof windows. The “adapted” method developed shall only be used **for the specific case of zones with only roof windows** with multiple orientations. As the  $C_p$  coefficient remains positive for a wider range of angles for facade windows (see **Figure 2**), applying this new method to zones with facade windows may lead to falsely consider cross-ventilation. Combining the two methods would lead to much more complex algorithms.

In this study, where roof windows could have positive  $C_p$  values even if they have a pitch between 30-60 degrees, we have shown, that:

- in case 2 (building surrounded by high obstacles), the new “adapted” cross-ventilation method provides results close to the simplified single-sided method from EN 16798-7:2017,
- in case 1 (building surrounded with lower building) cross-ventilation can theoretically occur quite often and the simplified single-sided method from EN 16798-7:2017 highly under-estimates the average airflow rate in this specific case.

Proposing this new adapted method for cross-ventilation to calculate the airflow rate in the specific case of room with only roof windows would allow to

better estimate the airflow rate in the room. This new “adapted” cross ventilation method could be used as an addendum to EN 16798-7:2017 for the EPB standard systematic review for this specific application of zones with only roof windows.

Nevertheless, while interpreting those results the following limitations shall be kept in mind:

- The given airflow rates are averaged airflow rates which by no mean are instantaneous airflow rates, assuming (among other things) an equiprobability of wind directions which may not be relevant in certain places
- Simplified equations used here have been developed in the context of EN 16798-7:2017 and compared to models performed in CONTAM and to on-site measurements (see (Larsen et al. 2018; Leprince, 2016.)). They slightly underestimate the airflow rate as EN 16798-7:2017 focuses on the calculation of the building energy use in periods when there is a cooling demand, and they have not been checked for very small temperature differences.
- $C_p$  coefficients used in this study are the ones provided in (Liddament 1996), where other sources provide other values.
- The airflow rates only apply when windows are open. In case of high-speed winds or high temperature differences, when windows may only be open for very short periods of time, the averaged airflow rate may not be relevant. ■

## Acknowledgements

The authors would like to thank VELUX A/S for funding this study.

## References

- Larsen, Tine Steen, Christoffer Plesner, Valérie Leprince, François Rémi Carrié, et Anne Kirkegaard Bejder. 2018. « Calculation Methods for Single-Sided Natural Ventilation: Now and Ahead ». *Energy and Buildings* 177 (October): 279-89. <https://doi.org/10.1016/j.enbuild.2018.06.047>.
- Leprince, Valérie; Carrié, François-Rémi. s. d. « Comparative analysis of window airing models proposed in prEN 16798-7 and influence of internal resistances ». In *CLIMA 2016 - proceedings of the 12th REHVA World Congress: volume 5. Aalborg: Aalborg University, Department of Civil Engineering. Aalborg University, Denmark.*
- Liddament, Martin W. 1996. *A Guide to Energy Efficient Ventilation: This Report Is Part of the Work of the IEA Energy Conservation in Buildings & Community Systems Programme, Annex V. Coventry: Annex V. Air Infiltration and Ventilation Centre.*

# Energy Savings with AeroSeal Ductwork Sealing in Europe



**NOLWENN HUREL**

PLEIAQ, 2 Avenue de Mérande, 73000 Chambéry, France  
[nolwenn.hurel@pleiaq.net](mailto:nolwenn.hurel@pleiaq.net)



**VALÉRIE LEPRINCE**

Cerema, 2 rue Antoine Charial, 69003 Lyon, France



**SIMON TÖLKE**

MEZ-TECHNIK GmbH, Bierwiesenstraße 7, 72770 Reutlingen, Germany

This paper presents the results of 7 ductwork sealing projects through aerosols injection in Europe. The ductwork leakages were reduced from 87% up to 98% with an average of 93%. The impact on the energy consumption is quantified, with savings reaching up to 36 k€/year (for a 30 000 m<sup>2</sup> building).

**Keywords:** Ductwork leakage, sealing, aerosol, energy savings, fan consumption, AeroSeal

For years, ventilation and air-conditioning systems have played an increasingly important role in ensuring sufficient air exchange in buildings. With time buildings are becoming more and more airtight to avoid energy losses through uncontrolled air leakage and mechanical ventilation systems are installed to ensure a good indoor air quality. What is a good approach in theory can fail in practice due to leaky ductwork. Various studies have shown a low awareness on this issue in most European countries [1], with leaky ductworks impacting the energy use, the indoor air quality or generating noise [2].

One solution applicable both to new ductwork systems not meeting the expected air tightness class and existing leaky ductwork, is a sealing through aerosols injection. This technique explained in [3] and patented as the AeroSeal process, allows to seal air duct systems from the inside within a short time and without having to search for leaks beforehand. Leakages with gaps of up to 15 mm are permanently eliminated by using a sealant that is certified according to VDI 6022. As reported by European resellers, almost 700 sealing projects have been carried out using this method since 2015 in Europe.

This paper presents the results of 7 ductwork sealing projects performed during the year 2021 on existing (mostly non-residential) buildings located in 7 different European countries: Germany, France, Ireland, Czech Republic, the Netherlands, Poland and Switzerland. An extended paper was presented at the Rotterdam

AIVC conference, including more data and calculation details, and presenting also on-site experience from the sealing operators [4].

## Methodology

### *AeroSeal air duct sealing technique*

The aerosol-based sealing process was developed in the 1990s at the University of Berkeley, USA [5], [6], and was patented as the AeroSeal process (see **Figure 1**). The innovation consists in sealing ductwork from the inside, within a short time and without having to search for leaks beforehand. Chemically speaking, this technique is based on an emulsion of water and vinyl acetate polymer, a stable, non-toxic and non-flammable mixture, that is aerosolized into 4–10 micron-sized particles [7].

The resulting aerosol is distributed under pressure inside the ventilation ductwork system [3]. The particles seal little by little leaks with gaps of up to 15 mm forming a robust air sealing that will last for years while staying pliable and flexible and remains effective over a wide range of operating pressures, temperatures and humidity levels found in residential, commercial and industrial air duct systems [7]. Contrary to a coating process, the particles deposit only at the leaks and not elsewhere in the ductwork.

Until today the AeroSeal process has been applied in more than 125 000 ductwork systems of both residential and non-residential buildings, mostly in the USA. In Europe

the product was introduced in the market in 2015 by Mez-Technik located in Germany and since then there have been almost 700 sealing projects in over 20 countries thanks to Aeroseal partners companies from 18 countries.

**Case study: selected 7 buildings across Europe**

In order to evaluate the performance of this aerosol-based sealing technique, a survey was sent to 7 Aeroseal partners across Europe to collect detailed data on ductwork sealing projects performed in 2021.

**Figure 2** presents the buildings' characteristics of the selected sealing projects, the reasons why a sealing was requested and the initial ductwork airtightness level. The building selection was made in order to cover a wide range of parameters for both the buildings (location, type, surface, year of construction) and the ventilation systems (flowrate capacities ranging from 6 000 m<sup>3</sup>/h for the CZ project to 301 407 m<sup>3</sup>/h for the IE project; exhaust, supply and balanced ventilation systems all represented).

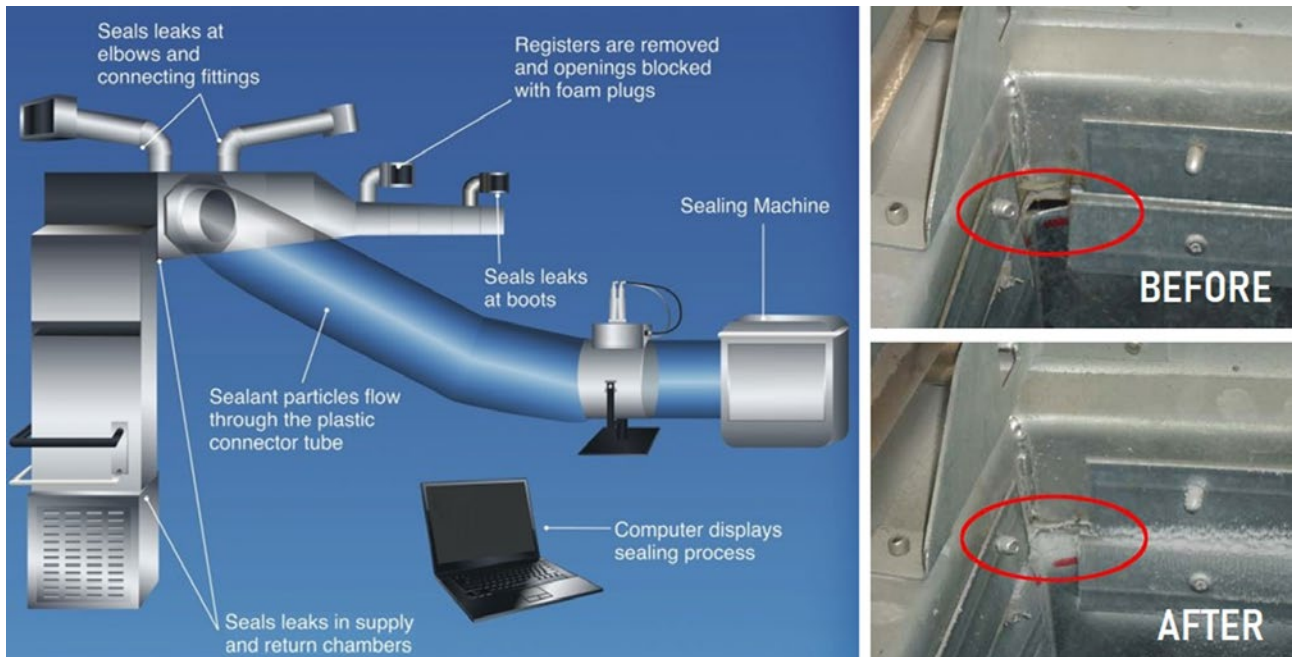


**Figure 1.** Aeroseal sealant technology (Image courtesy of Aeroseal LLC).

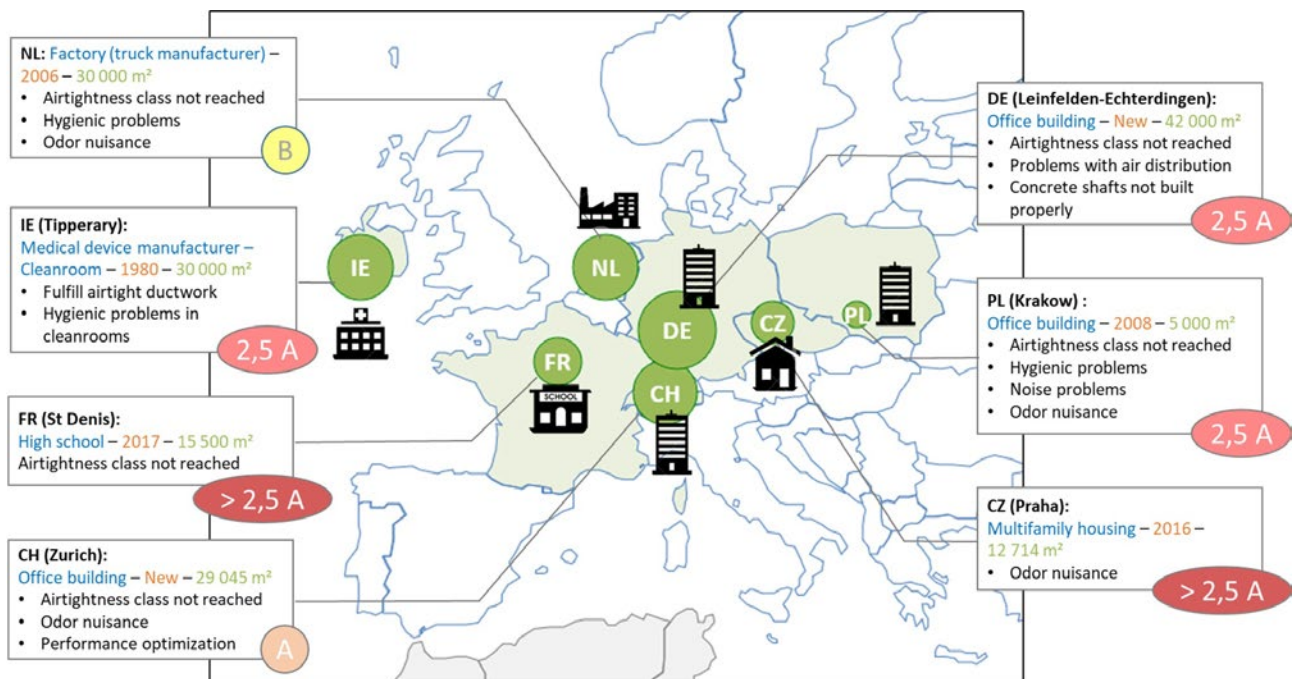


**Figure 2.** Details on the studied buildings, reasons for ductwork sealing, and initial ductwork airtightness level.

## Data Analysis: energy savings calculation

The energy savings on the fan power are estimated in this study considering that fans fully compensate for ductwork leakage. When the fan cannot, or only partially, compensate for leakage, it is the environmental air quality that is impacted [8].

Ductwork sealing can also induce significant heating/cooling savings [9] [2], when conditioned air leaks in a non-conditioned area. They were not calculated in this study as it would require detailed data that were not available [8].

### Fan power calculation

Apart from the IE project, the fan powers before/after sealing were not known by the survey respondents, and were therefore calculated as follows:

$$P_{AHU,i} = \frac{\Delta p_{AHU,i} \times Q_{AHU,i}}{\eta_{AHU,i} \times 3600} \quad (1)$$

With:

- $i = bef / aft$ : ductwork state: before / after the sealing
- $P_{AHU}$ : the power of the air handling unit (AHU) (W)
- $\Delta p_{AHU}$ : the pressure difference at the AHU (Pa)
- $Q_{AHU}$ : the air flowrate at the AHU (m<sup>3</sup>/h)
- $\eta_{AHU}$ : the AHU efficiency (-)

### Air flowrates calculation

The AHU flowrate after the sealing was considered to be the flowrate capacity provided:

$$Q_{AHU,aft} = Q_{AHU,nom} \quad (2)$$

The flowrate before the sealing is deduced from the value after and from the leakage flowrates ( $Q_{leak}$ ) measured before and after the sealing:

$$Q_{AHU,bef} = Q_{AHU,aft} + Q_{leak,bef} - Q_{leak,aft} \quad (3)$$

### Fan efficiency

The fan efficiency varies with its flowrate. After sealing it was calculated with Equation (1) when the flowrate and pressure were known. Otherwise, a default value of 0.4 was taken.

The fan efficiency before the sealing was estimated using an equation from the support Excel sheet of standard EN 16798-5-1:

$$\eta_{AHU,bef} \approx \sqrt{\frac{Q_{AHU,bef}}{Q_{AHU,aft}}} \times \eta_{AHU,aft} \quad (4)$$

## Results

### Leakage reduction

All sealing projects allowed significant leakage reductions in percentages, as illustrated in **Figure 3**. On average the leakage flowrates were indeed reduced by 93.4%, with a minimum of 87.2% for the IE project and a maximum of 97.6% for the FR project. This is done in a rather short time with cumulated aerosol injection times for the whole projects ranging from about 1 and a half hour (for the CZ project with the smallest ductwork area) to 62 hours (for the FR project with over 50 different AHU units).

### Impact of ductwork leakage on energy savings

The fan power savings by ductwork sealing with the AeroSeal process are calculated for all projects according to the methodology described in paragraph "Data Analysis: energy savings calculation" and presented in **Table 1**.

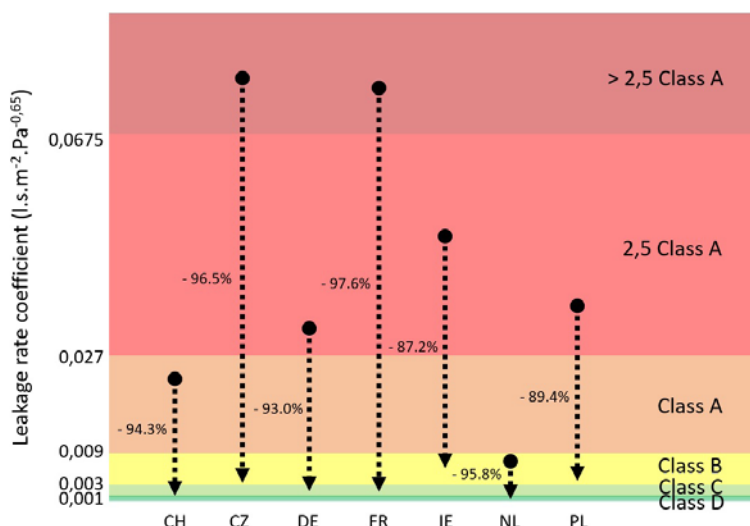


**Figure 3.** Ductwork leakage rate DECREASES with the AeroSeal sealing process.

The absolute fan power savings vary a lot depending on the sealing project (between 0.6 and 38 kW) due to the wide range of fan powers and initial leakage rates. In percentage of the initial total fan power, the savings represent from 1% (for NL project with the tightest initial ductwork) to 65% (for the FR project with the worst initial airtightness level).

The energy and cost savings are also calculated assuming a fan operating full time and according to national electricity prices. The IE project has the highest savings (about 331 000 kWh/year corresponding to about 36 000 €/year) since it is the project with the largest ductwork, one of the highest initial fan power and leakage rates. On the other hand, the CZ project has the lowest savings (about 5 000 kWh/year corresponding to about 900 €/year) despite having the highest initial leakage coefficient, as it is the project with the smallest ductwork area and initially lower fan power.

As illustrated in **Figure 4**, the percentage of initial fan power saved by ductwork sealing is proportional to the initial percentage of leakage compared to the flowrate capacity. The linear regression shows indeed a good correlation between these two parameters, with a coefficient of determination  $R^2$  of 0.987. As a result, it seems that for a given ductwork, the percentage

of initial fan power that can be saved by an Aerosol sealing process is about twice the percentage of leakage compared to the flowrate capacity:

$$\frac{(P_{AHU,bef} - P_{AHU,aft})}{P_{AHU,bef}} \approx 2 \times \frac{Q_{leak,bef}}{Q_{AHU,bef}} \quad (5)$$

The annual cost savings can therefore be roughly estimated as in Equation (6).

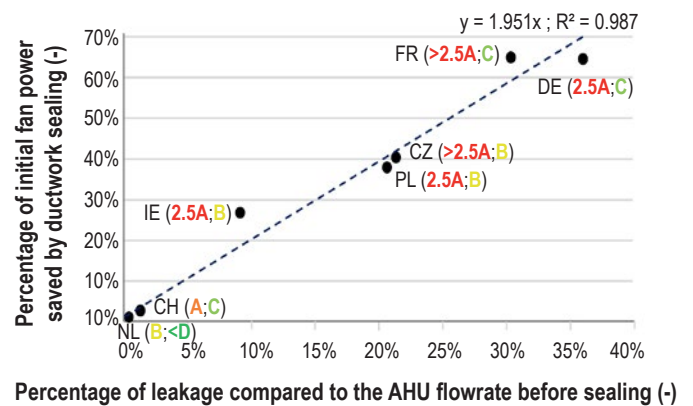


**Figure 4.** Percentage of initial fan power saved by sealing the ductwork according to the initial percentage of leakage compared to the AHU flowrate (airtightness classes before and after the sealing given into the brackets).

$$\text{savings (€)} \approx 2 \times P_{AHU,bef} (\text{kW}) \times \frac{Q_{leak,bef}}{Q_{AHU,bef}} \times t_{AHU,annual} (\text{h}) \times price_{elec} (\text{€/kWh}) \quad (6)$$

**Table 1.** Calculation of fan power, energy and cost savings by ductwork sealing.

Project reference	CH	CZ	DE1	FR	IE	NL	PL
Total ductwork area (m <sup>2</sup> )	440	131	1202	844.24	2750	800	2210
Aerosol injection time (h)	36.1	1.4	21.1	61.5	49.6	2.1	35.9
Electricity price (€/kWh)	0.204	0.180	0.228	0.110	0.110	0.178	0.150
Total AHU flowrate before sealing (103 m <sup>3</sup> /h)	128.7	7.1	18.1	28.0	299.9	271.8	79.0
Total required fan electrical power BEFORE sealing (kW)	149.1	1.405	5.089	15.72	139.3	140.0	29.99
Fan power savings							
Total saved fan power (kW)	3.9	0.57	3.08	10.3	37.8	1.6	11.5
Percentage of initial total fan power saved (-)	2.6%	41%	60%	65%	27%	1.1%	38%
Energy and cost savings for fan operating full time (8760 h/year)							
Total saved energy (103 kWh/yr)	34.1	5.0	26.9	90.0	331.0	14.0	100.3
Total cost savings (€/yr)	6 956	902	6 144	9 901	36 414	2 490	15 049

## Conclusions

The Aero seal process, already widely used worldwide, allows to seal ductworks from the inside after their installation. Technical details from 7 sealing projects performed in 2021 across Europe, on a large variety of buildings and ventilation systems, were collected through a survey and analyzed in this paper. It allows to conclude that the Aero seal ductwork sealing process:

- is **efficient**: ductwork leakages reduced on average by 93% (from 87% up to 98%);
- is **rather fast**: the cumulated injection time for the whole project varies from about 1 to 60 hours depending on the ventilation system's size and complexity (usually less than 1h per injection point);

- **saves fan energy use and money**: from 5 000 to 331 000 kWh per year leading respectively to about 900 € and 36 000€ of savings each year, depending on the initial fan consumption and airtightness level.

Moreover, it is observed with a linear correlation that the percentage of initial fan power that can be saved by an Aero seal sealing process is about twice the percentage of leakage compared to the flowrate capacity. This allows to roughly estimate of the savings before sealing the ductwork with Equation (6).

These findings rely on only 7 sealing projects but a future study on a large number of projects is expected as more technical details will now be systematically filled in by the operators for each sealed ductwork.■

## Acknowledgements

We would like to thank the Aero seal service providers which supported us and provided the specific project information: Air Innovators B.V. (Netherlands); Energy Air Sp. Z.o.o. (Poland); Ventilace EU a.s. (Czech Republic); Lippuner Energie- und Metallbautechnik AG (Switzerland); Map Clim (France); Spectrum Engineering Ltd. (Ireland); Windmüller Technik GmbH (Germany).

## References

- [1] V. Leprince, F. R. Carrié, and M. Kapsalaki, 'Building and ductwork airtightness requirements in Europe – Comparison of 10 European countries', in *AIVC*, Nottingham, UK, Sep. 2017.
- [2] V. Leprince, N. Hurel, and M. Kapsalaki, 'VIP 40: Ductwork airtightness - A review', *AIVC*, Apr. 2020.
- [3] M. Modera, 'Fixing Duct Leaks in Commercial Buildings', *Ashrae Journal*, Jun. 2005.
- [4] N. Hurel, V. Leprince, and S. Tölke, 'Field experience with ductwork airtightness improvement after completion in Europe', presented at the 42nd AIVC-10th TightVent- 8th venticool conference, Rotterdam, The Netherlands, Oct. 2022.
- [5] M. Modera, D. J. Dickerhoff, O. Nilssen, H. Duquette, and J. Geyselaers, 'Residential field testing of an aerosol-based technology for sealing ductwork', in *Proceedings of the 1996 Summer Study on Energy Efficiency in Buildings, 'Profiting from Energy Efficiency'*, USA, Washington DC, 1996.
- [6] F. R. Carrié and M. P. Modera, 'Particle Deposition in a Two-Dimensional Slot from a Transverse Stream', *Aerosol Science and Technology*, vol. 28, no. 3, pp. 235–246, Jan. 1998, doi: 10.1080/02786829808965524.
- [7] Mez-Aero seal, 'Aero seal Duct Seal Data Sheet'. [Online]. Available: [https://www.mez-technik.de/media/wysiwyg/Download/MEZ-AEROSEAL\\_Sealant-Data-Sheet\\_2022\\_EN.pdf](https://www.mez-technik.de/media/wysiwyg/Download/MEZ-AEROSEAL_Sealant-Data-Sheet_2022_EN.pdf).
- [8] N. Hurel and V. Leprince, 'Ductwork leakage: practical estimation of the impact on the energy overconsumption and IAQ', presented at the 42nd AIVC-10th TightVent- 8th venticool conference, Rotterdam, The Netherlands, Oct. 2022.
- [9] N. Hurel and V. Leprince, 'Impact of ventilation non conformities: calculation methodology and on-site examples', presented at the 42nd AIVC-10th TightVent- 8th venticool conference, Rotterdam, The Netherlands, Oct. 2022.

# Integration of Domestic Ventilation Systems with Vertical Axis Wind Turbine Ventilation Technology

This study focuses on the investigation of a new concept of domestic ventilation systems integrated with a vertical wind turbine ventilation technology. The results indicated that the proposed wind turbine technology could potentially be capable of exerting significant influence on ventilation performance, meeting the UK's benchmark for air extraction and supply flow rate.

**Keywords:** Turbine ventilator, Resilient cooling, Ventilation, CFD, Wind Energy

The use of natural ventilation components as an enhancement for ventilation systems has become more desirable in the building sector. Mechanical ventilation systems are responsible for almost 40% of the total energy consumption. Applications of low carbon ventilation technologies, for example powerless ventilators, offer a prominent solution for reducing energy consumption in buildings. Powerless ventilators hold a potential to facilitate ventilation, reduce energy consumption and improve IAQ through the use of natural energy sources (Khan et al., 2008; Tan et al., 2016).

This study hypothesises the development of a new concept of home ventilation system that employs a wind driven turbine ventilator, as a means to reduce



**JIRAYUT SITTHIPIUK**  
School of Engineering and  
Built Environment, Edinburgh  
Napier University, Edinburgh,  
Scotland.  
jirayut.sitthipuk@napier.ac.uk

energy consumption and improve indoor air quality in a building. Additionally, the aim is to achieve a detailed understanding of the proposed system, in terms of ventilation performance for both air extraction and the supply of air by the turbine ventilator.

## Methodology

The model of a vertical wind turbine ventilator was created, as shown in **Figure 1a**, and consists of two parts: fresh air intake and turbine extractor. The principle of the turbine ventilator design was to provide active and passive ventilation through using the air intake vent for air supplying and the rotating turbine for extracting stale air. The study adopted Jadhav et al. (2016)'s CFD simulation approach of the wind tunnel domain setup for numerical simulations. The approach replicates the physical test rig for a wind tunnel. The whole computational domain is divided into two main regions: the flow domain and the chamber (see **Figure 1b**).

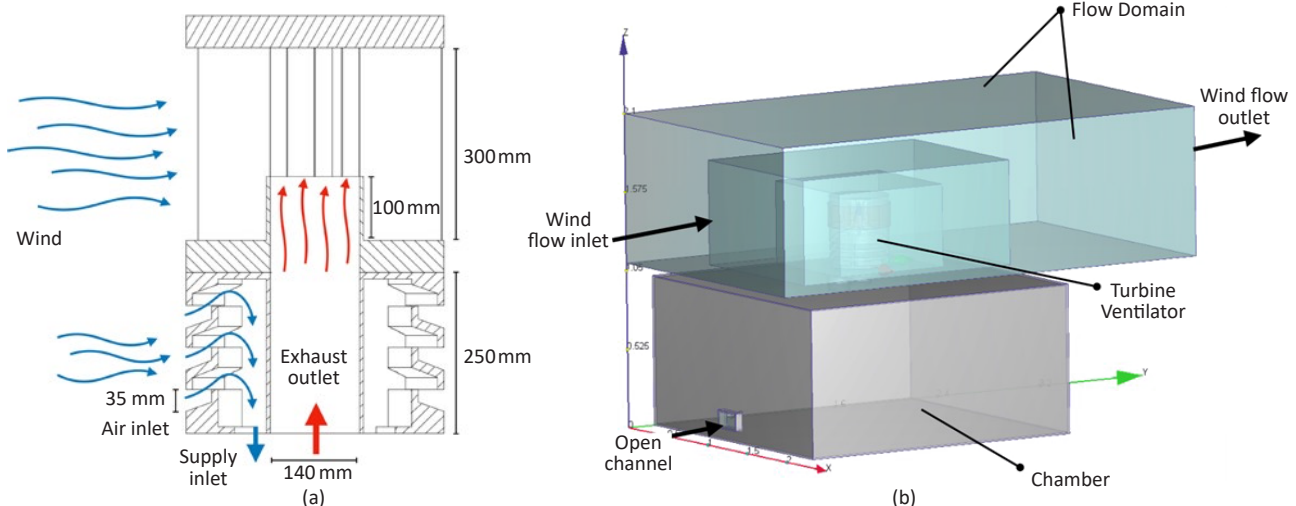


**Figure 1.** Schematic: (a) Turbine ventilator principle and (b) CFD computational domain setup.

Boundary conditions were assigned to each face of the computational domain. The entry of the computational domain upstream was defined as a uniform velocity-inlet boundary condition. The rotation of turbine ventilators started when the wind speed was higher than 2 m/s (Rimdžius et al., 2018). A pressure outlet boundary condition was assigned to the end of the domain downstream of the turbine ventilator, in which the pressure was set equal to 0. The k-epsilon turbulence model was used due to its robustness and proficiency in economically simulating a wide range of mean flow characteristics for turbulent flow conditions with reasonable accuracy (Jadhav et al., 2016).

## Results

### Performance investigation of air extraction flow rate

The initial investigation was carried out by performing CFD simulations of the proposed model with two different blade profiles: 2 blades (2B-TV) and 8 blades (8B-TV). This allows us to quantify the influence of the turbine blade profile on the ventilation performance in terms of exhaust volume flow rate. The highlighted zones in **Figure 2a** indicate the influence on pressure distributions on the 2B-TV model.

With the incoming flow on the convex side of the returning blade deflecting the rotation of the turbine ventilator, the highlighted region (the red circle shown in **Figure 2a & 2b**) is stagnant and creates a large pressure gradient on the blade convex (Tian et al., 2019). As a result, the flows started swirling in the middle region of the rotor, which creates a vortex, allowing the airflow to be influenced and therefore extracted from the duct (see **Figure 2c**)

On the other hand, the 8B-TV model exhibited better performance for developing the swirling flows, as shown in **Figure 2e**. The flows started entering the inner domain of the turbine ventilator from the top left corner and leaving through the bottom, causing the inner flows swirling in the interior of the turbine ventilator (see **Figure 2f**). Hence, the 8B-TV profile had a great impact on the swirling flow pattern, which leads to an increase in exhaust airflow rate. The CFD results of the 2B-TV and 8B-TV for air extraction performance were shown in **Figure 3**. It is noticeable that the 8B-TV greatly outperformed the 2B-TV by 66% beyond a wind speed above 2 m/s, which manages to meet the UK's minimum requirement of air extraction rate with the extracted volume flow rate of 35.59 l/s at wind speed of 3 m/s.

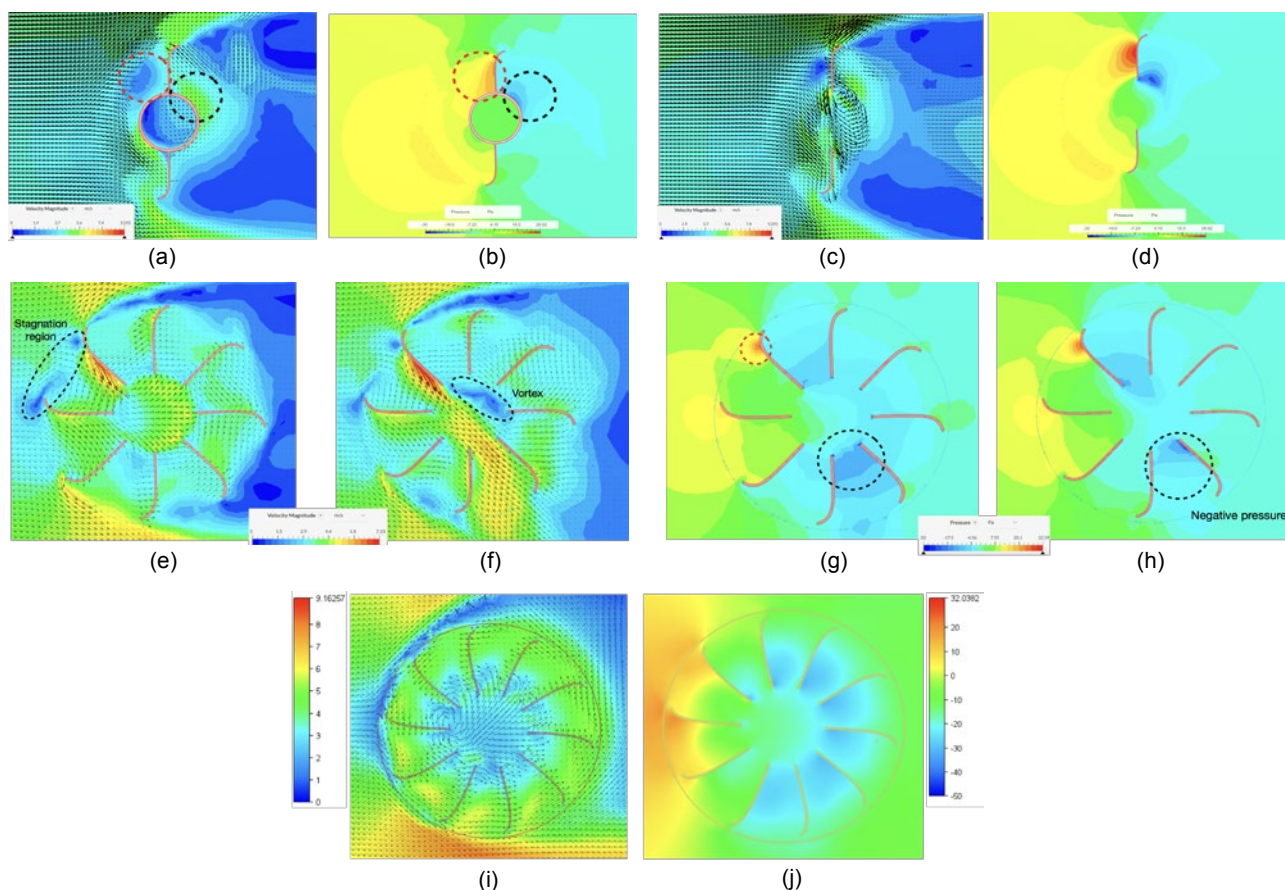


**Figure 2.** Velocity and pressure contours of 2B-TV, 8B-TV and modified 10B-TV.

To further explore ventilation performance of the turbine ventilator, a decrease in blade height was considered in this study to determine the differences in performance of the turbine blades to be more efficient at a lower wind speed. Moreover, the number of blades was also increased for the modified model (10B-TV). **Figure 2i** shows that the flow behaviour was similar to the flow characteristics of the 8B-TV. However, in this case, the flows entered the inner domain from downstream as more inner flow swirled within the rotor. A vortex took place in the centre of the rotor domain as the flows started swirling. Despite the result of the modified 10B-TV exerting an exhaust airflow rate of 45.81 l/s at 6 m/s, it still underperformed when compared to the 8B-TV model by approximately 50%, as shown in **Figure 3**.

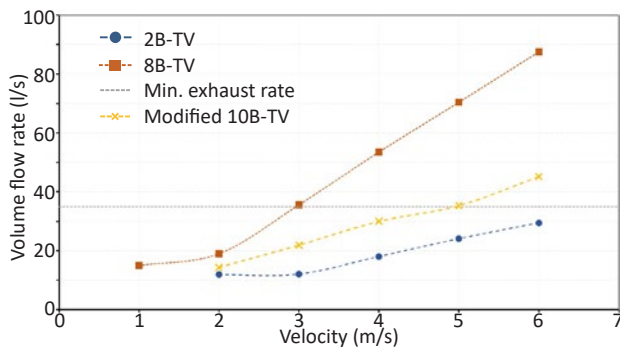


**Figure 3.** Comparison of air extraction performance between 2B-TV, 8B-TV and modified 10B-TV.

### Performance investigation of air supply flow rate

The performance on air supply rates was assessed against an induced flow rate entering through the air intake vent (AIV). The results of CFD simulations show the induced flows passing through the opening on the windward side of the channel (see **Figure 4**). Moreover, the recirculation zones were formed on the outer wall at lower edge of the louver bend (red circles in **Figure 4a**) after the airflow entered the inlet opening. This then develops the high-pressure area causing a loss in the air flow, which leads to a decreasing flow rate in the air supply channel. The CFD result of the volume flow rates induced by the AIV is shown in **Figure 5**, with the maximum flow rate of 38.25 l/s at 6 m/s. In

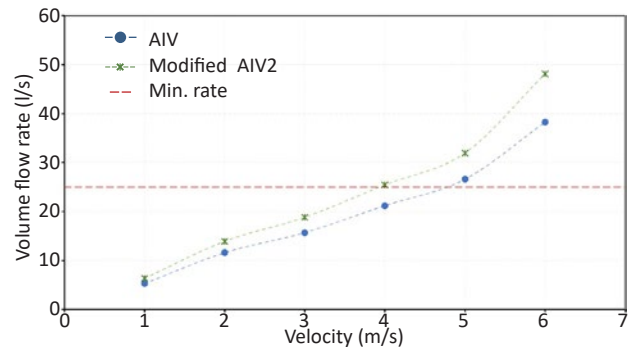


**Figure 5.** Comparison of ventilation performance for air supply between the AIV and modified AIV2.

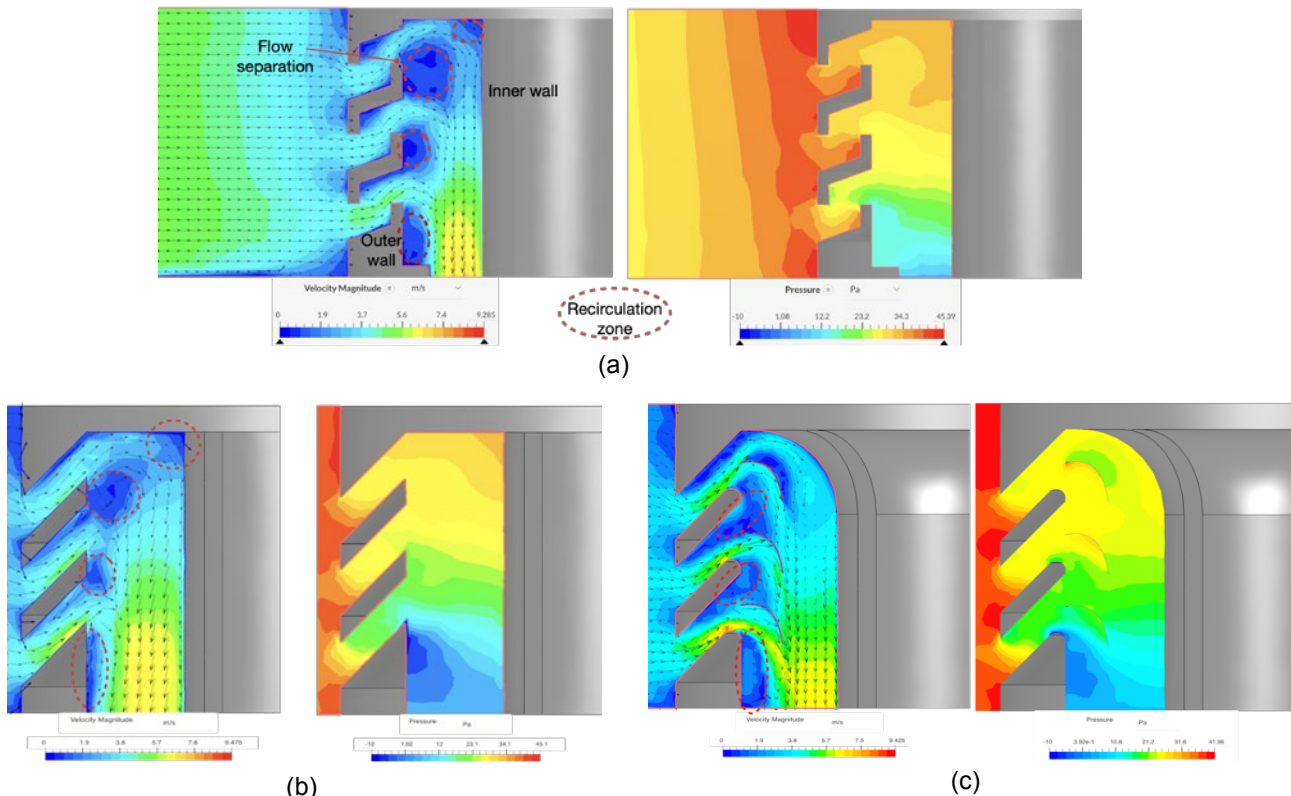


**Figure 4.** Velocity and pressure contours: (a) AIV, (b) modified AIV1 and (c) modified AIV2.

addition, it also meets the minimum ventilation rate for air supply of 25 l/s when the wind speed is 5 m/s.

Features of the AIV profile were altered to further enhance its ventilation performance. **Figure 4b** shows that the size of the recirculation zones (in the red circles) of the modified AIV1 was reduced, which improved the ventilation performance by 5% compared to the AIV. In contrast, the modified AIV2 in **Figure 4c** outperformed the AIV by almost 20% due to an increase in an airflow rate of 48.11 l/s at 6 m/s, with the results are compared in **Figure 5**.

### Conclusion

The application of a powerless turbine ventilator to induce exhaust air flow rate through the roof is effective and efficient for the industrial building (Khan et al., 2008). However, it is deemed as unnecessary

for domestic ventilation systems, mainly due to the required working environment, visual pollution for some homeowners and unreliable resources available for operation. It has been overlooked in ventilation strategies when compared to HVAC, but it is considered to be more efficient in terms of both energy saving and ventilation performance.

As the proposed turbine ventilator is a primary design, the study shows a promising potential for the proposed home ventilation system integrated with the turbine ventilator. With further improvements, this new concept of ventilation system could be a greener alternative for future home ventilation for new builds or conventional houses. It will be cheaper and greener for domestic dwellings if a new ventilation system integrated with a low carbon turbine ventilator that maximises a natural source of wind energy for ventilation and energy saving can be developed. ■

### Reference

- Jadhav GK, Ghanegaonkar PM and Garg S (2016) Experimental and CFD analysis of turbo ventilator. *Journal of Building Engineering* 6: 196-202.
- Khan N, Su Y and Riffat SB (2008a) A review on wind driven ventilation techniques. *Energy and Buildings* 40(8): 1586-1604.
- Rimdžius D, Bielskus J, Martinaitis V, et al. (2018) Experimental Evaluation of Turbine Ventilators Performance under Different Test Conditions. *E3S Web of Conferences* 64.
- Tan YC, Ismail M and Ahmad MI (2016) Turbine Ventilator as Low Carbon Technology. *Renewable Energy and Sustainable Technologies for Building and Environmental Applications*. pp.167-174.
- Tian W, Mao Z and Ding H (2019) Numerical study of a passive-pitch shield for the efficiency improvement of vertical axis wind turbines. *Energy Conversion and Management* 183: 732-745.

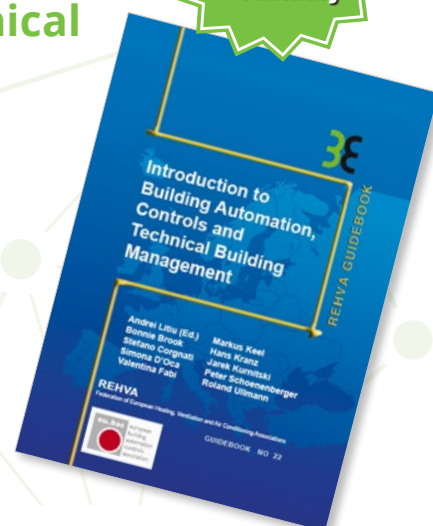
## REHVA EUROPEAN GUIDEBOOKS

### GB No.22 – Introduction To Building Automation, Controls And Technical Building Management

This guidebook aims to provide an overview on the different aspects of building automation, controls and technical building management and steer the direction to further in depth information on specific issues, thus increasing the readers' awareness and knowledge on this essential piece of the construction sector puzzle.

REHVA  40 RUE WASHINGTON 1050 BRUSSELS, BELGIUM  
 +32-2-5141171  INFO@REHVA.EU  WWW.REHVA.EU

Guidebook  
of the month  
- February



# Statistical analysis of the French building airtightness database



BASSAM MOUJALIED<sup>1,2</sup>



ADELINE MÉLOIS<sup>1,2</sup>



VALÉRIE LEPRINCE<sup>3</sup>



GAËLLE GUYOT<sup>1,2</sup>

<sup>1</sup> Cerema, BPE Research Team, 46 rue Saint Théobald, F-38081, L'Isle d'Abeau, France

<sup>2</sup> LOCIE, Université Savoie Mont Blanc, CNRS UMR5271, F-73376, France

<sup>3</sup> Cerema, Direction Territoire et Ville, 2 rue Antoine Charial, F-69426 Lyon, France

The French database of building airtightness was created in 2007 following the implementation of the national qualification scheme for building airtightness measurement. It currently contains about 570,000 measurements. This paper summarizes the results of the analysis of the database regarding the evolution of air permeability, and the impact of detected leakages.

This article is based on a paper presented at the 42nd AIVC - 10th TightVent & 8th venticool Conference “Ventilation Challenges in a Changing World” held on 5-6 October 2022 in Rotterdam, Netherlands.

**Keywords:** building airtightness, measurements, database, field data, detected leakages

With the constant evolution of the French EP-regulations, good building airtightness has become mandatory to reach required energy performance. The EP-regulation RT2012 introduced for the first time in 2013 minimum requirements for building airtightness in all new residential buildings. The air permeability, expressed by the French indicator  $q_{EA}$  ( $Q_{4Pa-surf}$  in French: air leakage rate at 4 Pa divided by the loss surface area excluding the basement floor) must be lower than  $0.6 \text{ m}^3 \cdot \text{h}^{-1} \cdot \text{m}^2$  for single-family houses (i.e. around  $n_{50} = 2.3 \text{ h}^{-1}$ ) and  $1.0 \text{ m}^3 \cdot \text{h}^{-1} \cdot \text{m}^2$  for multi-family buildings. The new EP-regulation RE2020 has strengthened the requirements since January 2022 by:

- introducing a new minimum requirement for non-residential (a limit value of  $1.7 \text{ m}^3 \cdot \text{h}^{-1} \cdot \text{m}^2$  for office buildings and schools of less than  $3000 \text{ m}^2$  of surface);

- and adding penalties for measurements by sampling (final result multiplied by 1.2) or tests performed before the completion of all work impacting the envelope air permeability (final result incremented by  $0.3 \text{ m}^3 \cdot \text{h}^{-1} \cdot \text{m}^2$ ).

Compliance must be justified either by an airtightness test performed by a qualified tester or by applying a certified quality framework. Thanks to this requirement, more than 60,000 airtightness tests have been carried out each year since 2015. Each test performed by a qualified tester is recorded in the French database on building airtightness, which is therefore growing rapidly (more than half million in 2020). The structure of the database is presented by Mélois (Mélois *et al.*, 2019). It is composed of 39 data fields on the building, the measurement procedure and the test results.

### Database Overview

Figure 1 shows the evolution of the number of building airtightness measurements and the distribution of measurements depending on the use of the building.

The database currently contains about 570,000 measurements. It takes into account the measurements made in France until 2021. The implementation of the regulatory requirement of the former EP-regulation RT2012 has initiated since 2013 a strong increase in the annual number of tests that fluctuates today between 65,000 and 80,000 approximately.

Residential buildings account for almost all of measurements (68% for single-family dwellings with 388,442 tests,

and 28% for multi-family buildings with 157,469 tests). Only 4% of tests are carried out in non-residential buildings (35,958 tests). This is due to the mandatory requirement that applies only to residential buildings.

### Changes of air permeability in the last decade

The results presented here are expressed according to the air permeability French indicator  $Q_{4Pa-surf}$ , as explained in the introduction. Only measurements performed upon completion are analysed hereafter in order to perform relevant comparisons.

Figure 2 presents the change over the last decade of building air permeability and its distribution.

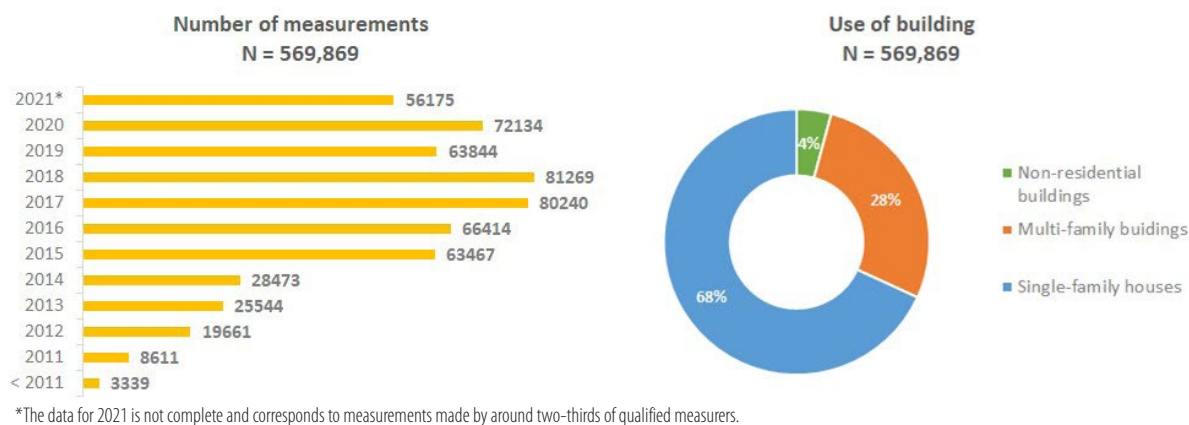


Figure 1. Evolution of the number of building airtightness test in France (left) and distribution of measurements depending on the use of the building.

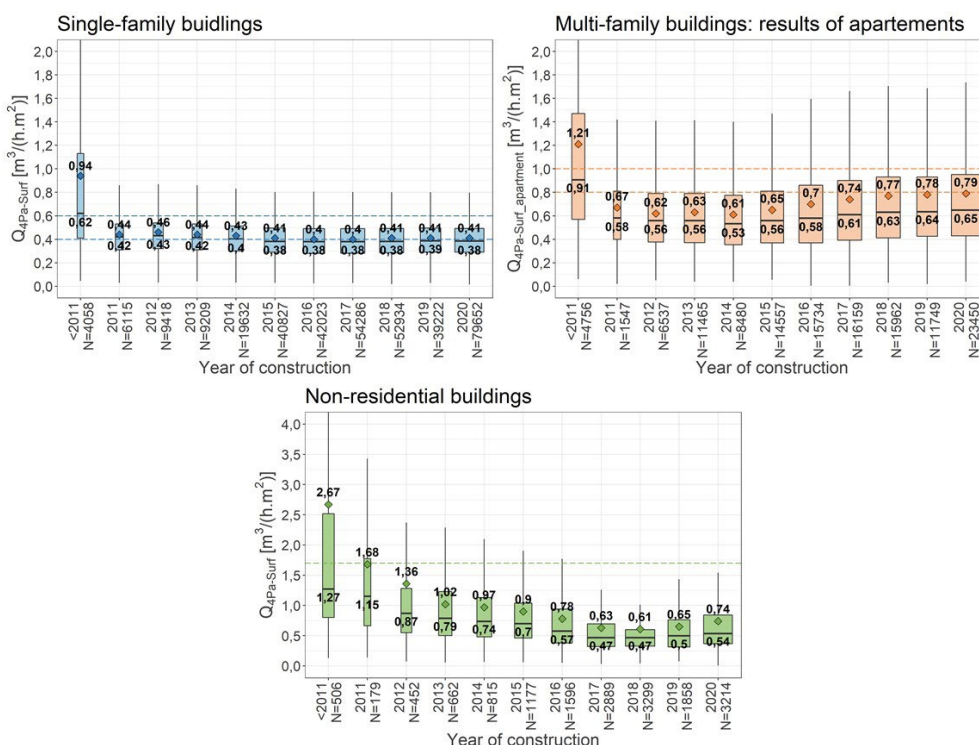


Figure 2. Boxplot of the building air permeability according to the year of construction in single-family, multi-family and non-residential buildings.

For single-family dwellings, the air permeability values decrease quickly in the first years and both median and mean values of  $Q_{4Pa-surf}$  stabilize around  $0.4 \text{ m}^3 \cdot \text{h}^{-1} \cdot \text{m}^2$  (median and mean values of  $n_{50}$  are  $1.70$  and  $1.86 \text{ h}^{-1}$  respectively) from 2015, clearly below the limit value of the mandatory requirement ( $0.6 \text{ m}^3 \cdot \text{h}^{-1} \cdot \text{m}^2$ ).

For multi-family buildings, the air permeability values also decrease quickly in the first years and then increase slightly from 2015. This is probably because every new building is now tested and not only exemplary ones that were applying for an EP-label. Indeed, the application of the mandatory requirement in multi-family buildings has been delayed by two years compared to single-family dwellings. The median and mean values of  $Q_{4Pa-surf}$  tend to stabilize around  $0.65$  and  $0.8 \text{ m}^3 \cdot \text{h}^{-1} \cdot \text{m}^2$  respectively (median and mean values of  $n_{50}$  are  $1.43$  and  $1.78 \text{ h}^{-1}$  respectively). They are both clearly below the limit value of the mandatory requirement ( $1.0 \text{ m}^3 \cdot \text{h}^{-1} \cdot \text{m}^2$ ).

For non-residential buildings, as seen above, the number of measurements is much lower. However, results show an annual increase in the number of measurements since 2011, with more than 3,000 non-residential buildings tested in 2020. As for the multi-family buildings, air permeability drops rapidly during the first years, then begins to increase slightly

over the last three years as the number of buildings measured increases. The median and mean values of  $Q_{4Pa-surf}$  tend to stabilize around  $0.55$  and  $0.75 \text{ m}^3 \cdot \text{h}^{-1} \cdot \text{m}^2$  respectively (median and mean values of  $n_{50}$  are  $1.82$  and  $2.38 \text{ h}^{-1}$  respectively).

### Analysis of the detected leakages

During each test, a detailed qualitative leakage detection is performed by testers in accordance with the Standard ISO 9972 (AFNOR, 2015) and the French standard FD P50-784 (AFNOR, 2016). Leakages are classified according to the leakage categories of FD P50-784 (see appendix A) with 8 main categories and 46 sub-categories (see appendix A).

Figure 3 shows the frequency of detected leakages by category in single-family, multi-family and non-residential buildings. Leakages through doors and windows (category C), electrical components (category F) and around penetrations through the envelope (category D) are the most frequent leakages detected in all buildings.

In order to analyse the impact of leakages on the air permeability, we have constructed 46 subsamples corresponding to the 46 subcategories of leakages. Each subsample contains the data where a particular leakage

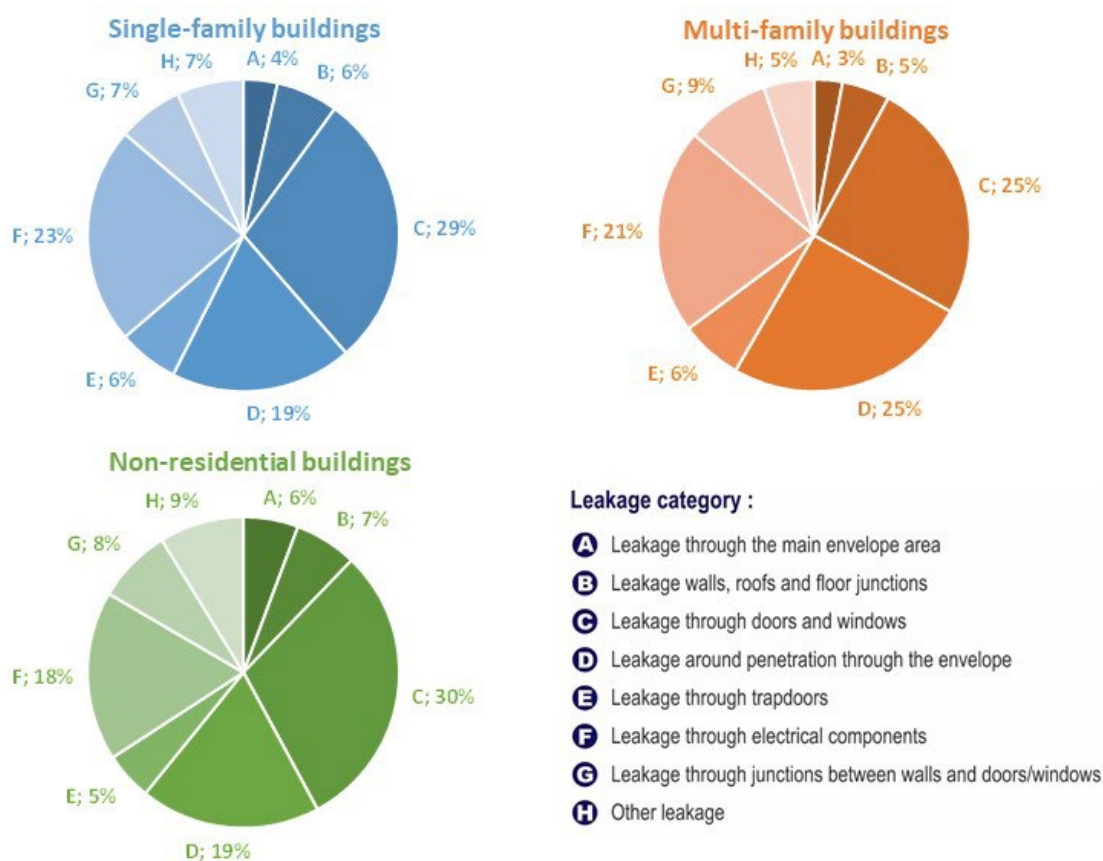
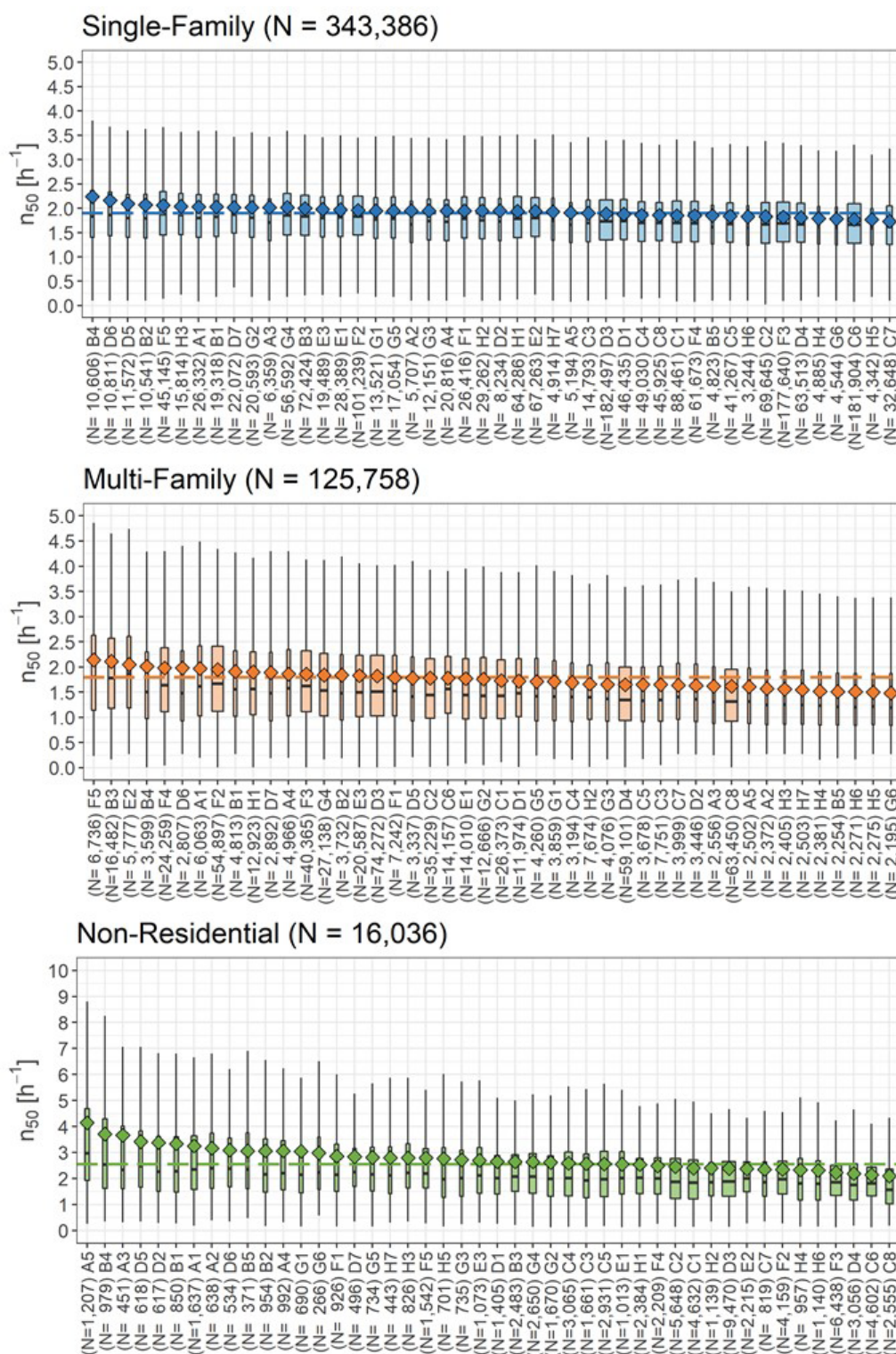


Figure 3. Frequency of detected leakages in single-family, multi-family and non-residential buildings.

is observed. We then compared the mean value of air permeability of each subsample to that of the entire sample using Wilcoxon tests. For this analysis, we used the air change rate at 50 Pa “ $n_{50}$ ” as indicator to analyse air permeability variations, as it has the lowest error with respect to repeatability, reproducibility, and wind impact (Moujalled *et al.*, 2021).

**Figure 4** shows the comparison between the boxplots of  $n_{50}$  of all leakage subsamples and the mean value of the entire sample. Leakage subsamples are sorted in decreasing order of the mean value of  $n_{50}$ . We can identify the leakage subsamples with highest values  $n_{50}$ , the corresponding leakage can thus be considered to have greatest impact on the airtightness ( $p$ -value  $\ll 0.01$ ).



**Figure 4.** Boxplots of the measured air change rate at 50 Pa  $n_{50}$  in single-family, multi-family and non-residential buildings depending on the type of the detected leakage.

**Table 1** shows the top five leakages with the highest values of mean  $n_{50}$  in single-family, multi-family and non-residential buildings. It is interesting to note that the B4 leak (junction between wall and ceiling or sloped roof) is among those with a significant impact on airtightness in all three types of buildings, even though it is not very frequent. Overall, leakages through the main envelope area (A) and the junctions between walls and floors (B) are less frequent but have a significant impact on the air tightness of the building. As the search for leakages is not exhaustive during a test, a bias might exist in the detection of the leakages: leakages can be found only where the testers have looked for.

## Conclusions

Since its creation in 2007, the French database of building airtightness has been annually fed by measurements performed by qualified testers. The total number of measurements is now about 570,000 with a majority of residential buildings (68% single dwellings, 28% multi-family buildings against 4% non-residential buildings). This is due to the mandatory requirements of the former EP-regulation RT2012 that was implemented in 2013 only for new residential buildings. It has initiated since 2013 a strong increase in the annual number of tests that fluctuates today between

65,000 and 80,000 approximately. Measurements from 2015 can thus be considered as representative of new French residential buildings. With the new requirement in the current regulation RE2020 for non-residential buildings, we can expect to see a large increase in the number of tests in office buildings and schools in the coming years, similar to residential buildings.

In new single-houses, the mean air permeability is about  $0.4 \text{ m}^3/(\text{h}\cdot\text{m}^2)$  at 4 Pa which is significantly below the mandatory threshold value ( $0.6 \text{ m}^3/(\text{h}\cdot\text{m}^2)$ ) and 94% of all houses meet the mandatory requirement. In new multi-family buildings, the mean air permeability is about  $0.8 \text{ m}^3/(\text{h}\cdot\text{m}^2)$  at 4 Pa which is significantly below the mandatory threshold value ( $1.0 \text{ m}^3/(\text{h}\cdot\text{m}^2)$ ) and 94% of all buildings meet the mandatory requirement. In new non-residential buildings, for which there is no mandatory test, the airtightness has improved over the years and is now equivalent to the new multi-family buildings level: 93% of the tested buildings are better than the default value of the RT 2012 ( $1.7 \text{ m}^3\cdot\text{h}^1\cdot\text{m}^2$ ). The analyses of detected leakages enable us to identify the most critical leakages that are not always the most frequent ones: leakages through the main envelope area and the junctions between walls and floors are less frequent but have a significant impact on the air tightness of the building. ■

**Table 1.** The top five leakages with the greatest impact on air permeability.

Type of building	Leakages with highest values of mean $n_{50}$ (Occurrence)
Single-family	<p><b>B4-Junction between wall and ceiling or pitched roof (3%)</b></p> <p>D6-Beam connection with floor or ceiling (3%)</p> <p>D5-Beam or joist connection with walls (3%)</p> <p>B2-Junction between two vertical walls (3%)</p> <p>F5-Lighting components (13%)</p>
Multi-family	<p>F5-Lighting components (5%)</p> <p>B3-Junction between wall and floor (13%)</p> <p>E2-Attic trap door (absent or ineffective seal) (5%)</p> <p><b>B4-Junction between wall and ceiling or pitched roof (3%)</b></p> <p>F4-Wiring inside internal walls (19%)</p>
Non-residential	<p>A5-False ceiling panels (8%)</p> <p><b>B4-Junction between wall and ceiling or pitched roof (6%)</b></p> <p>A3-mortar/glue junction between masonry blocks, wall panels (3%)</p> <p>D5-Beam or joist connection with walls (4%)</p> <p>D2-Vapour barrier membrane through which duct, pipe, beams, hatches (4%)</p>

Classification of leakages according to the French standard FD P50-784 (AFNOR, 2016).

Leakage category	Leakage sub-category
A - Main envelope area	A1 - Other leakage on main envelope area A2 - Vapour barrier membrane (or similar complex): adhesive junction between strips, puncture or tearing A3 - Mortar/glue junction between masonry blocks, wall panels A4 - Puncture (e.g.: wall plug) or unsealed junctions between panels A5 - False ceiling panels
B – Wall, roof and floor junctions	B1 - Other leakage through wall and slab junctions B2 - Junction between two vertical walls B3 - Junction between wall and floor B4 - Junction between wall and ceiling or pitched roof B5 - Junction between vapour barrier membrane and slab
C – Doors and windows	C1 - Other leakage on windows and glazed doors C2 - Window / glazed doors: junction between frame and opening panels C3 - Window & glazed doors: junction between glass and frame defective seal) C4 - Landing door or fire door: poor compression of seals (excluding threshold bar) C5 - Landing door or fire door: absent or ineffective threshold bar C6 - Sliding door: Excessive space between glass panels. and the frame C7 - Sliding door: Evacuation of condensates C8 - Rolling shutter casing
D -Penetration through the envelope	D1 - Other element through a wall D2 - Vapour barrier membrane through which due pipe, beams, hatches D3 - Crossing Floor, walls and/or partitions (any type of pipes and electrical wiring...) D4 - Ventilation air terminals: leaks at periphery of exhaust/supply air vents D5 - Beam or joist connection with walls D6 - Beam connection with floor or ceiling D7 - Stairs: Junction flooring/stairs or vertical walls/stairs
E - Trapdoor	E1 - Another trapdoor E2 - Attic trap door (absent or ineffective seal) E3 - Trapdoor to vertical technical duct (absent or ineffective seal)
F - Electrical component	F1 - Other electrical component F2 - Electrical board F3 - Wiring inside external walls F4 - Wiring inside internal walls F5 - Lighting components
G - Door / window and wall junctions	G1 - Other leakage through wall and door/window junction G1 - Junction between walls and windows or glazed door G3 - Junction between walls and landing door or Fire door G4 - Junction between internal panels and window and glazed door G5 - Junction between internal panels and landing door or Fire door G6 - Junction between vapour barrier membrane and door or window
H - Other	H1 - Other leakage H2 - wood-burner, fireplace insert or boiler. or combustion-air air vent H3 - Extractor hood with external evacuation H4 - Trap door for smokes evacuation H5 - Zenithal lighting roof lights H6 - Elevator door (frame - connecting door...) H7 - Arrival air extraction or not described in the thermal calculation

## References

- AFNOR (2015) 'NF EN ISO 9972. Thermal performance of buildings - Determination of air permeability of buildings - Fan pressurization method'.
- AFNOR (2016) 'FD P50-784. Thermal performance of buildings - Implementation guide for NF EN ISO 9972'.
- Mélois, A.B. et al. (2019) 'Improving building envelope knowledge from analysis of 219,000 certified on-site air leakage measurements in France', *Building and Environment*, 159, p. 106145.
- Moujalled, B. et al. (2021) 'Mid-term and long-term changes in building airtightness: A field study on low-energy houses', *Energy and Buildings*, 250, p. 111257.

# REHVA is happy to welcome a new supporter!



Worldwide leader in light and sustainable construction, Saint-Gobain designs, manufactures and distributes materials and services for the construction and industrial markets.



Its integrated solutions for the renovation of public and private buildings, light construction and the decarbonization of construction and industry are developed through a continuous innovation process and provide sustainability and performance.

#### More information:

<https://www.saint-gobain.com/en>

**We are happy to welcome Saint-Gobain in the REHVA Family!**

## BECOME A REHVA SUPPORTER

REHVA, the **Federation of European HVAC Associations** represents more than 120.000 building services engineers from 27 countries. REHVA is dedicated to the improvement of health, comfort and energy efficiency in all buildings and communities.

REHVA supporter companies share the mission of REHVA: promoting latest HVAC technologies and advocating for energy efficient buildings with high indoor environmental quality. The benefits of REHVA Supporters are multiple: they range from increased European visibility, through networking with experts and HVAC engineers from across Europe, till the access to latest research outcomes and educational materials in the HVAC field.

### Services to REHVA Supporter Companies

- EU level networking opportunities with engineers, HVAC designers, researchers and stakeholders in the field of building services
- The Supporters' Bulletin focusing on EU directives, regulations and standards tailored for supporters (bi-monthly)
- Promotion in the REHVA Journal six times a year
- REHVA Journal in paper copy
- Access to restricted online services: eGuidebooks, HVAC Terminology, EU Policy Tracking, REHVA Committee documents, workshops and courses videos.
- Up to 60% discount for REHVA Guidebooks' orders
- Promotion on the REHVA website - [www.rehva.eu](http://www.rehva.eu)
- Up to 40% discount advertisements in the REHVA Journal
- REHVAClub events (at Annual Conference, REHVA seminars, cocktails, etc.) organized for Supporters with speakers from the European Commission and EU level stakeholder organizations
- Free copy of new REHVA Guidebooks and 20% discount on list price for extra copies

### Pricing

- The annual fee for REHVA Supporters is only 3.000 €!
- Additionally, REHVA offers Platinum, Gold, Silver and Bronze Supporter Packages which offer complementary promotion opportunities to its Supporters.
- For more information visit [www.rehva.eu/about-us/join-rehva](http://www.rehva.eu/about-us/join-rehva) or contact us at [info@rehva.eu](mailto:info@rehva.eu)



Visit us  
at the ISH  
in Frankfurt.

## Small devices, big impact.

The intelligent utilisation of energy protects against climate change and lowers operating costs. With the small and extremely effective actuators, valves, sensors and meters from the world market leader Belimo, you have perfect solutions for efficiently controlling, monitoring and optimising energy flows in buildings. This enables you to ensure a healthy room climate – in new buildings as well as in existing ones.

You can experience all our innovations and our product range in practical applications at our trade fair booth.

See you soon – we look forward to meeting you.



ISH 2023 | Frankfurt am Main  
13. – 17.3. | Hall 10.2 | Booth C75

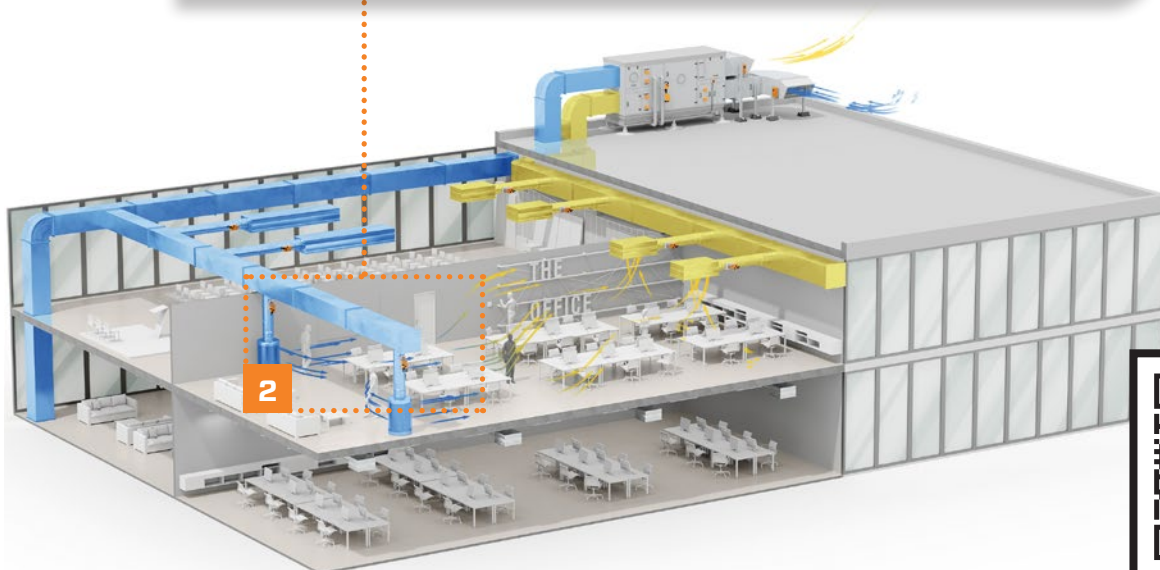
# ISH

# The Seven Essentials of Healthy Indoor Air

## 2. Accurate amount of air to the zone and controlled removal of contaminated air

Air handling units usually supply air to several zones in a building. It is important that each room receives the exact amount of fresh air it needs. If the number of people in a room increases, e.g., in a larger meeting room, one would expect the air supply to increase accordingly. Similarly,

the polluted air must also be removed from the room. To ensure this, zones and rooms must be supplied individually with variable air volume (VAV). If, for example, a room sensor detects excessively high CO<sub>2</sub> content, the VAV units are opened and the room is flooded with additional fresh air.



Learn more about Belimo's 7 essentials of healthy indoor air:  
[https://www.belimo.com/ch/en\\_GB/indoor-air-quality/7-essentials-iaq](https://www.belimo.com/ch/en_GB/indoor-air-quality/7-essentials-iaq)



# Exhibitions, Conferences and Seminars

## February 2023

28 Feb – 3 March 2023 World Sustainable Energy days ([wsed.at](http://wsed.at)) Wels, Austria

## March 2023

6–8 March 2023 HVAC Cold Climate Conference 2023 ([ashrae.org](http://ashrae.org)) Anchorage, Alaska

13–17 March 2023 ISH 2023 ([ish.messefrankfurt.com](http://ish.messefrankfurt.com)) Frankfurt am Main, Germany

14–16 March 2023 ACREX 2023 ([acrex.in](http://acrex.in)) Mumbai, India

## May 2023

10–11 May 2023 Developing Economies Conference 2023 ([ashrae.org](http://ashrae.org)) Mumbai, India

11–12 May 2023 REHVA Annual Meeting ([rehva.eu](http://rehva.eu)) Brussels, Belgium

20–23 May 2023 IAQVEC 2023 ([iaqvec2023.org](http://iaqvec2023.org)) Tokyo, Japan

## June 2023

11–14 June 2023 HB2023 Europe Conference, “Beyond disciplinary boundaries – Transdisciplinary perspectives on multisensory stimulation for innovative and creative solutions in a Post-Covid era” ([ukaachen.de](http://ukaachen.de)) Aachen, Germany

24–28 June 2023 2023 ASHRAE Annual Conference ([ashrae.org](http://ashrae.org)) Tampa, FL

## August 2023

14–16 August 2023 SuDBE 2023 ([sudbeconference.com](http://sudbeconference.com)) Espoo, Finland

## September 2023

28–30 September 2023 EFS 2023 ([efs2023.uc.pt](http://efs2023.uc.pt)) Prague, Czech Republic

## October 2023

4–5 October 2023 43rd AIVC – 11th TightVent & 9th venticool Conference: Ventilation, IEQ and health in sustainable buildings ([aivc2023conference.org](http://aivc2023conference.org)) Aalborg University, Copenhagen, Denmark

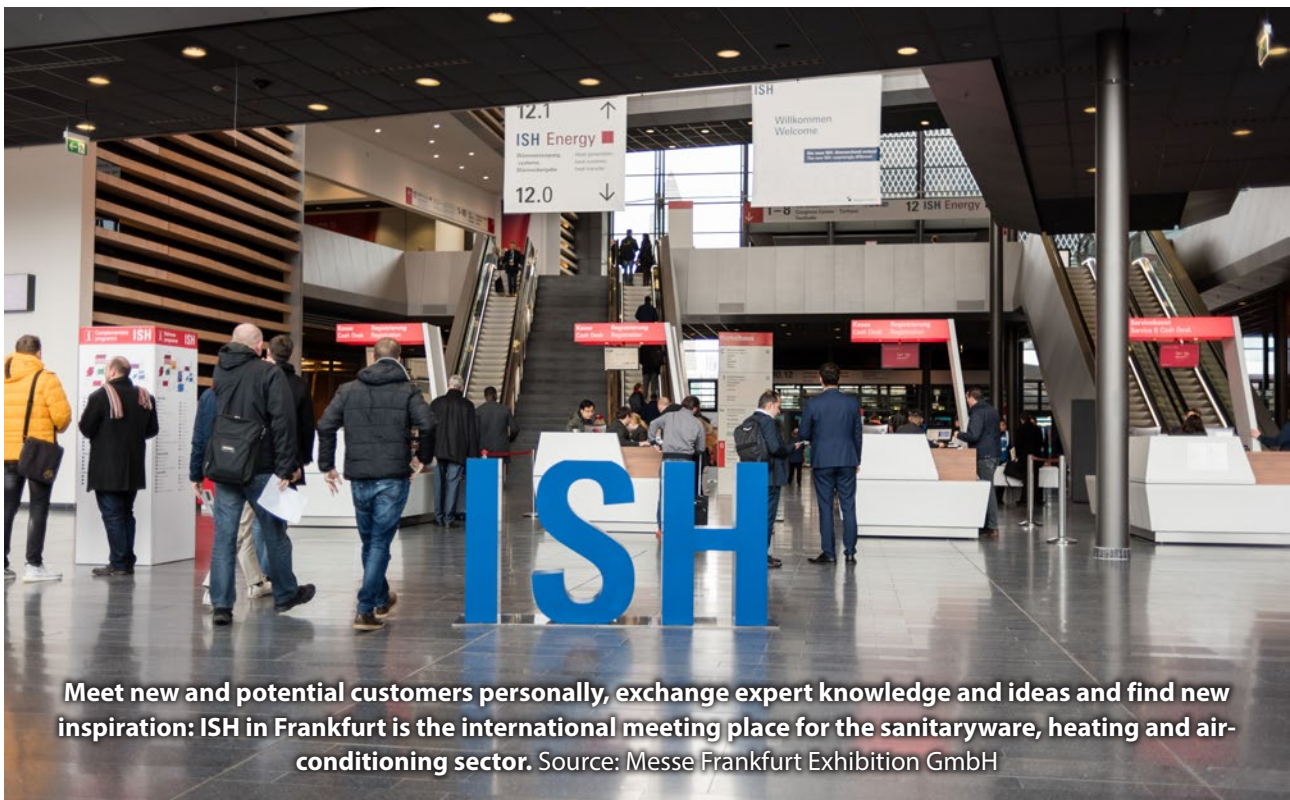
25–27 October 2023 2023 Decarbonization Conference for the Built Environment ([ashrae.org](http://ashrae.org)) Washington D.C., USA

Due to the COVID-19 circumstances, the dates of events might change. Please follow the event's official website.



# ISH 2023 interim result: growing anticipation

The focus of ISH - The world's leading trade fair HVAC + Water, from 13 to 17 March 2023, is on marketable solutions for a sustainable future. Currently, the organisers are expecting around 2,000 companies to present their solutions for renewable sources of energy, sustainable water usage and clean air at the leading international trade event for the HVAC and water sector.



ISH from 13 to 17 March 2023 is to be held under the motto, 'Solutions for a sustainable future'. For five days, everything at the world's leading trade fair for HVAC + Water will revolve around innovations that contribute to achieving climate-protection targets and a responsible and efficient use of resources. "The interim result is a source of growing anticipation for us. At present, we expect around 2,000 exhibitors to participate and take advantage of the power of attraction exercised by ISH for their businesses. They are spread fairly evenly across the two main sections of the fair, ISH Water and ISH Energy. Accordingly, the coming ISH is an unrivalled opportunity for them to present their solutions to an international audience of trade visitors, to profit from networking effects and to exchange valuable knowledge", explains Stefan Seitz, ISH Brand Management Director.

With 70 percent of exhibitors coming from outside Germany, the 2023 edition of the world's biggest meeting place for the sanitaryware, heating and air-conditioning sector is distinguished by a high level of internationality. Besides the many German companies, the majority of exhibitors will be making their way to Frankfurt from Italy, Turkey, Spain,

China, Poland, France, the Netherlands, Austria, Belgium, Sweden and Switzerland. They are spread across the two main sections of the fair, ISH Water and ISH Energy. The focus of the ISH Water section is on modern bathroom design and sustainable technology in the use of water as a valuable resource. In Halls 1, 2, 3, 4, 5 and 6, visitors will find innovative products and solutions for the lifestyle-oriented bathroom,

## EVENTS UPCOMING

a hygienic drinking-water installation, quick and easy installation and fastening technologies and software solutions.

The spectrum of products at ISH Energy in Halls 8, 9, 10, 11 and 12 ranges from innovative heat generation, especially sustainable heat-pump technology, modern heat distribution, delivery and systems, via intelligent home and building automation, to cooling, air-conditioning and ventilation technology under the motto, 'Air is essential for life'.

The ISH Contactor offers an up-to-date overview of all exhibitors taking part in the fair at [www.ish.messefrankfurt.com/contactor](http://www.ish.messefrankfurt.com/contactor).

### The top themes: the future in sight

'Solutions for a sustainable future' is the motto of ISH 2023 where everything will revolve around innovations that contribute to achieving climate-protection targets and a responsible and efficient use of resources. Buildings, which account for around 40 percent of energy consumption, can play an important role in this. Thus, sustainability is the most important issue facing the sector and the determining factor for all top themes. In the ISH Energy section, the focus is on the expansion of renewable energies, decarbonisation, greater energy efficiency, heat-pump technology and the use of hydrogen. This is reflected by the top themes, 'Solutions for Heat Transition and Climate Protection' and 'Energy Efficiency & Sustainability'. An integral part of ISH, the subject of air, also makes an important contribution to the superordinate goal of CO2 reduction and energy saving and will be given due prominence in 2023 by the top theme of 'Indoor Air Quality'. In the ISH Water section, the spotlight with 'Resource Water' is on the sustainable use and supply-side security of drinking water. The second top theme, the 'Sustainable Bathroom' puts the emphasis on ecological factors in the bathroom.

### A blend of expert knowledge, trending themes and networking

A multi-faceted programme of events awaits everyone from the sanitaryware, heating and air-conditioning business, e.g., from the installation trade, the retail side, the industry, planning offices, the building and housing sector and public authorities and utilities. For the first time, the thematic grouping of events in the form of hotspots will ensure rapid orientation at the fair. Full details for the wide-ranging programme of events at ISH 2023 can be found at [www.ish.messefrankfurt.com/events](http://www.ish.messefrankfurt.com/events).

### ISH Digital Extension

The digital platform accompanying the trade fair will run concurrently with ISH 2023 in Frankfurt and for a week afterwards. From 13 to 24 March 2023, the [ISH Digital Extension](#) offers participants the chance to take part in the fair virtually. One advantage is the opportunity to make targeted contacts. Thanks to an AI-aided matchmaking system, it will be possible for participants to find potential customers or suppliers and to make contact with them either at the fair or digitally. Moreover, individual items on the programme of events can be seen as on-demand videos whenever it suits the user. ■

### ISH – The world's leading trade fair HVAC + Water

ISH opens its doors in Frankfurt am Main from 13 to 17 March 2023.



For more information, please visit our website at: [www.messefrankfurt.com](http://www.messefrankfurt.com)



# 11<sup>th</sup> SuDBE International Conference

Sustainable Development in the Building and Environment (SuDBE)

## Important Dates

Abstract submission deadline

Mar. 15<sup>th</sup>, 2023

Full paper submission deadline

Jun. 15<sup>th</sup>, 2023

Conference date

Aug. 14-18<sup>th</sup>, 2023



## Themes

- Green and Sustainable Building Development Response to Climate Changes
- Practice and Development of Healthy Building
- Indoor Environment (air quality, thermal comfort, acoustic, light)
- Low-carbon and Intelligent Buildings (energy, system, and operation)
- Innovative Geo-techniques and Structural Engineering
- Urban Ecological Infrastructures
- Sustainable Urban Renewal
- Youth Scholars Forum
- Students Forum

## Schedule

August 14 <sup>th</sup>	Check-in and Registration
August 15-16 <sup>th</sup>	Plenary and Technical, Workshop Sessions
August 17-18 <sup>th</sup>	Technical Tour

## Registration Fee

**Participation fee:** 650€  
**Student:** 400€

**Note:** registration fee includes a lunch, a coffee break and a welcome dinner on Aug. 15<sup>th</sup> and a lunch and a coffee break on Aug. 16<sup>th</sup>.

The 11<sup>th</sup> International Conference on Sustainable Development in the Building and Environment will be held in Espoo, Finland from 14<sup>th</sup> to 18<sup>th</sup> of August 2023. We wish you take away new innovative ideas and spark new research and implementations in practice.

<http://sudbeconference.com/>

## Efs 2023

5<sup>th</sup> ENERGY FOR SUSTAINABILITY INTERNATIONAL CONFERENCE  
TOWARDS A SUSTAINABLE AND RESILIENT FUTURE

28 – 30 September 2023 | Prague, Czech Republic

## IMPORTANT DEADLINES

28<sup>th</sup> FEBRUARY

Submission of abstracts

15<sup>th</sup> MARCH

Notification of acceptance of abstracts

30<sup>th</sup> APRIL

Paper submission

31<sup>st</sup> MAY

Final acceptance notification

15<sup>th</sup> JUNE

Final paper submission

### CONTACTS

efs2023@efs.uc.pt  
efs2023.uc.pt

Solving the issue of energy scarcity calls for, not only the supply of clean, reliable and inexpensive energy, but also for the increase of energy efficiency at the stages of conversion, distribution and final consumption of energy. Tackling this issue requires a multidisciplinary approach.

Under the theme of "Towards a resilient and sustainable future", the goal of the Efs 2023 Conference is to generate discussion on how to create an energy sustainable future for the people and the planet by promoting the exchange of knowledge, innovative ideas and past experiences between participants from multiple scientific fields.



ATIC vzw—asbl — Belgium  
[www.atic.be](http://www.atic.be)



BAOVK — Bulgaria  
[www.baovk.bg](http://www.baovk.bg)



STP — Czech Republic  
[www.stpcr.cz](http://www.stpcr.cz)



DANVAK — Denmark  
[www.danvak.dk](http://www.danvak.dk)



EKVÜ — Estonia  
[www.ekvy.ee](http://www.ekvy.ee)



FINVAC — Finland  
[www.finvac.org](http://www.finvac.org)



AICVF — France  
[www.aicvf.org](http://www.aicvf.org)



VDI—e.V. — Germany  
[www.vdi.de](http://www.vdi.de)



ÉTÉ — Hungary  
[www.eptud.org](http://www.eptud.org)



MMK — Hungary  
[www.mmk.hu](http://www.mmk.hu)



AiCARR — Italy  
[www.aicarr.org](http://www.aicarr.org)



LATVIJAS SILTUMA, GĀZES UN ŪDENS  
 TEHNOLOĢIJAS INŽENIERU SAVIENĪBA

AHGWTEL/LATVAC — Latvia  
[www.lsgutis.lv](http://www.lsgutis.lv)



LITES — Lithuania  
[www.listia.lt](http://www.listia.lt)



AIIRM — Republic of Moldova  
[www.aiirm.md](http://www.aiirm.md)



TVVL — The Netherlands  
[www.tvvl.nl](http://www.tvvl.nl)



NEMITEK — Norway  
[www.nemitek.no](http://www.nemitek.no)



PZITS — Poland  
[www.pzits.pl](http://www.pzits.pl)



ORDEM DOS ENGENHEIROS — Portugal  
[www.ordemengenheiros.pt](http://www.ordemengenheiros.pt)



AFCR — Romania  
[www.criofrig.ro](http://www.criofrig.ro)



AGFR — Romania  
[www.agfro.ro](http://www.agfro.ro)



AIIR — Romania  
[www.aiiro.ro](http://www.aiiro.ro)



KGH c/o SMEITS — Serbia  
[www.smeits.rs](http://www.smeits.rs)



SSTP — Slovakia  
[www.sstp.sk](http://www.sstp.sk)



SITHOK — Slovenia  
<https://web.fs.uni-lj.si/sithok/>



ATECYR — Spain  
[www.atecyr.org](http://www.atecyr.org)



SWEDVAC — Sweden  
[www.energi-miljo.se](http://www.energi-miljo.se)



DIE PLANER — Switzerland  
[www.die-planer.ch](http://www.die-planer.ch)



TTMD — Turkey  
[www.ttmd.org.tr](http://www.ttmd.org.tr)



CIBSE — United Kingdom  
[www.cibse.org](http://www.cibse.org)

# SUPPORTERS

*Leaders in Building Services*



Daikin Europe – Belgium  
[www.daikin.eu](http://www.daikin.eu)



EPEE – Belgium  
[www.epeeglobal.org](http://www.epeeglobal.org)



EVIA – Belgium  
[www.evia.eu](http://www.evia.eu)



Velux – Denmark  
[www.velux.com](http://www.velux.com)



Granlund – Finland  
[www.granlund.fi](http://www.granlund.fi)



Halton – Finland  
[www.halton.com](http://www.halton.com)



Uponor – Finland  
[www.uponor.com](http://www.uponor.com)



Eurovent Certita Certification –  
 France  
[www.eurovent-certification.com](http://www.eurovent-certification.com)



LG Electronics – France  
[www.lgeaircon.com](http://www.lgeaircon.com)



Saint-Gobain – France  
[www.saint-gobain.com](http://www.saint-gobain.com)



Viega – Germany  
[www.viega.com](http://www.viega.com)



Aermec – Italy  
[www.aermec.com](http://www.aermec.com)



Evapco Europe – Italy  
[www.evapco.eu](http://www.evapco.eu)



Rhoss – Italy  
[www.rhoss.com](http://www.rhoss.com)



Purmo Group – The Netherlands  
[www.purmogroup.com](http://www.purmogroup.com)



Royal Haskoning DHV –  
 The Netherlands  
[www.royalhaskoningdhv.com](http://www.royalhaskoningdhv.com)



SMAY – Poland  
[www.smay.eu](http://www.smay.eu)



E.E.B.C. – Romania  
[www.eebc.ro](http://www.eebc.ro)



Dosetimpex – Romania  
[www.dosetimpex.ro](http://www.dosetimpex.ro)



Testo – Romania  
[www.testo.com](http://www.testo.com)



Camfil – Sweden  
[www.camfil.com](http://www.camfil.com)



Fläkt Group – Sweden  
[www.flaktgroup.com](http://www.flaktgroup.com)



Lindab – Sweden  
[www.lindab.com](http://www.lindab.com)



Swegon – Sweden  
[www.swegon.com](http://www.swegon.com)



Systemair – Sweden  
[www.systemair.com](http://www.systemair.com)



Belimo Automation – Switzerland  
[www.belimo.com](http://www.belimo.com)



Arçelik – Turkey  
[www.arcelikglobal.com](http://www.arcelikglobal.com)



Friterm Termik Cihazlar  
 Sanayi ve Ticaret – Turkey  
[www.friterm.com](http://www.friterm.com)



Zoonex – United Kingdom  
[www.zoonexsystems.com](http://www.zoonexsystems.com)

## REHVA ASSOCIATE ORGANISATIONS:



EVHA – European Union  
[www.evha.eu](http://www.evha.eu)



Enerbrain srl – Italia  
[www.enerbrain.com](http://www.enerbrain.com)



Enviromech – United Kingdom  
[www.enviromech.co.uk](http://www.enviromech.co.uk)



ISIB – Turkey  
[www.isib.org.tr](http://www.isib.org.tr)



ECI – Belgium  
[copperalliance.org](http://copperalliance.org)



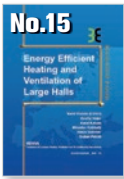
Romanian Chamber of Energy Auditors (O.A.E.R.)

O.A.E.R. – Romania  
[www.oaer.ro](http://www.oaer.ro)



# REHVA EUROPEAN GUIDEBOOKS

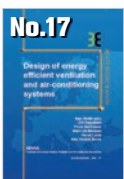
REHVA Guidebooks are written by teams of European HVAC experts



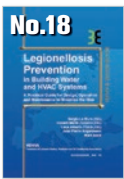
**No.15 Energy Efficient Heating and Ventilation of Large Halls.** This Guidebook is focused on modern methods for design, control and operation of energy efficient heating systems in large spaces and industrial halls. The book deals with thermal comfort, light and dark gas radiant heaters, panel radiant heating, floor heating and industrial air heating systems. Various heating systems are illustrated with case studies.



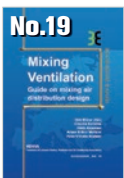
**No.16 HVAC in Sustainable Office Buildings - A bridge between owners and engineers.** This Guidebook discusses the interaction of sustainability and heating, ventilation and air-conditioning. HVAC technologies used in sustainable buildings are described. This book also provides a list of questions to be asked in various phrases of building's life time. Different case studies of sustainable office buildings are presented.



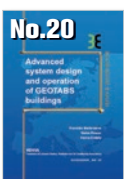
**No.17 Design of energy efficient ventilation and air-conditioning systems.** This Guidebook covers numerous system components of ventilation and air-conditioning systems and shows how they can be improved by applying the latest technology products. Special attention is paid to details, which are often overlooked in the daily design practice, resulting in poor performance of high quality products once they are installed in the building system.



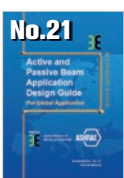
**No.18 Legionellosis Prevention in Building Water and HVAC Systems.** This Guidebook is a practical guide for design, operation and maintenance to minimize the risk of legionellosis in building water and HVAC systems. It is divided into several themes such as: Air conditioning of the air (by water - humidification), Production of hot water for washing (fundamentally but not only hot water for washing) and Evaporative cooling tower.



**No.19 Mixing Ventilation.** In this Guidebook most of the known and used in practice methods for achieving mixing air distribution are discussed. Mixing ventilation has been applied to many different spaces providing fresh air and thermal comfort to the occupants. Today, a design engineer can choose from large selection of air diffusers and exhaust openings.



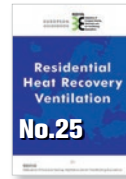
**No.20 Advanced system design and operation of GEOTABS buildings.** This Guidebook provides comprehensive information on GEOTABS systems. It is intended to support building owners, architects and engineers in an early design stage showing how GEOTABS can be integrated into their building concepts. It also gives many helpful advices from experienced engineers that have designed, built and run GEOTABS systems.



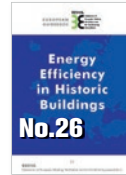
**No.21 Active and Passive Beam Application Design Guide.** is the result of collaboration by worldwide experts. It provides energy-efficient methods of cooling, heating, and ventilating indoor areas, especially spaces that require individual zone control and where internal moisture loads are moderate. The systems are simple to operate and maintain.



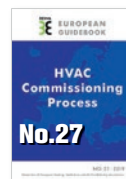
**No.22 Introduction to Building Automation, Controls and Technical Building Management.** This Guidebook aims to provide an overview on the different aspects of building automation, controls and technical building management and steer the direction to further in depth information on specific issues, thus increasing the readers' awareness and knowledge on this essential piece of the construction sector puzzle.



**Residential Heat Recovery Ventilation.** Heat recovery ventilation is expected to be a major ventilation solution while energy performance of buildings is improved in Europe. This European Guidebook prepared by REHVA and EUROVENT experts includes the latest ventilation technology and knowledge about the ventilation system performance, intended to be used by HVAC designers, consultants, contractors, and other practitioners.



**Energy Efficiency in Historic Buildings.** These guidelines provide information to evaluate and improve the energy performance of historic buildings, fully respecting their significance as well as their cultural heritage and aesthetic qualities. The guidelines are intended for both design engineers and government agencies.



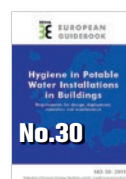
**HVAC Commissioning Process.** This Guidebook describes the HVAC Commissioning Process compatible with the routines in the building sector almost everywhere around the world. This is the first work that both describes the process in a very hands-on manner and details the commissioning activities for various types of systems, complete with theoretical background, guidance & checklists.



**NZEB Design Strategies for Residential Buildings in Mediterranean Regions - Part 1.** The aim of this Guidebook is to develop a basic framework of a design guideline for planners, designers and engineers involved in the passive/architectural design of buildings and the selection process of the HVAC systems to deliver the most appropriate and cost-effective solutions for NZEB in Mediterranean climates.



**Quality Management for Buildings.** This Guidebook gives a brief overview on quality management services Technical Monitoring (TMon) and Commissioning (Cx) to building owners, developers and tenants. Avoiding technical details, it shows the tremendous economic potential, gives insights on the most important technical aspects and provides hands-on advice for application in projects.



**Hygiene in Potable Water Installations in Buildings.** This REHVA Guidebook provides information on the design, installation, commissioning, use, operation and maintenance of all water installations in buildings. Central waterworks supply over 95% of the population with potable water round the clock and with virtually no interruptions.



**NZEB Design Strategies for Residential Buildings in Mediterranean Regions - Part 1.** The main objective behind this Guidebook is to present and promote the use of equipment, technology and systems appropriate to the cooling-demand-dominated requirements of the Mediterranean climate.



**Energy Efficient Renovation of Existing Buildings for HVAC professionals.** This Guidebook shows the baseline for specific energy efficiency and other renovation measures in existing buildings for which the HVAC systems play an important role. It presents the best available techniques and solutions that can be used as part of the energy modernization of the HVAC systems.